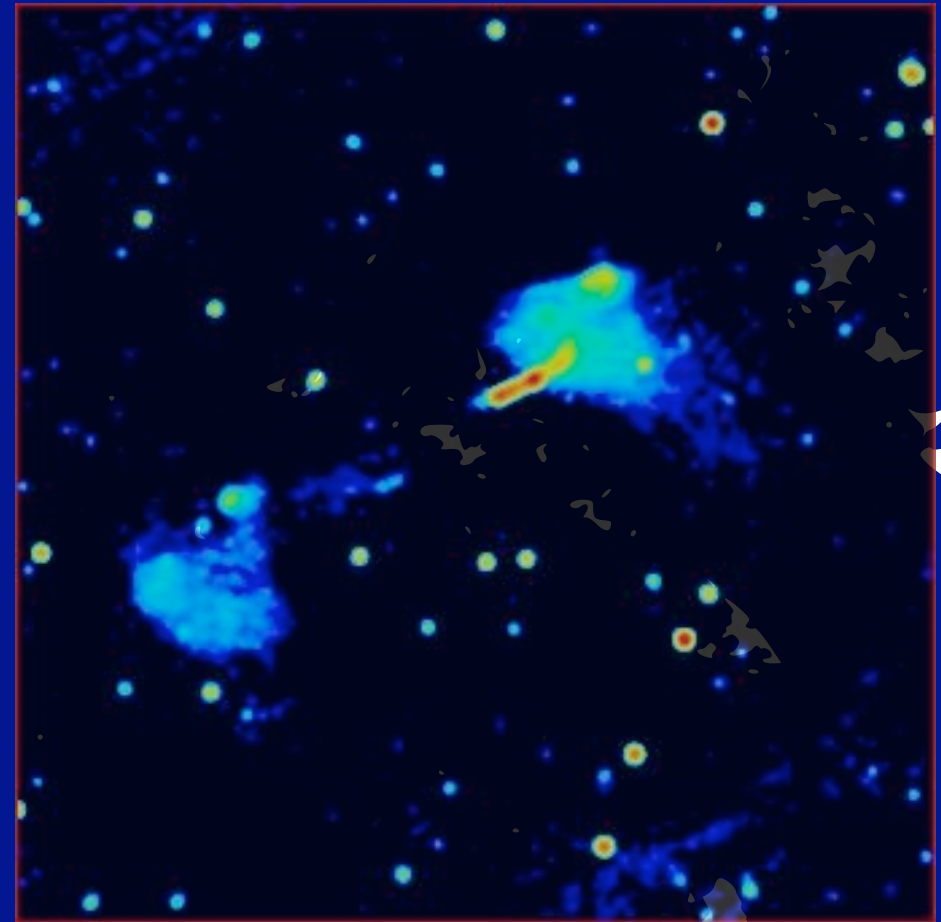


Misaligned AGNs from Radio to Gamma

Paola Grandi

INAF
IASF-BO



Overview

AGN community is mainly working on three fundamental questions:

- Black Holes to test general relativity

- **Accretion and jet link**

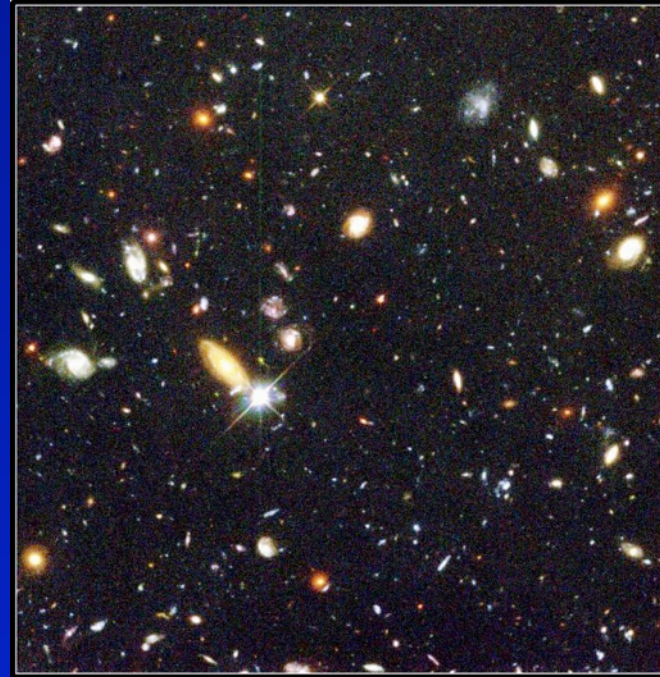
- Black hole formation and evolution

Outline of this lesson

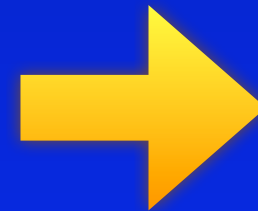
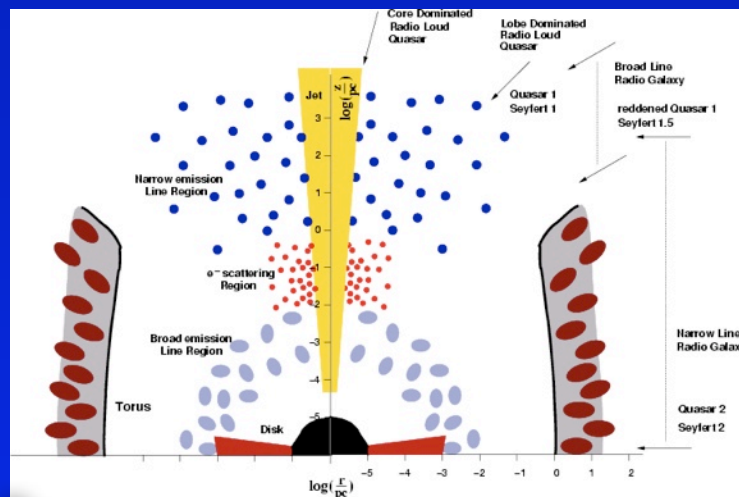
1. AGN Tour
2. Accretion Processes
3. Jets
4. Accretion in MAGNs
5. Jets - Lobes in MAGNs

1. AGN in general

A small fraction 20% of galaxies has a very bright nucleus



2-3 pc



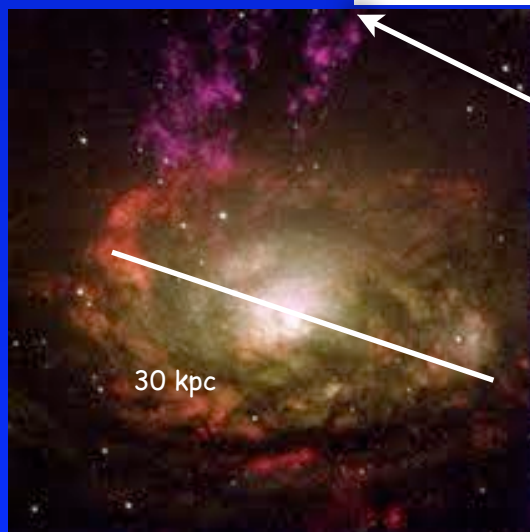
A small fraction 15-20% of AGN are Radio Loud (RL).

An AGN is Radio Loud when $F_{5\text{GHz}}/F_B > 10$
(controversial classification)

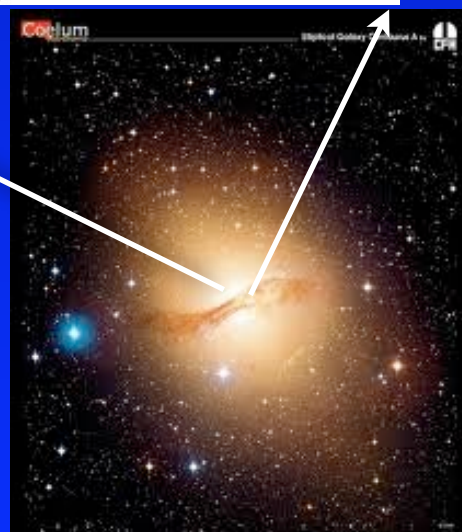
otherwise is Radio Quiet (RQ)

RQ => Elliptical and Spiral

RL => Elliptical

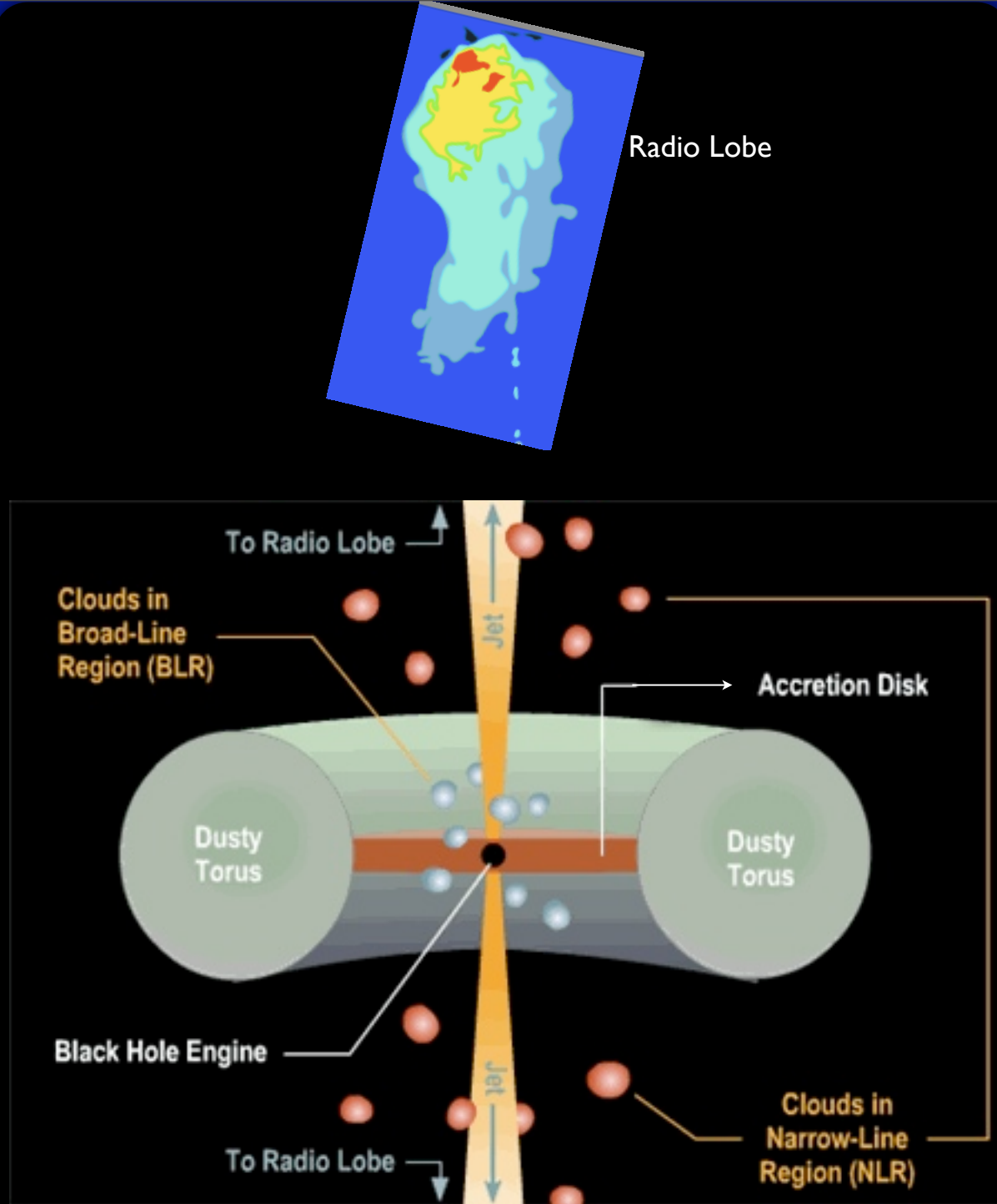


Spiral



Elliptical

Some numbers for a typical AGN

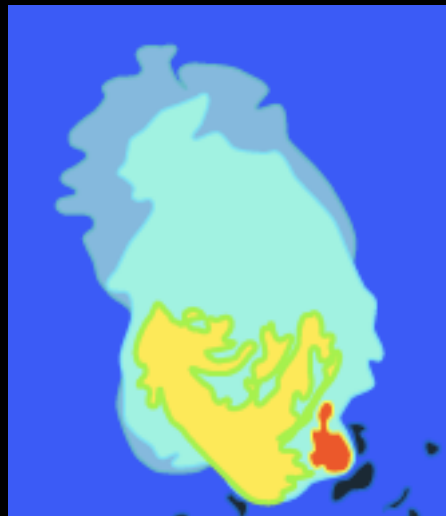


BH Mass	$\sim 10^8 M_{\odot}$
Luminosity	$\sim 10^{44} \text{ erg s}^{-1}$
BH radius	$\sim 3 \times 10^{13} \text{ cm}$
BLR radius	$\sim 2 - 20 \times 10^{16} \text{ cm}$
NLRG radius	$\sim 10^{18} - 10^{20} \text{ cm}$

In RL AGNs

Jet can be observed at $\sim 10^{17} \text{ cm}$

Jet ends at Kc distances forming radio lobes



2. Accretion



Accretion is the physical process by which black hole aggregates matter from their surroundings. The gravitational energies that such matter must release for accretion to occur is a powerful source of luminosity L .

The efficiency of the process is: $L = \eta \dot{M} c^2$

{ with $\eta \propto M/R$ (compactness of the system)
and \dot{M} accretion rate in $M_{\odot} yr^{-1}$

In case of a black hole the size is defined in term of the Schwarzschild radius

$$R_s = \frac{GM}{c^2} \sim 3 \times 10^3 M_8 \text{ cm}$$

Eddington Luminosity L_E is the luminosity at which the outward force of the radiation pressure is balanced by the inward gravitational force

$$L_E = \frac{4\pi G m_p c}{\sigma_e} M \sim 1.3 \times 10^{38} (M/M_{\odot}) (\text{erg s}^{-1})$$

accretion on to a black hole must power the most luminous phenomena in the universe

$$L_{acc} = \frac{GM}{R} \dot{M} = \eta c^2 \dot{M}$$

Quasars: $L \approx 10^{46} \text{ erg/s}$ requires $\dot{M} = 1 M_{sun} / \text{yr}$

X—ray binaries: $L \approx 10^{39} \text{ erg/s}$ $10^{-7} M_{sun} / \text{yr}$

Gamma—ray bursters: $L \approx 10^{52} \text{ erg/s}$ $0.1 M_{sun} / \text{sec}$

Accretion processes around black holes involve rotating gas flow. Therefore the accretion flow structure is determined by solving simultaneously four conservation equations:

1. conservation of vertical momentum
2. conservation of mass
3. conservation of energy
4. conservation of angular momentum

Four solutions are currently known. In these solutions viscosity transports angular momentum outward, allowing the accretion gas to spiral in toward the BH. Viscosity acts a source of heat that is radiated away.

The most famous solutions are:

- i) Shakura & Sunyaev thin optically thick disk model (standard model)
- ii) Optically thick Advection-Dominated Accretion Flow (ADAF)

Energy Equation

$$q^+ = q^- + q^{adv}$$

Thin Accretion Disk

(Shakura & Sunyaev 1973;
Novikov & Thorne 1973;...)

Most of the viscous heat
energy is radiated

$$q^- \approx q^+ \gg q^{adv}$$

$$L_{rad} : 0.1 \dot{M} c^2$$

Advection-Dominated Accretion Flow (ADAF)

(Ichimaru 1977; Narayan & Yi
1994, 1995; Abramowicz et al.
1995)

Most of the heat energy is
retained in the gas

$$q^- \ll q^+ \approx q^{adv}$$

$$L_{rad} \ll 0.1 \dot{M} c^2$$

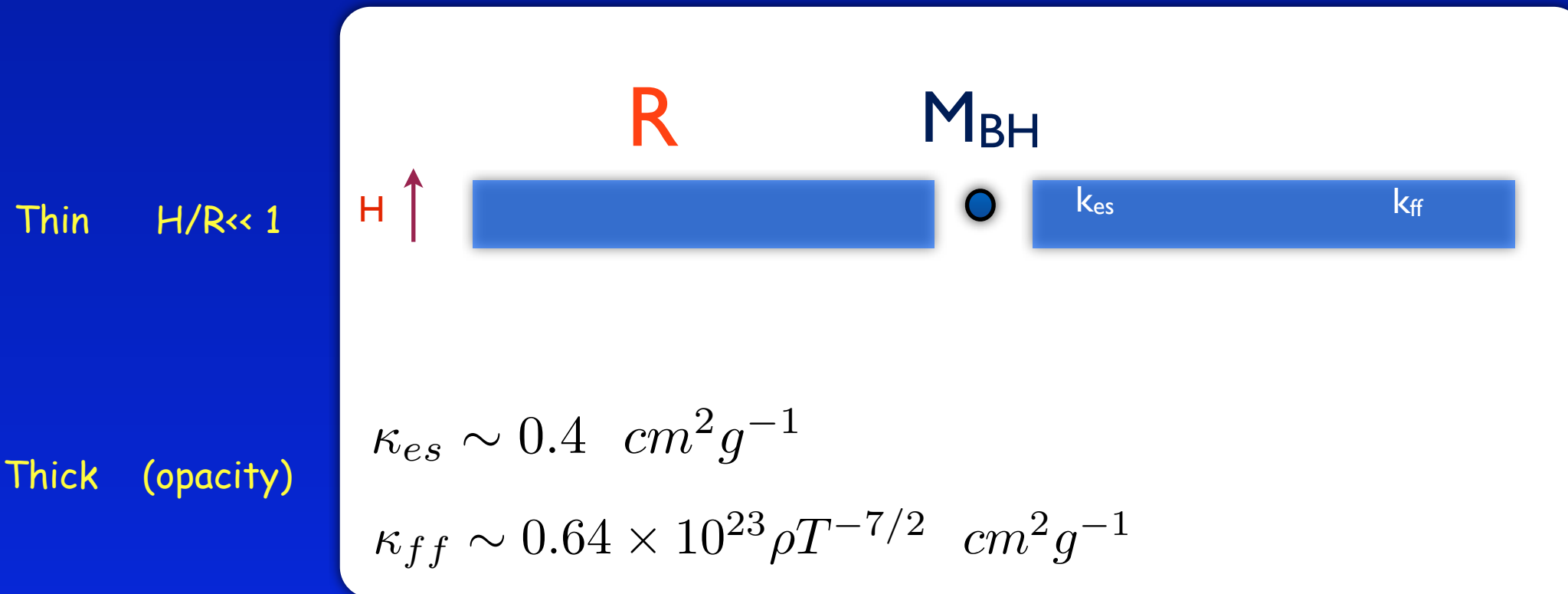
$$L_{adv} : 0.1 \dot{M} c^2$$

q^+ is the energy generated by viscosity per unit volume

q^- is the radiative cooling per unit volume

q^{adv} represents the advective transport of energy

Shakura & Sunyaev thin optically thick disk model (standard model)



The main contributor to the opacity of the matter come from Thompson scattering on free electrons and free free absorption

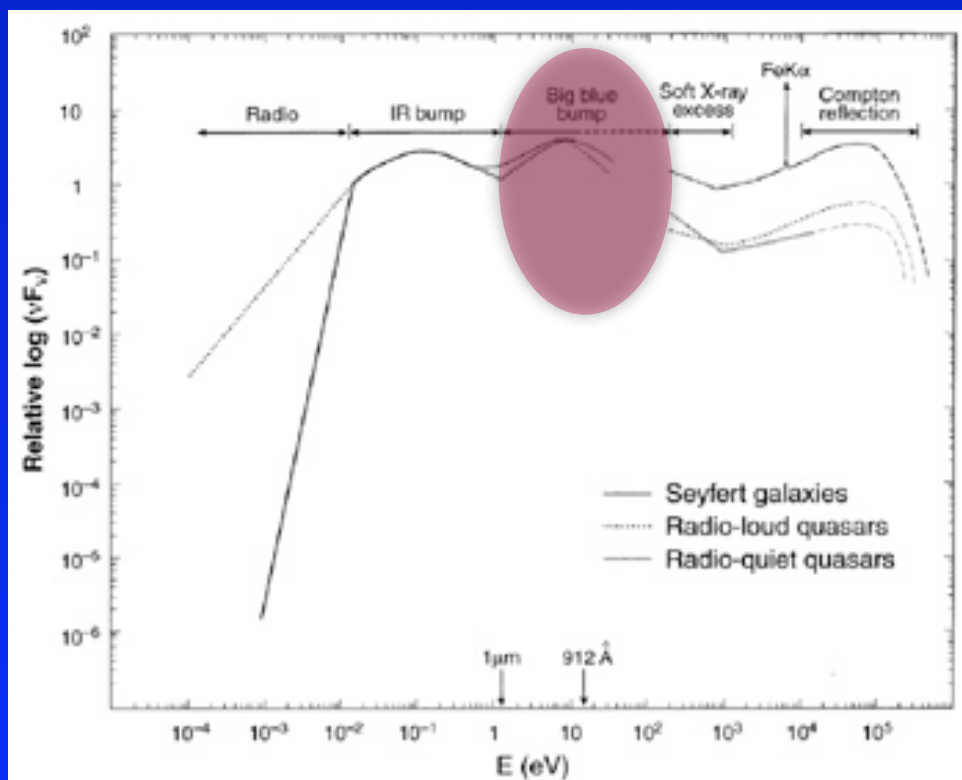
electron scattering is the main source of opacity in the inner hot part of the disk

free-free absorption dominates in the outermost colder part of the disk

If the the disk is optically thick, we can approximate the local emission as blackbody and the effective temperature of the photosphere

$$T(r) \sim 6.3 \times 10^5 \left(\frac{\dot{M}}{\dot{M}_E} \right)^{1/4} M_8^{-1/4} \left(\frac{r}{R_s} \right)^{-3/4} \text{ K}$$

For AGN with $M_{BH} = 10_8 = 10^8 M_\odot$ $\dot{M} \sim \dot{M}_E = \frac{L_E}{\eta c^2}$



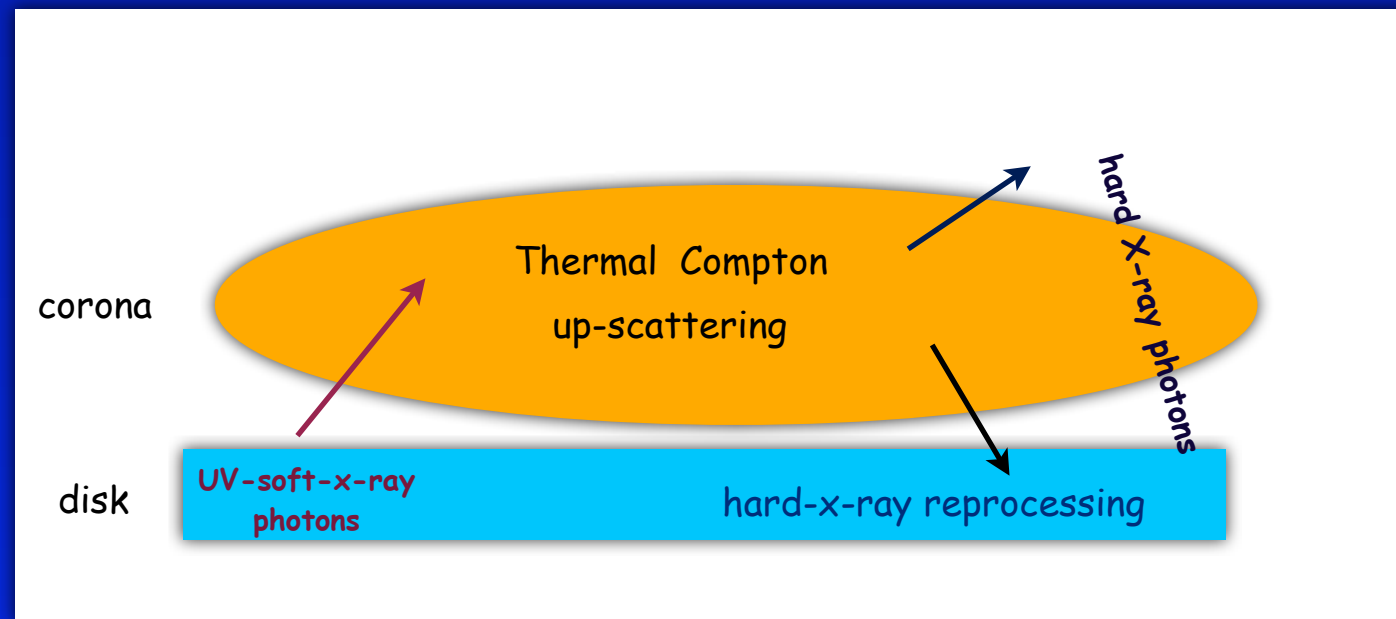
the peak occurs at UV-soft-X-ray region

$$\frac{\partial B}{\partial \nu} = 0 \quad B(\nu) \propto \nu^3 [e^{\frac{h\nu}{kT}} - 1]^{-1}$$

$$\nu_{max} = 2.8kT/h \sim 10^{16} \text{ Hz}$$

But the accretion flows are probably more complex...

SS Disk + Corona



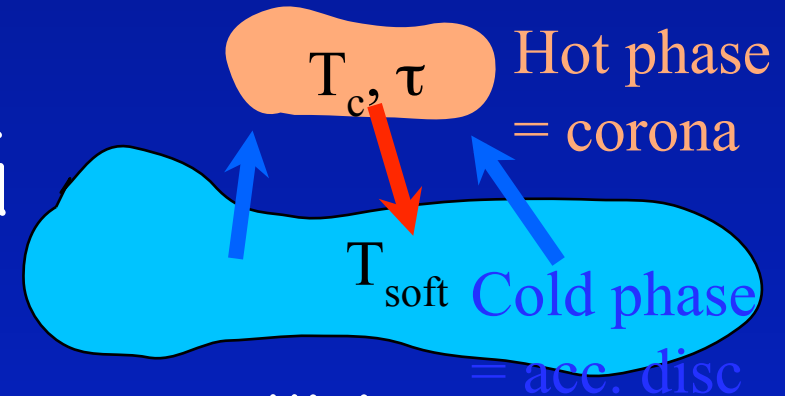
- Thermal Comptonization
- Hard X-ray-reprocessing
 - Iron Line
 - Compton hump

In the plane parallel limit only half of hard X-ray flux escapes from the source while the other half impinges on the cool disk.

The latter is in part (10-20%) reflected giving rise to the observed spectral hump in the 10-30 keV range; in small part it is reemitted as an Fe fluorescence line, but the largest part (80-90%) is absorbed, reprocessed and reemitted into black body photons which contribute to the soft photon input for Comptonization.

Thermal Comptonization

Comptonization on a thermal plasma of electrons characterized by a temp. T and optical depth τ



- ✓ mean relative energy gain per collision

$$\frac{\Delta E}{E} \simeq \left(\frac{4kT}{mc^2} \right) + 16 \left(\frac{kT}{mc^2} \right)^2 \quad \text{for } E \ll kT$$

$$\leq 0 \quad \text{for } E \gtrsim kT$$

- ✓ mean number of scatterings

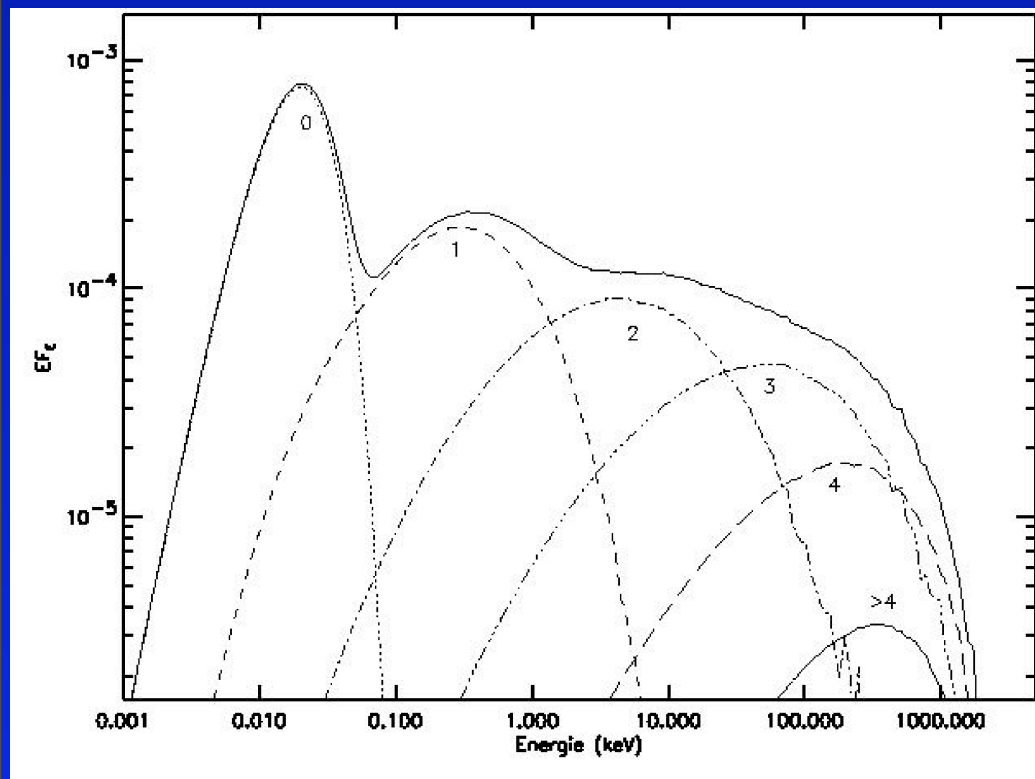
$$N \simeq (\tau + \tau^2)$$

➔ Compton parameter $y = \frac{\Delta E}{E} N$

$$E_f = E_i e^y$$

Thermal Comptonization Spectrum: the continuum

$$F_E \propto E^{-\Gamma(kT, \tau)} \exp\left(-\frac{E}{E_c(kT, \tau)}\right)$$



$$\Gamma(\tau, kT)$$

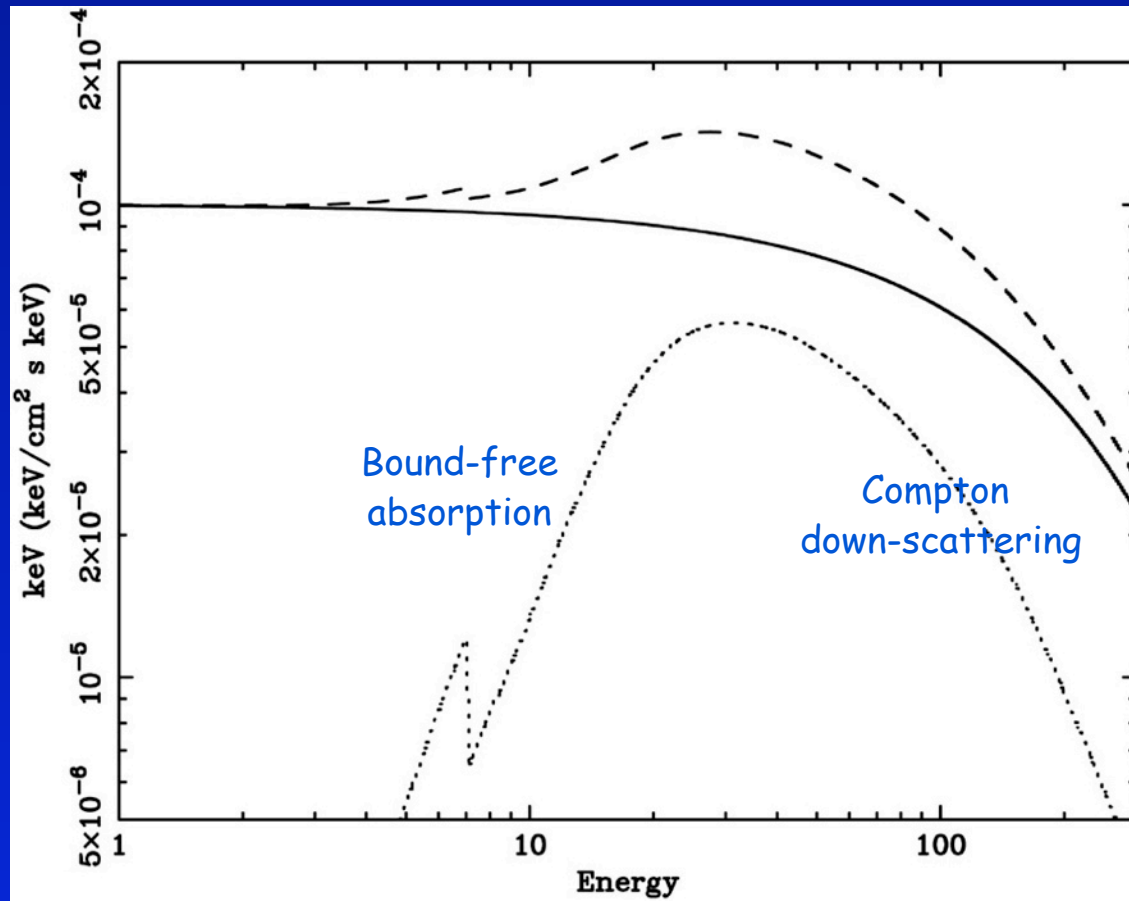
The exact relation between spectral index and optical depth depends on the geometry of the scattering region.

$$E_c \simeq kT$$

As photons approach the electron thermal energy, they no longer gain energy from scattering, and a sharp rollover is expected in the spectrum.

The observed high energy spectral cutoff yields information about the temperature of the underlying electron distribution.

Reflection



At low energies <10 keV the high Z ions absorb the X-rays. A major part of the opacity above 7 keV is due to Fe k-edge opacity.

At high energies the Compton shift of the incident photons becomes important

$$\Delta\nu/\nu \sim -h\nu/m_e c^2$$

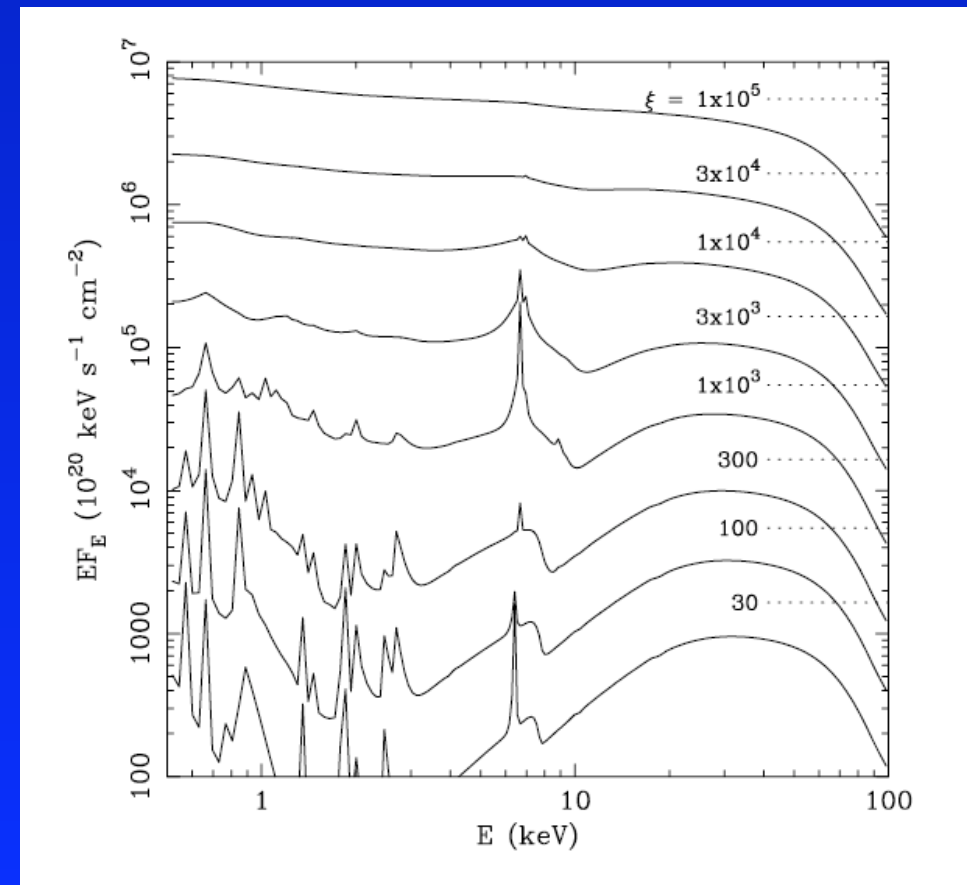
The shape of the Compton reflection depends on the ionization state of the slab.

For very high values of the ionization parameter

$$\xi \propto F_x/n$$

the slab becomes a perfect mirror.

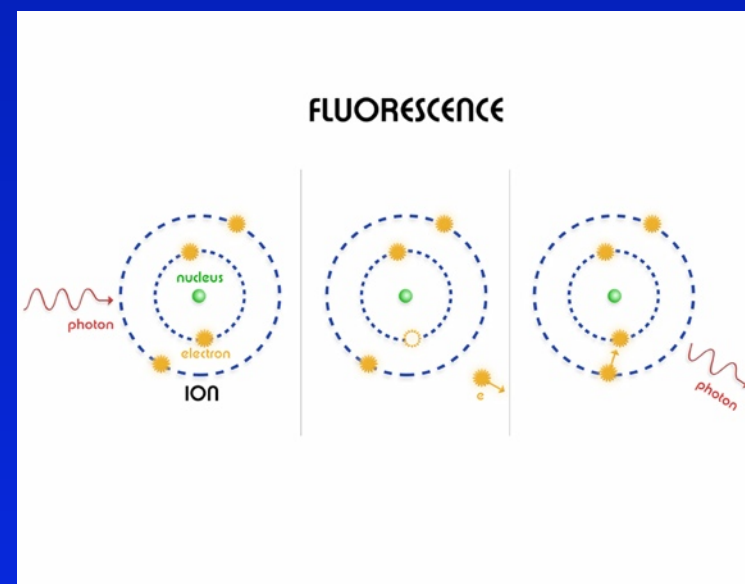
F_x is the incident X-ray flux
 n is the density of the disk



Iron Line

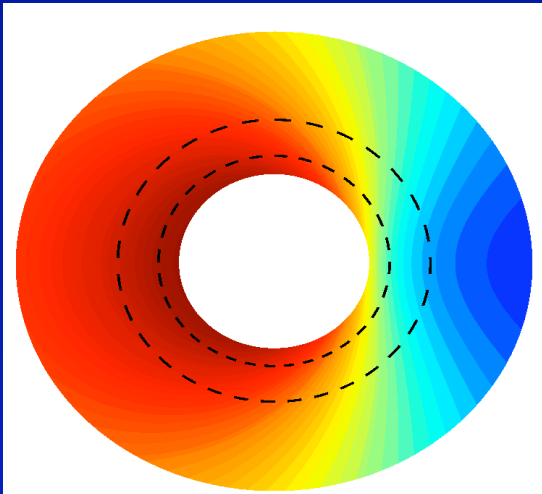
The fluorescent iron line is produced when one of the 2 K-shell ($n=1$) electrons of an iron atom (or ion) is ejected following photoelectric absorption of an X-ray.

Following the photoelectric event, the resulting excited state can decay in one of two ways. An L-shell ($n=2$) electron can then drop into the K-shell releasing 6.4~keV of energy either as an emission line photon (34 % probability) or an Auger electron (66 % probability).

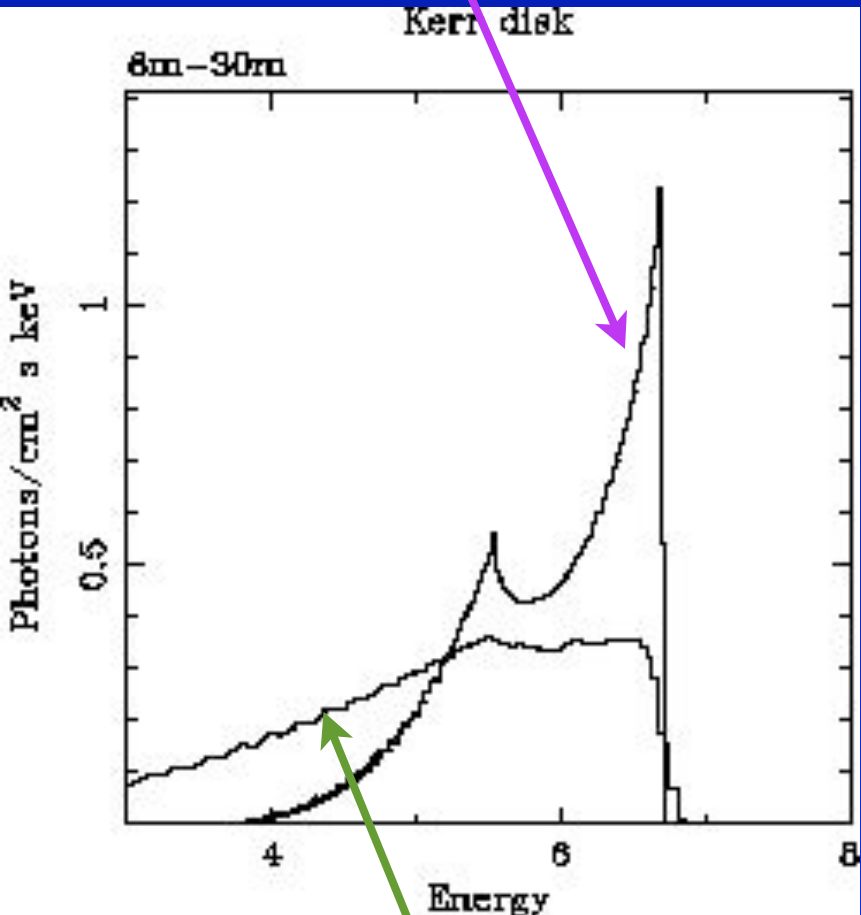


For ionized iron, the outer electrons are less effective at screening the inner K-shell from the nuclear charge and the energy of both the photoelectric threshold and the K line are increased

BROAD LINE

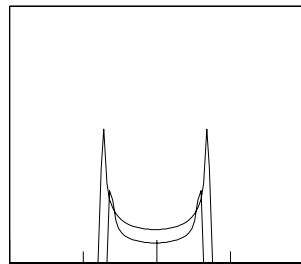


$R_{\text{INNER}} \sim 6 \text{ GM}/c^2$
Schwarzschild BH

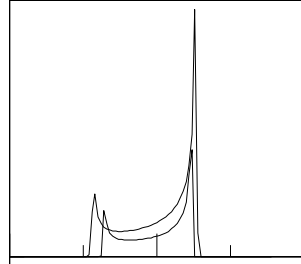


Kerr BH
 $R_{\text{INNER}} \sim 1.25 \text{ GM}/c^2$

Newtonian

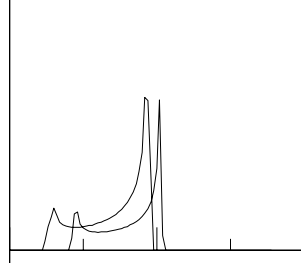


Special relativity



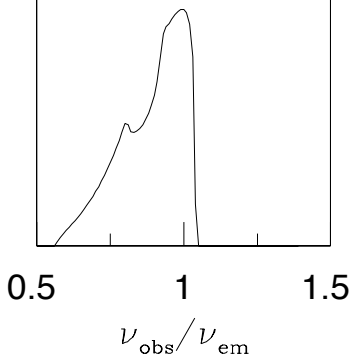
Transverse Doppler shift
Beaming

General relativity



Gravitational redshift

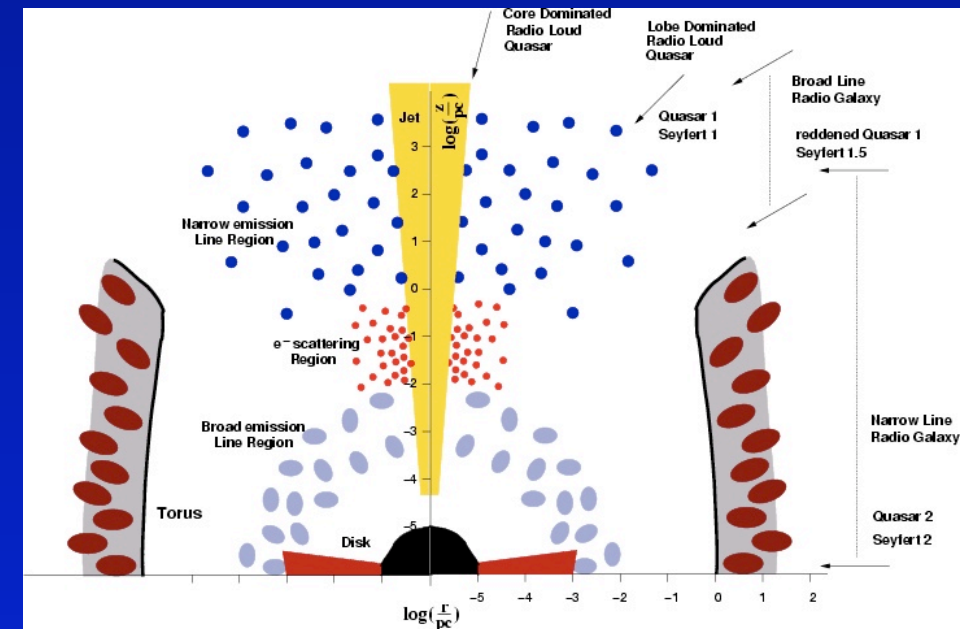
Line profile



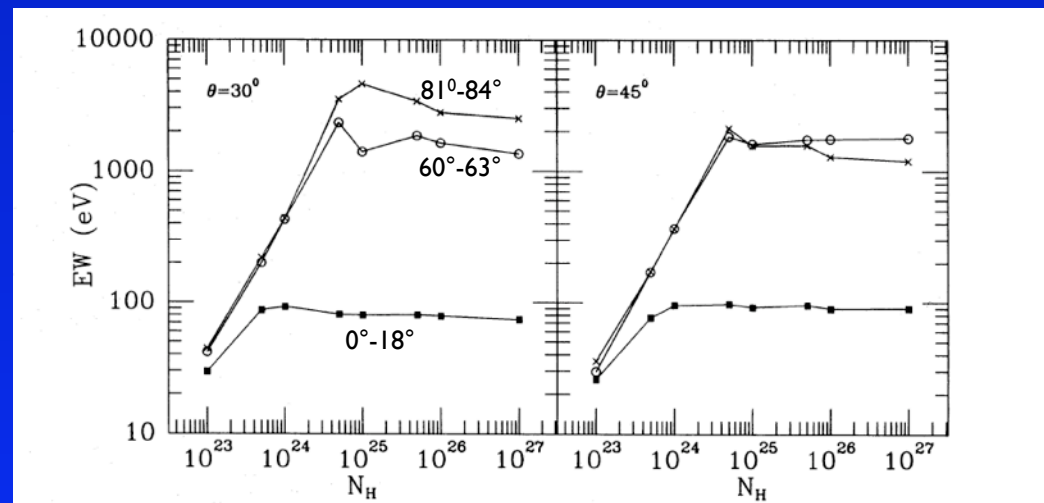
0.5 1 1.5
 $\nu_{\text{obs}}/\nu_{\text{em}}$

The iron line is probably a combination of two components

- Narrow component from torus/BLR
- Broad component from disk

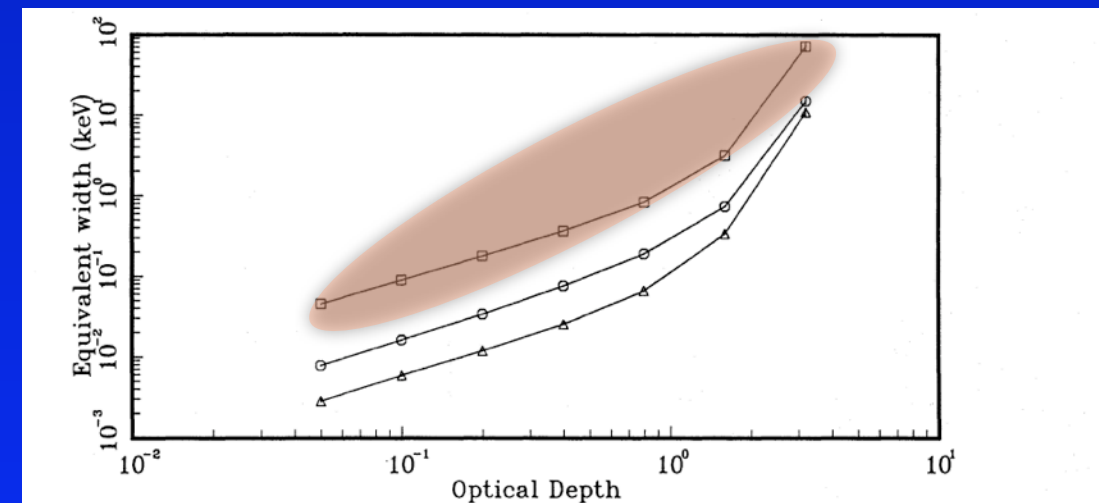


Toroidal distribution



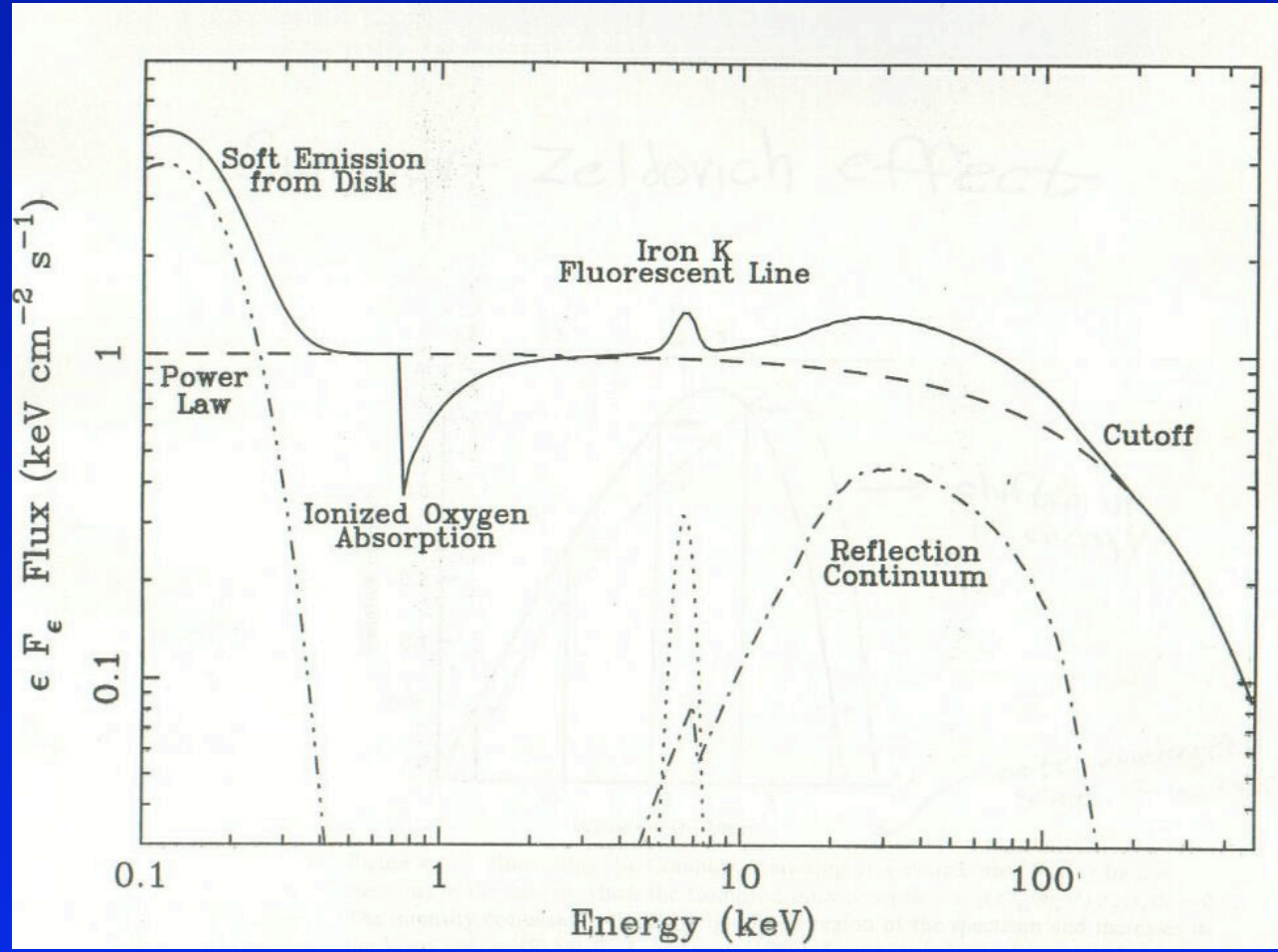
EW of the line produced by a torus for two values of the torus open angle

Spherical distribution



For a column density of the BLR clouds of the order of 10^{23} cm^{-2} , $\tau = \sigma_{FeK} \times N_H \sim 10^{-1}$

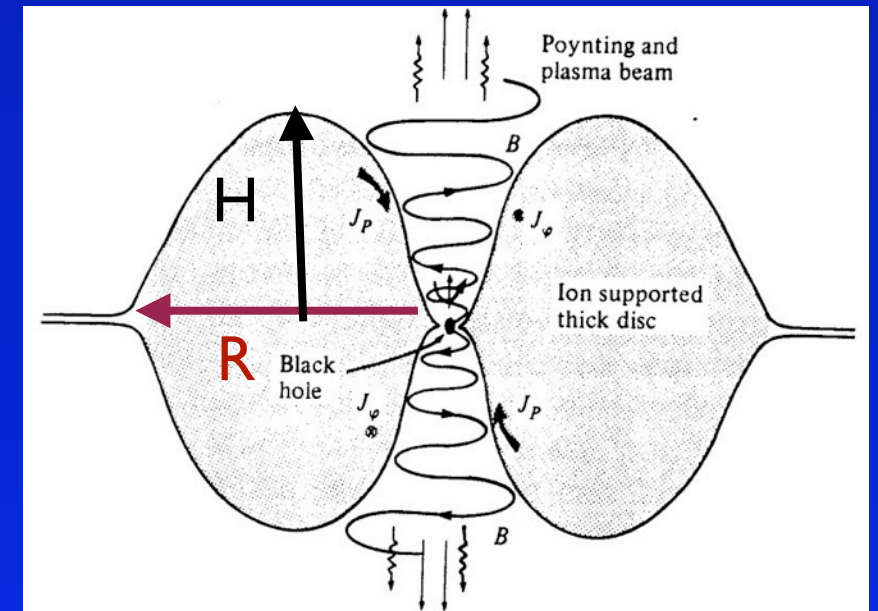
$$\sigma_{FeK}(E) = 1.2 \times 10^{-24} (E/7.1 \text{ keV})^{-3} \text{ cm}^2 / H$$



ADAF

In this solution the accreting gas has a very low density and is unable to cool efficiently. The viscous energy is stored in the gas as thermal energy instead of being radiated and is advected onto the BH. Ions and electrons are thermally decoupled.

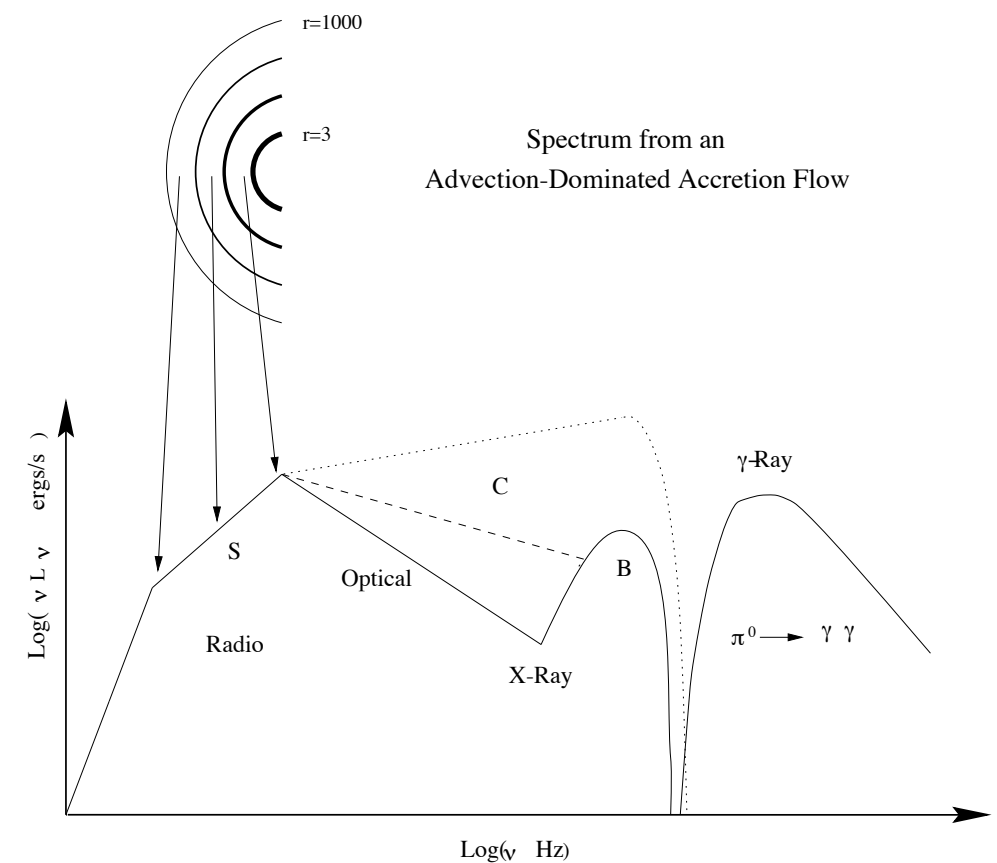
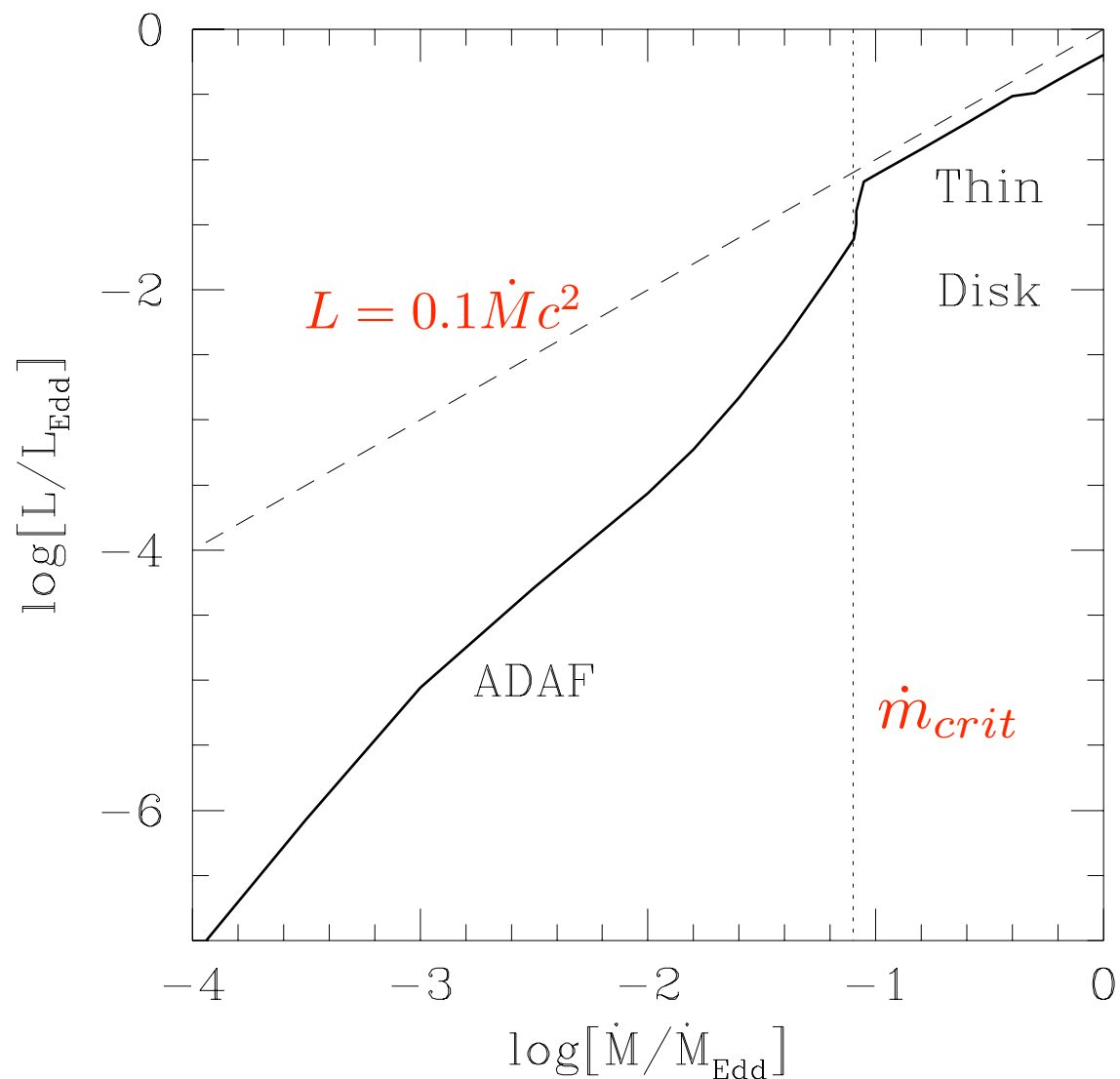
- Very Hot: $T_i \sim 10^{12} \text{K}$ (R_s/R), $T_e \sim 10^9\text{-}10^{11} \text{K}$ (since ADAF loses very little heat).
- Geometrically thick: $H \sim R$ (most of the viscosity generated energy is stored in the gas as internal energy rather than being radiated, the gas puffs up)
- Optically thin (because of low density)



The ADAF solution exists only for $\frac{\dot{M}}{\dot{M}_E}$ less than a critical value $\dot{m}_{crit} \sim \alpha^2$

$$\frac{\dot{M}}{\dot{M}_E} \leq 0.05 - 0.1$$

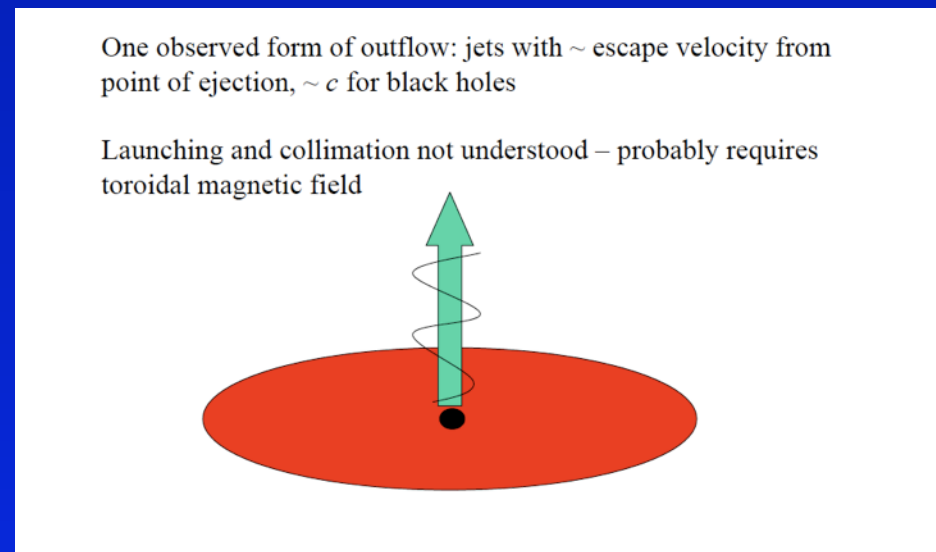
α viscosity parameter



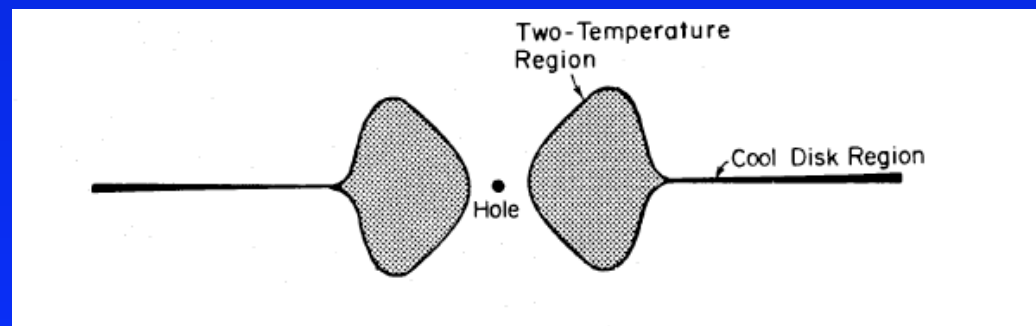
But the accretion flows are probably more complex...

ADAF \Rightarrow ADIOS

In ADVECTION-DOMINATED INFLOW-OUTFLOW SOLUTIONS (ADIOS) only a small fraction of the gas supplied actually falls on to the black hole, and that the binding energy it releases is transported radially outward by the torque so as to drive away the remainder in the form of a wind/jet.



ADAF + Truncated disk

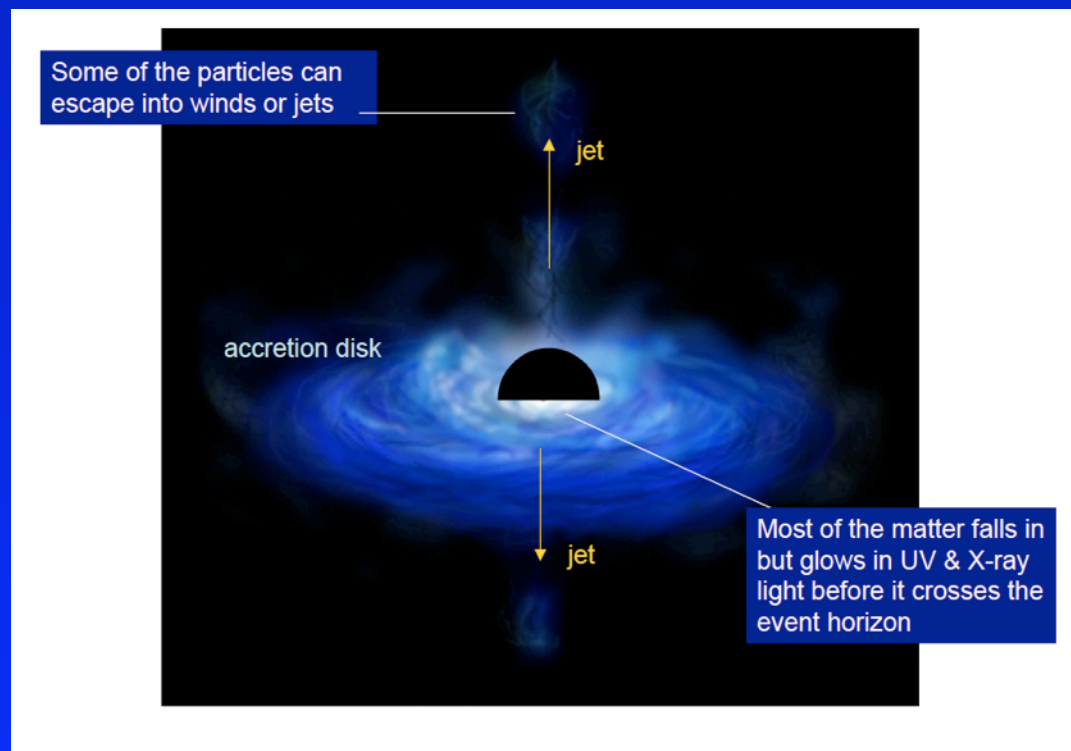


3. Jet



Extragalactic Jet

Jets are giant plasma outflows through which the BH transfers huge amount of energy, momentum and angular momentum very large distance to the ambient.



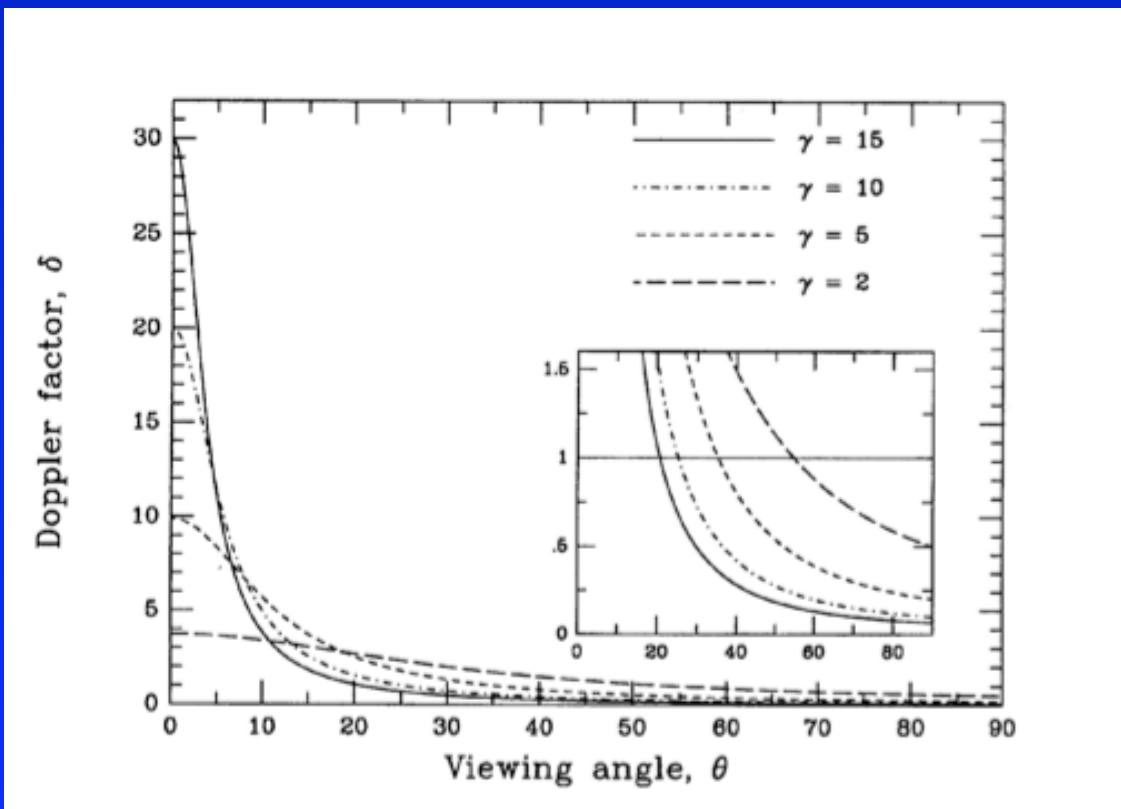
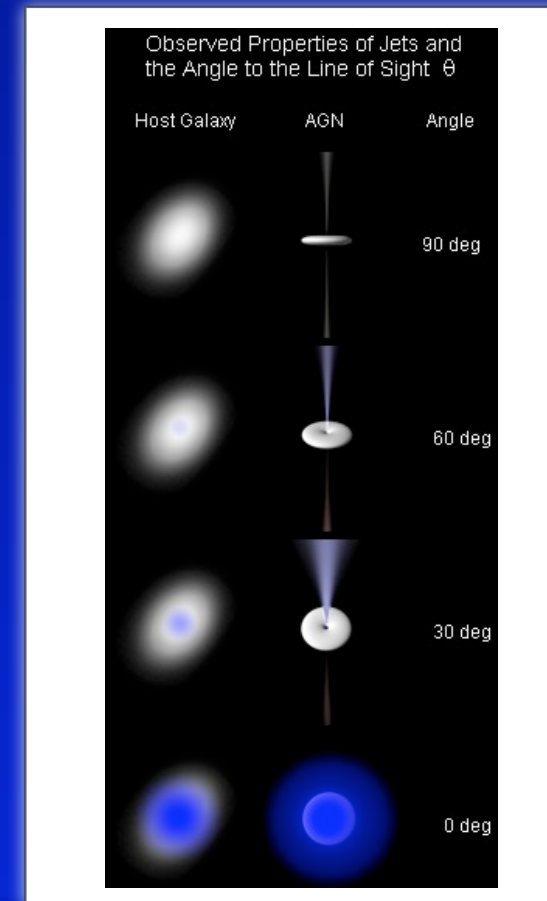
Beethoven's 5th Symphony



Doppler Factor $\delta(\beta, \theta)$
is a key parameter for the jet study

$$\delta = [\gamma(1 - \beta \cos\theta)]^{-1}$$

$\beta = v/c$ is the bulk velocity
 $\gamma = (1 - \beta^2)^{-1/2}$ is the Lorentz factor
 θ is the angle between the jet axis and the line of sight



The Doppler factor relates intrinsic and observed flux for a moving source at relativistic speed $v = \beta c$.

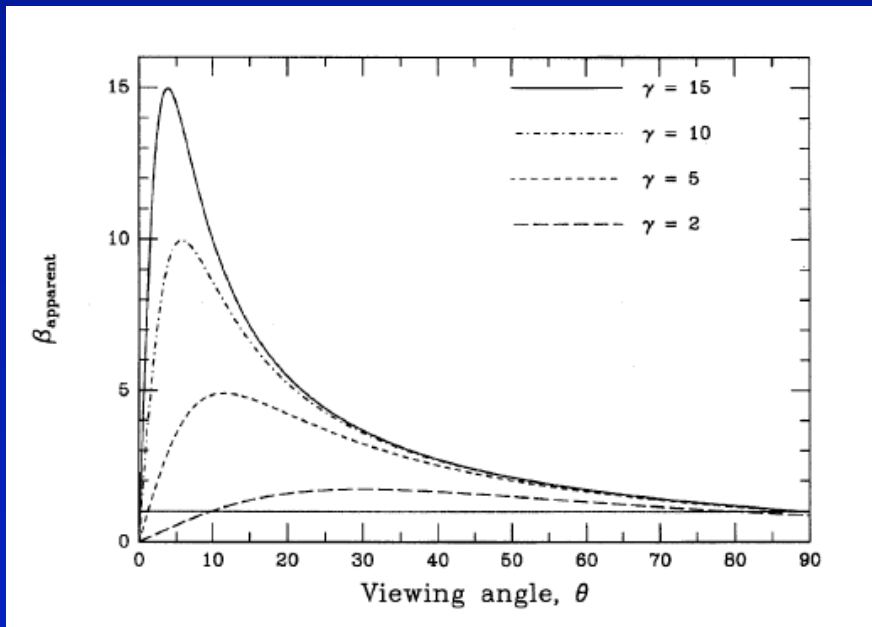
For an **intrinsic** power law spectrum:

$$F'(\nu') = K (\nu')^{-\alpha}$$

the **observed** flux density is

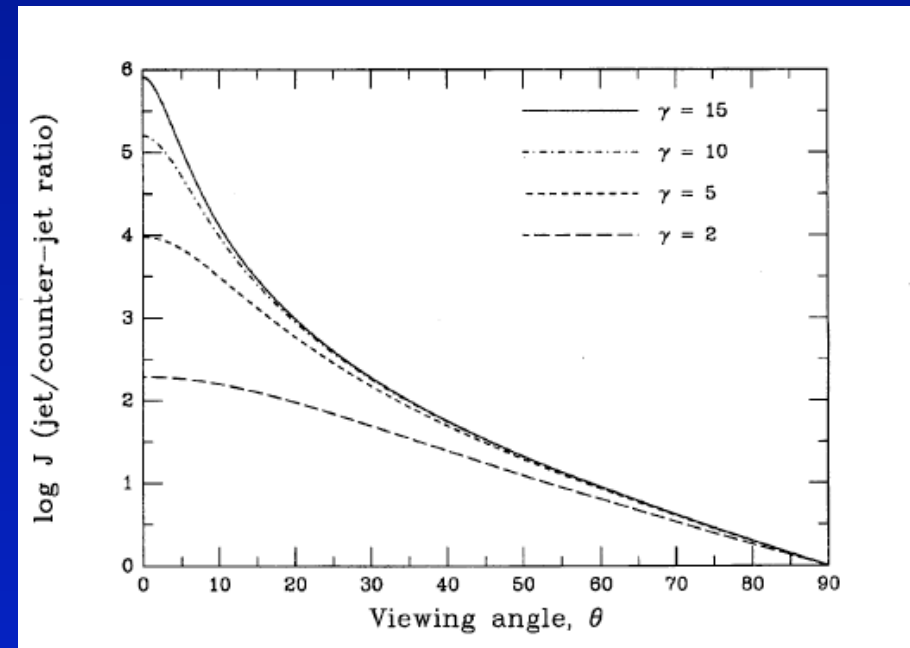
$$F_{\nu}(\nu) = \delta^{3+\alpha} F'_{\nu'}(\nu)$$

APPARENT VELOCITY

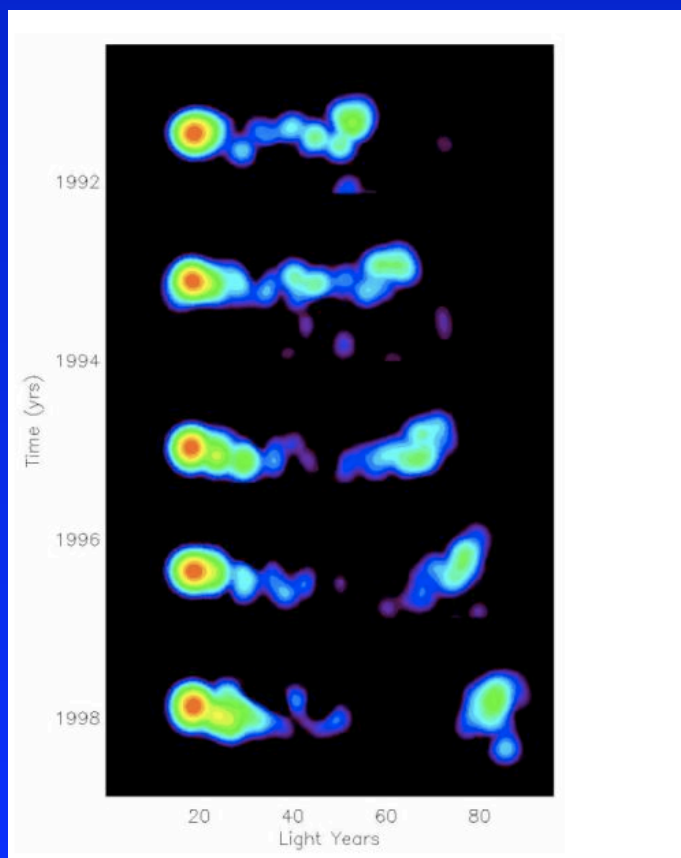


$$\beta_a = \frac{\beta \sin \theta}{1 - \beta \cos \theta}$$

Jet-Counter Jet



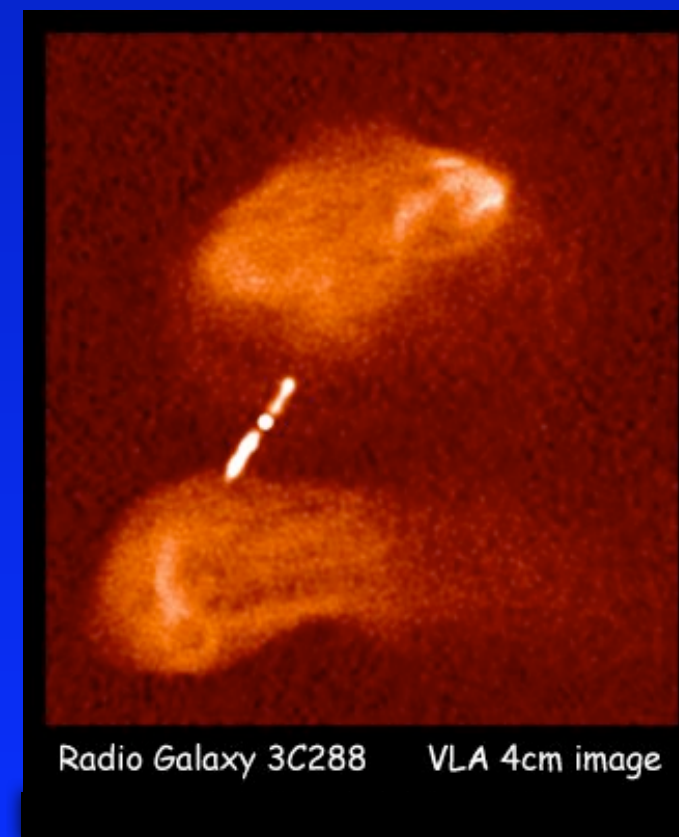
$$J = \left(\frac{1 + \beta \cos \theta}{1 - \beta \cos \theta} \right)^{2 + \alpha}$$



VLBI 22GHz image of
3C279

The bright spot at the right appears to have moved 25 light years in seven years

$$\beta_a \sim 3.6$$

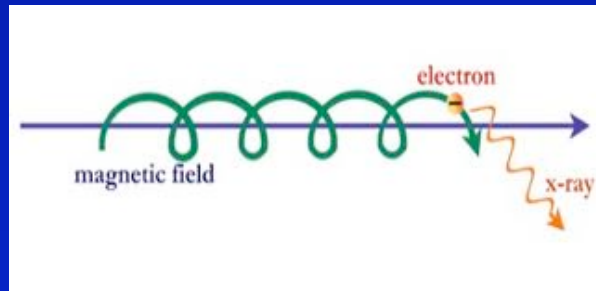


Radio Galaxy 3C288 VLA 4cm image

Jet Physical Processes

Synchrotron

Radiation from relativistic electrons spiraling in a magnetic field

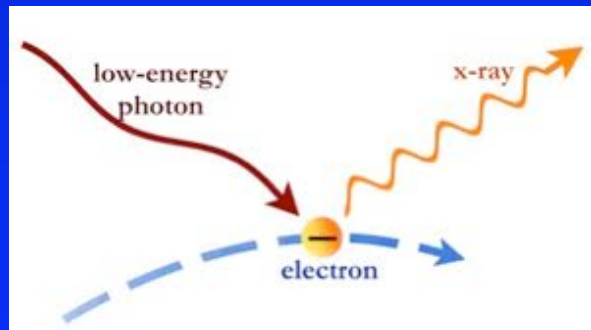


$$N(\gamma_e) = K\gamma_e^{-p}, \quad \gamma_{min} < \gamma_e < \gamma_{max}, \quad p = 1 + 2\alpha$$

$$\epsilon_{sin}(\nu) \propto KB^{\alpha+1}\nu^{-\alpha} \quad \text{erg cm}^{-3} \text{ s}^{-1} \text{ sr}^{-1}$$

Inverse Compton

When the electron is not at rest, but has an energy greater than the typical photon energy, there can be a transfer of energy from the electron to the photon. This process is called inverse Compton to distinguish it from the direct Compton scattering, in which the electron is at rest, and it is the photon to give part of its energy to the electron



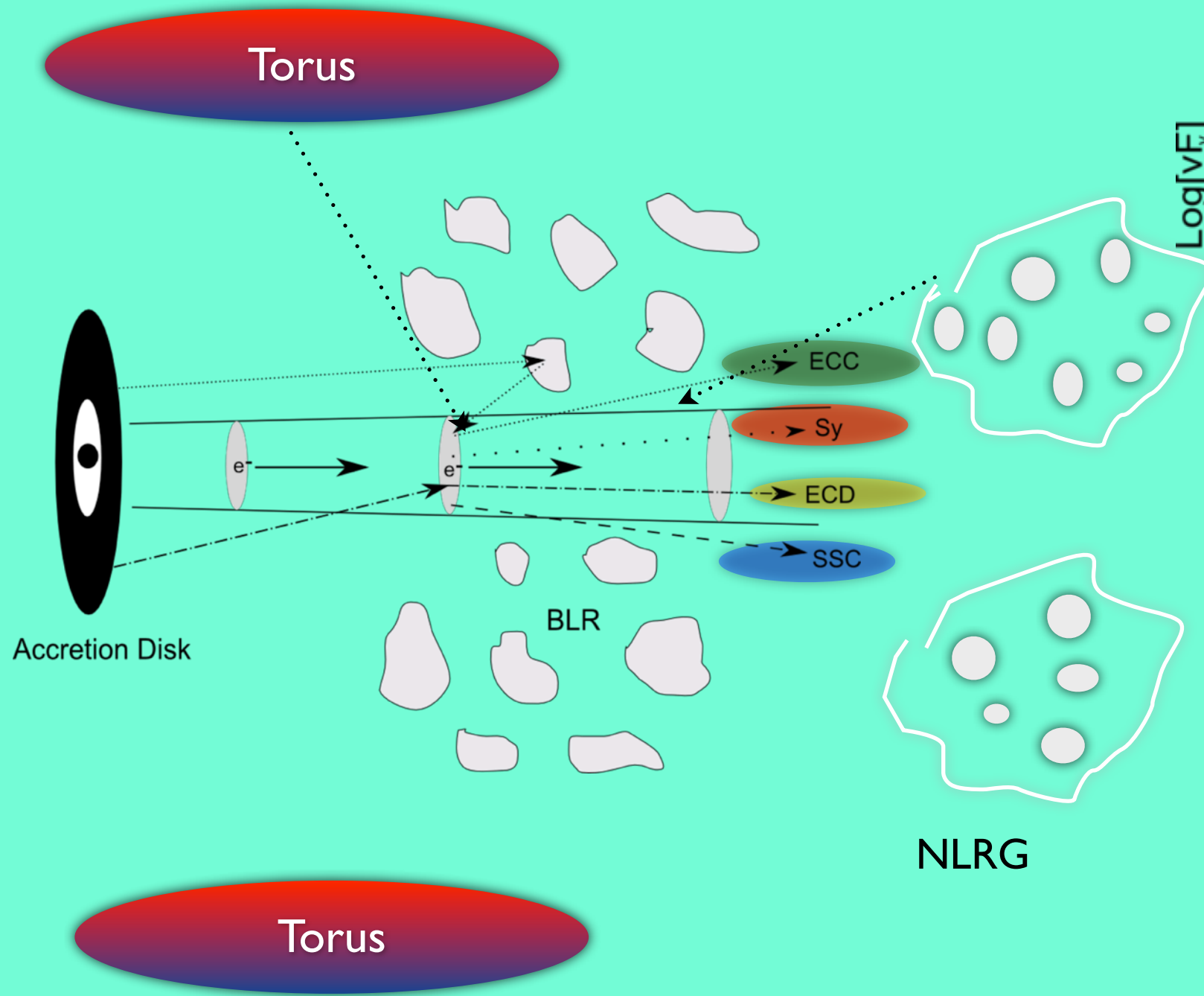
$\nu_c/\nu_0 \sim \gamma^2$ is the average gain in energy of the scattered photons.

$$\epsilon_c(\nu_c) \propto K\nu_c^{-\alpha} \int \frac{U_r(\nu)\nu^\alpha}{\nu} d\nu \quad \text{erg cm}^{-3} \text{ s}^{-1} \text{ sr}^{-1}$$

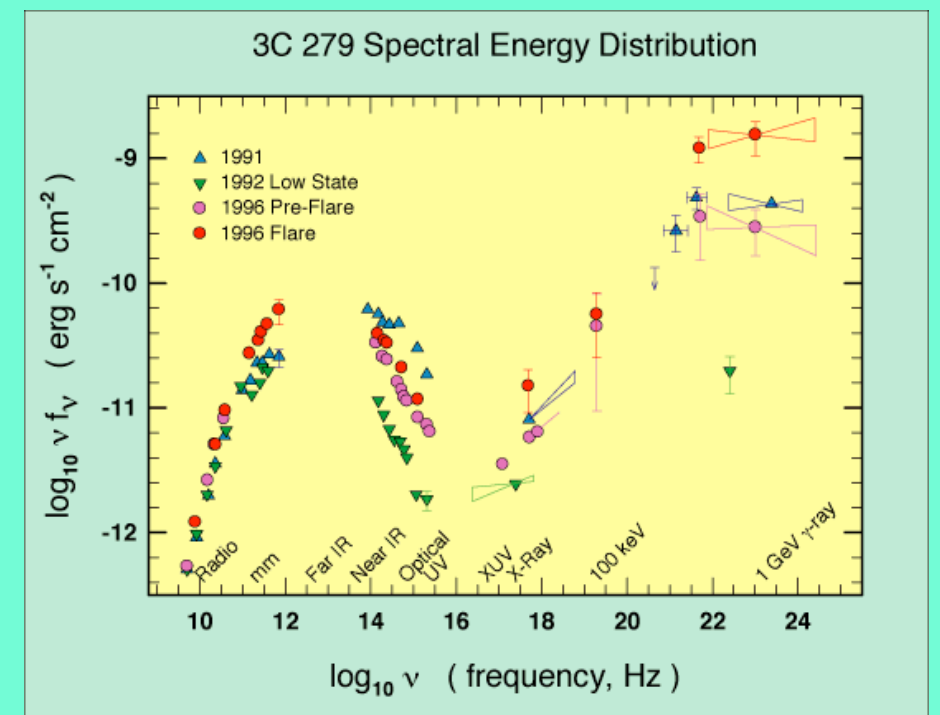
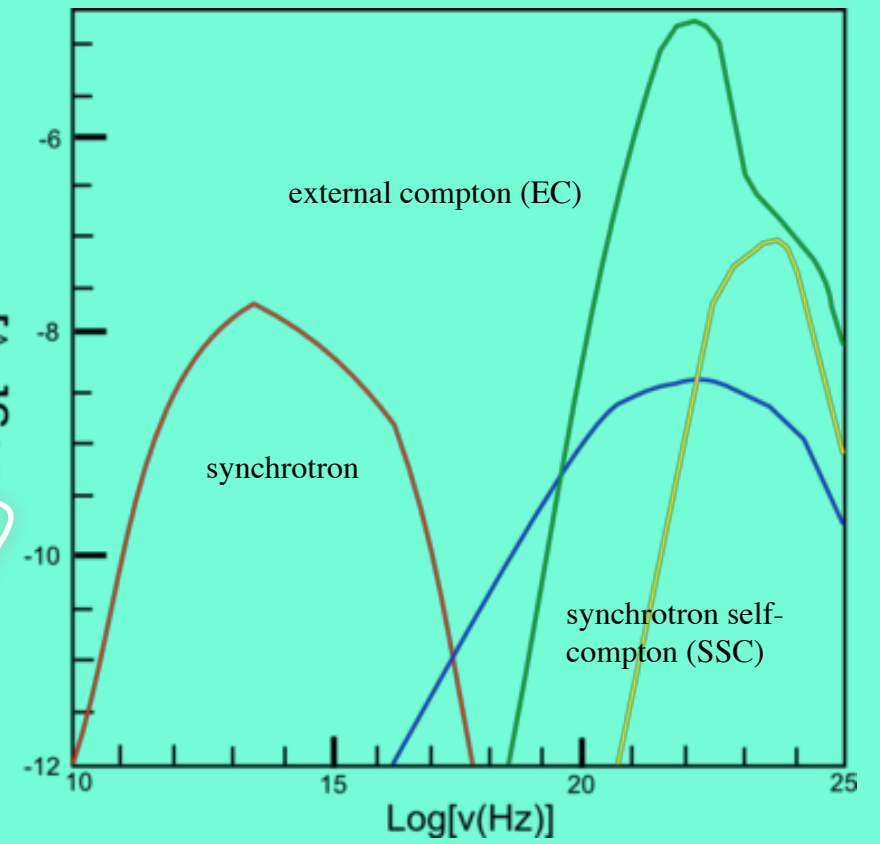
U_r is the radiation energy density

Jet Physical Processes

see Ghisellini's lesson



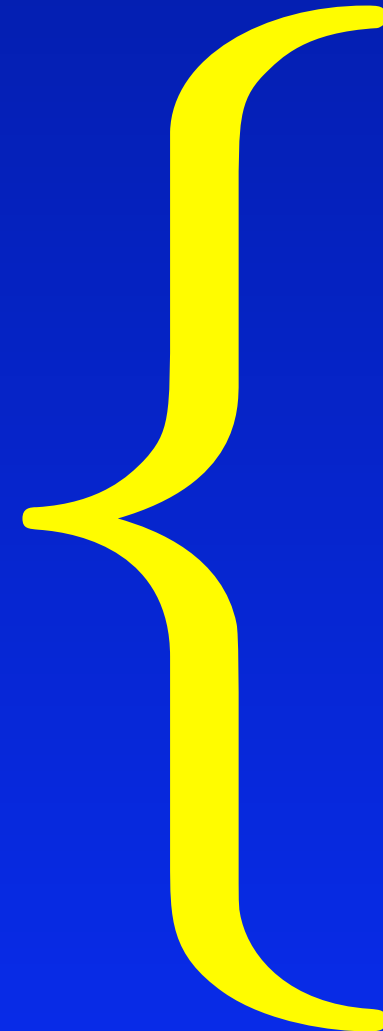
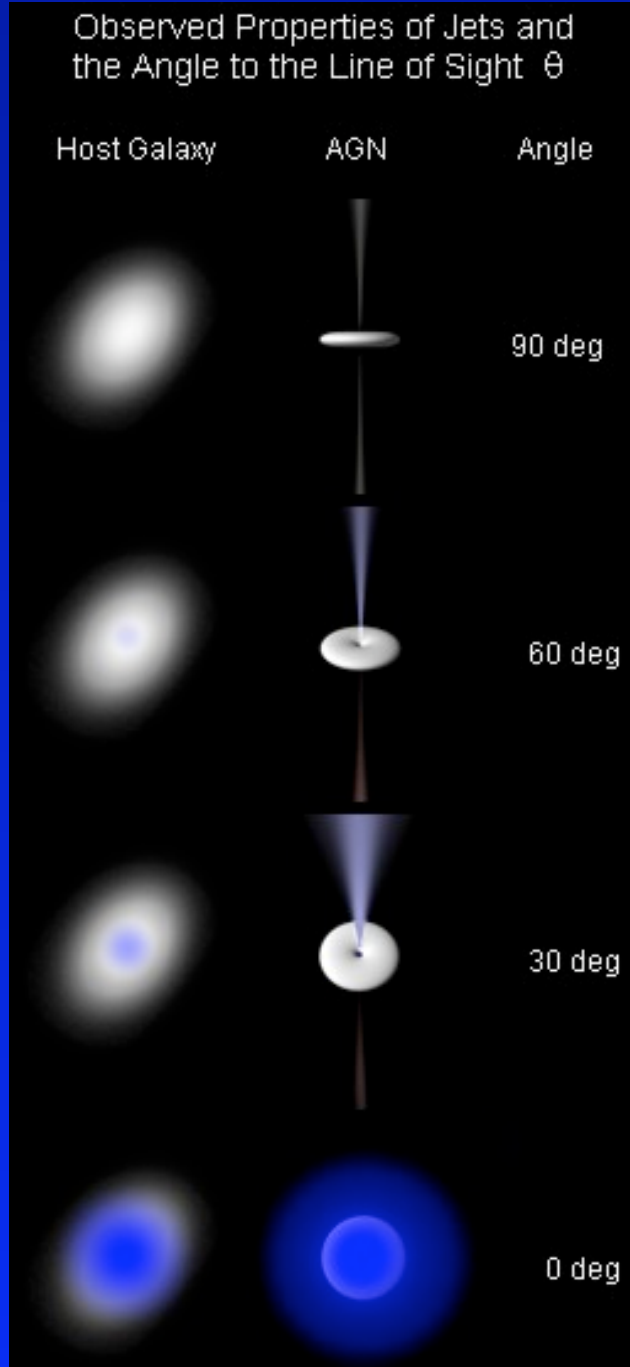
+ a contribution from NLRG and torus



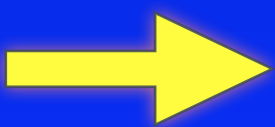
4. Accretion in MAGNs: observations, studies and debates



Misaligned AGN versus Blazar



Misaligned AGNs

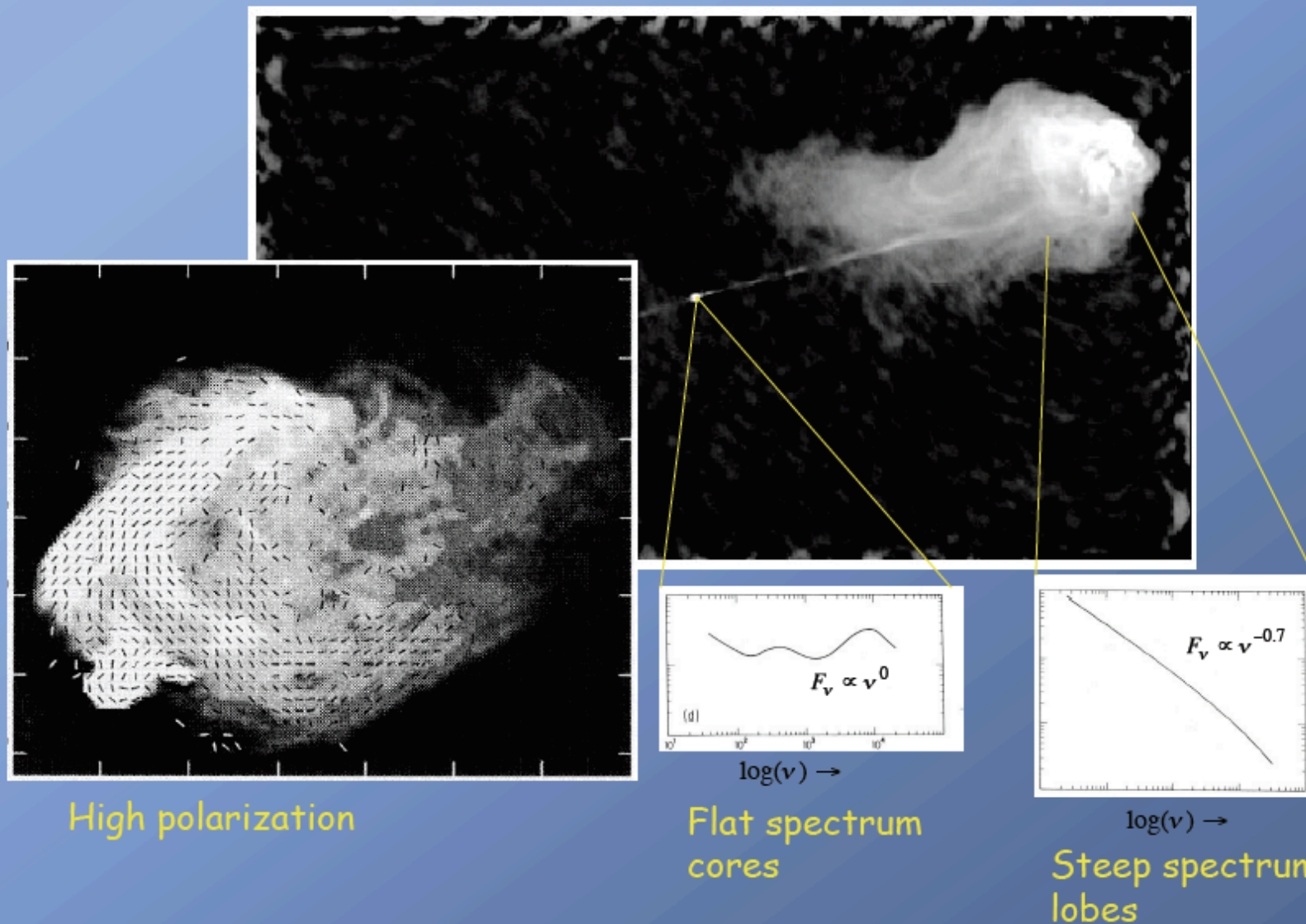


Blazars:
BL Lacs, FSRQs

WHAT WE INTEND FOR MISALIGNED AGNs: A PRAGMATIC APPROACH

Misaligned sources (RG, SSRQ) are AGNs showing
steep radio spectra ($\alpha_r > 0.5$) or/and

Radio properties



High polarization

Flat spectrum
cores

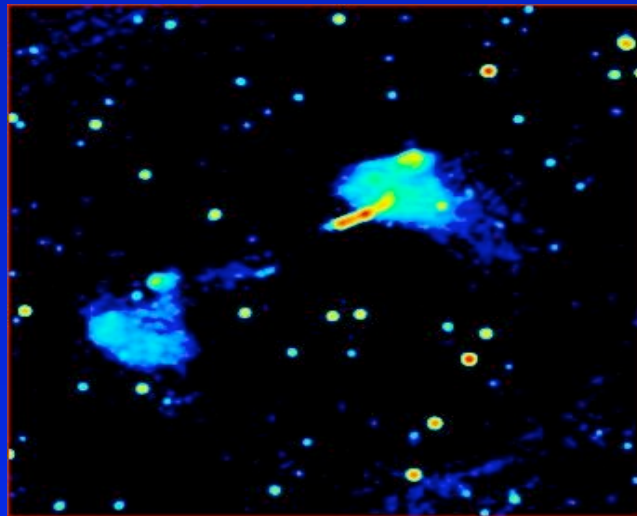
Steep spectrum
lobes

resolved and possibly symmetrical structures in radio maps

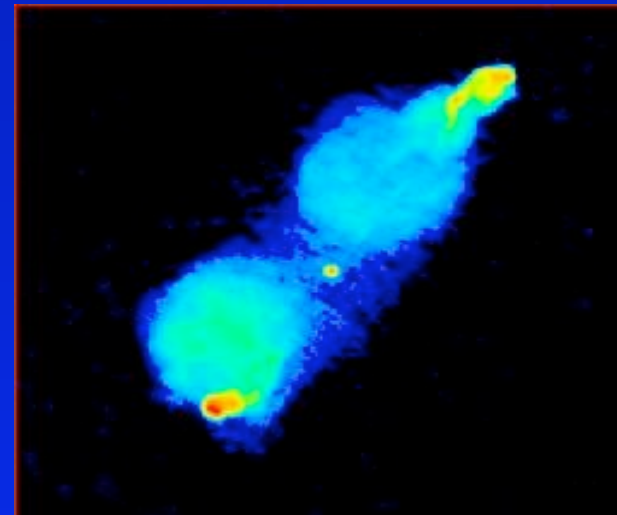
FR I The separation between the points of peak intensity in the two lobes is smaller than half the largest size of the source. ($R < 0.5$). $P_{178 \text{ MHz}} < 10^{25} \text{ Watt Hz}^{-1} \text{ sr}^{-1}$

FR II: The separation between the points of peak intensity in the two lobes is greater than half the largest size of the source ($R > 0.5$). $P_{178 \text{ MHz}} > 10^{25} \text{ Watt Hz}^{-1} \text{ sr}^{-1}$

NGC6251 - FRI

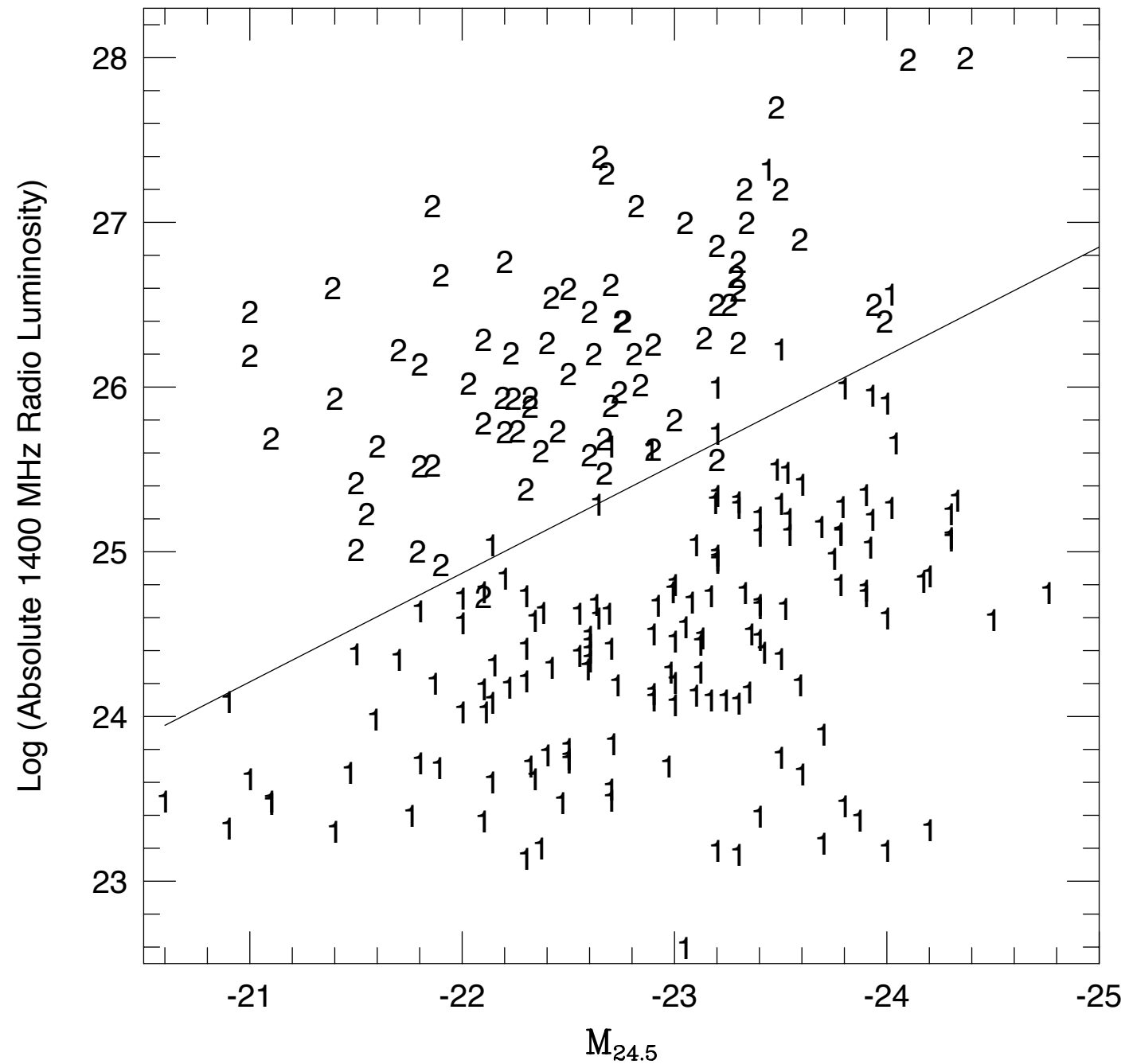


3C 390.3 - FR II



FRI are considered the PARENT POPULATION of BL LACs

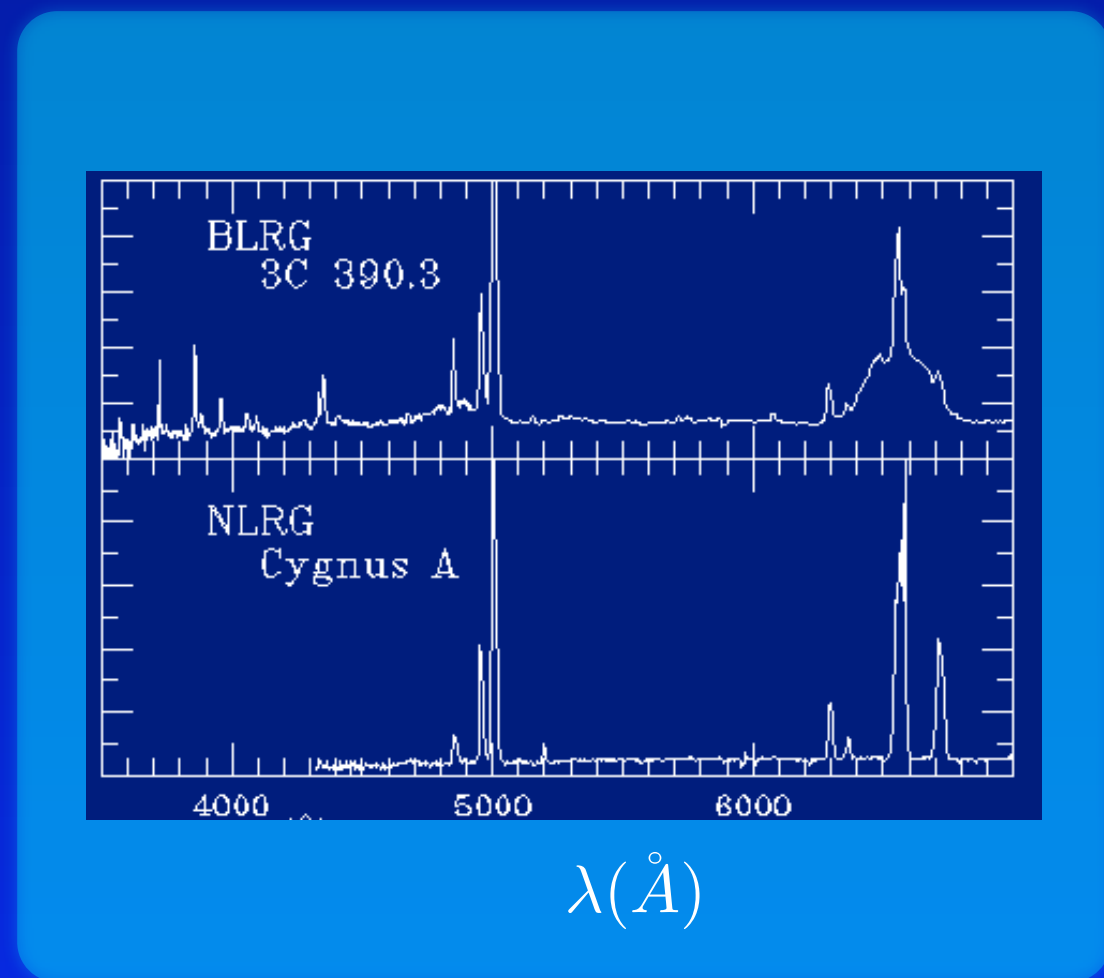
FR II are considered the PARENT POPULATION of FSRQs (SSRQs are in between)



Very optical bright FRIs are also seen at high radio powers.

Optical classifications:

<p>BLRG</p> <p>Quasars</p>	<p>bright continuum and broad emission lines from hot high velocity gas</p>	<p>FRII</p>
<p>NLRG/HEG</p>	<p>weak continuum and only narrow emission lines</p>	<p>FRII</p>
<p>NLRG/LEG</p>	<p>narrow emission lines: $EW_{[OIII]} < 10 \text{ \AA}$ and /or $O[II]/[OIII] > 1$</p>	<p>FRII FRI</p>



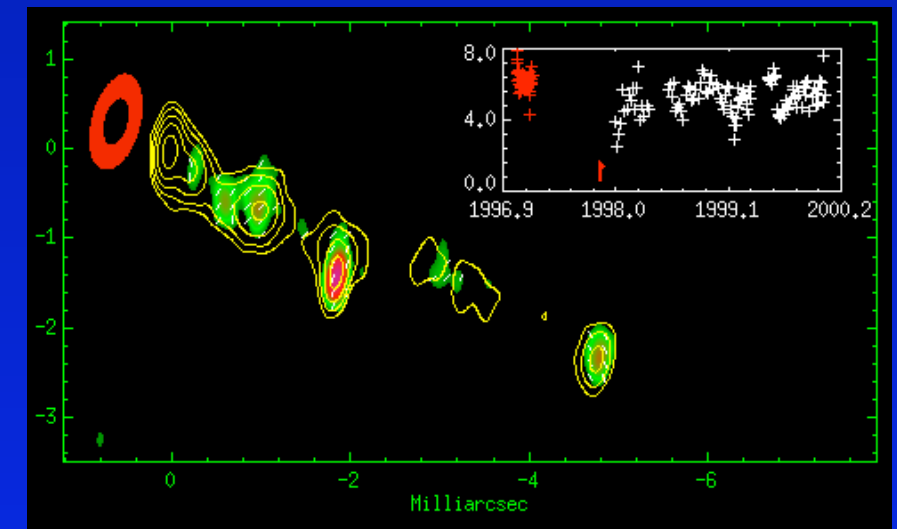
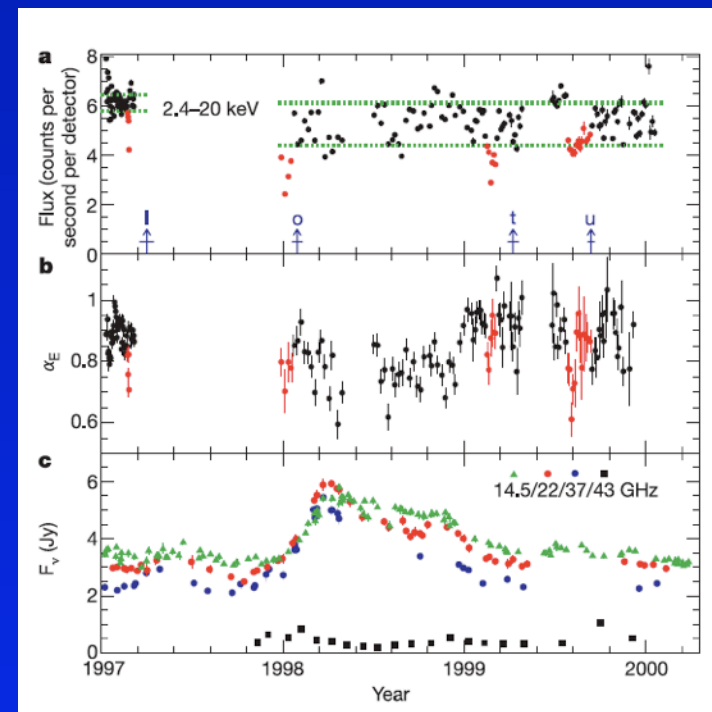
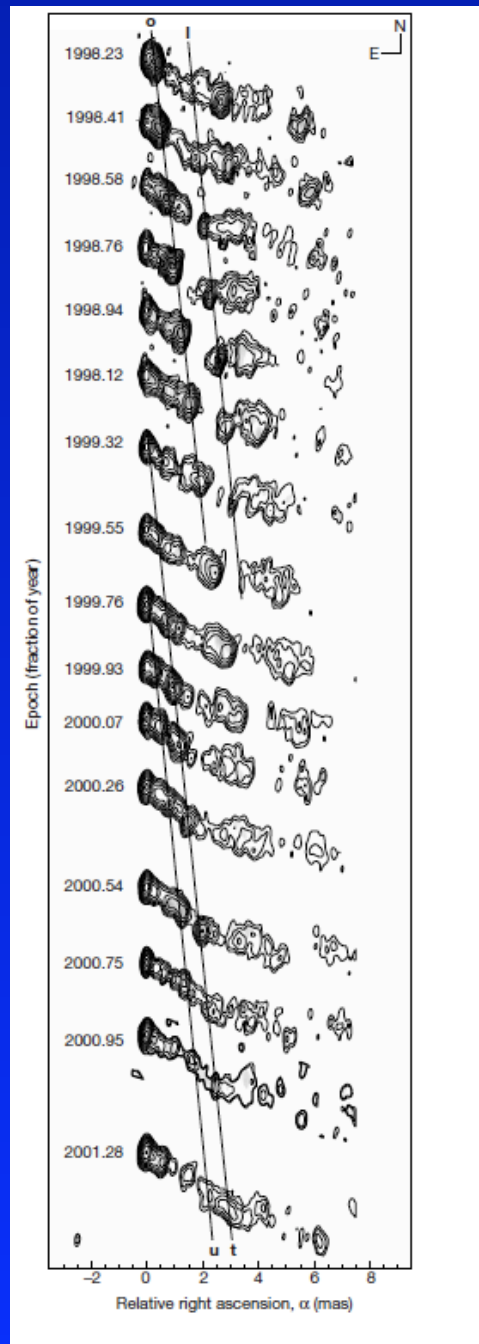
What kind of accretion occurs in AGN with strong jets?

Why is this question important?

Growing evidences indicate that accretion and ejected flows are closely related in all AGNs (non only in powerful radio sources) implying common physical mechanisms. Thus the fundamental question to address is how these mechanisms work under different physical conditions. In particular, the relation between the launch/quench of the jet and the disk accretion regime, is of primary importance.

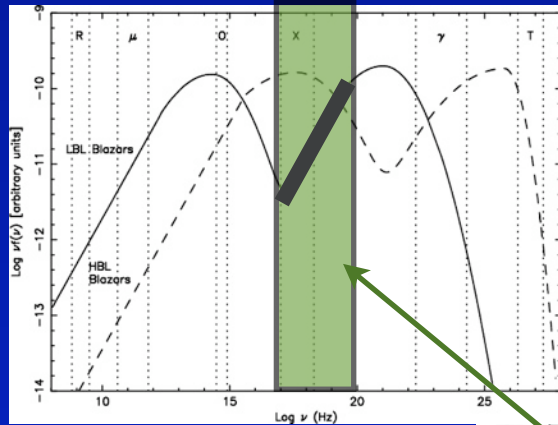
The first observational evidence of an Accretion-Jet link: 3C120

Roughly every ten months, the X-ray-emitting SS accretion disk around of 3C 120 becomes suddenly dim, and a month later the telltale bright spot of radio emission appears in the jet.



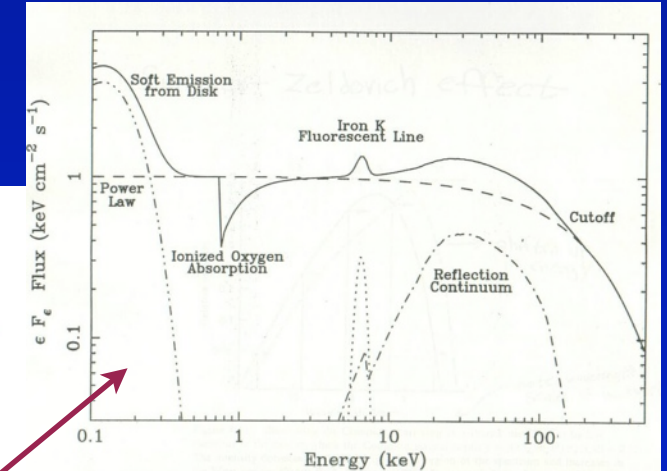
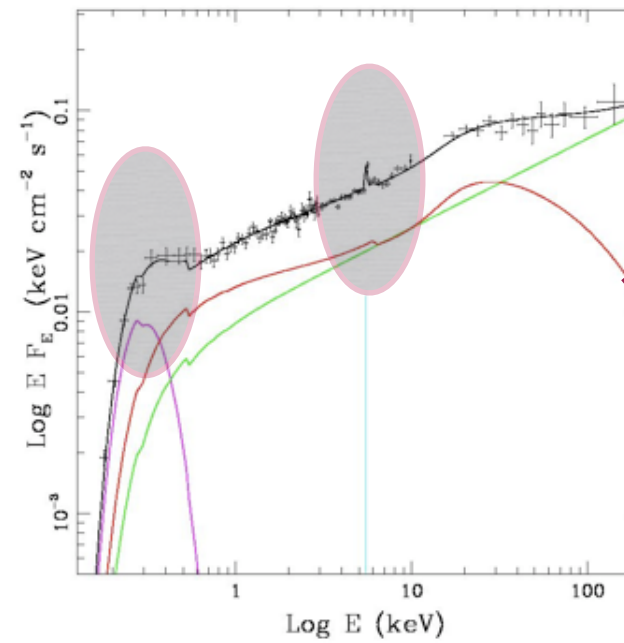
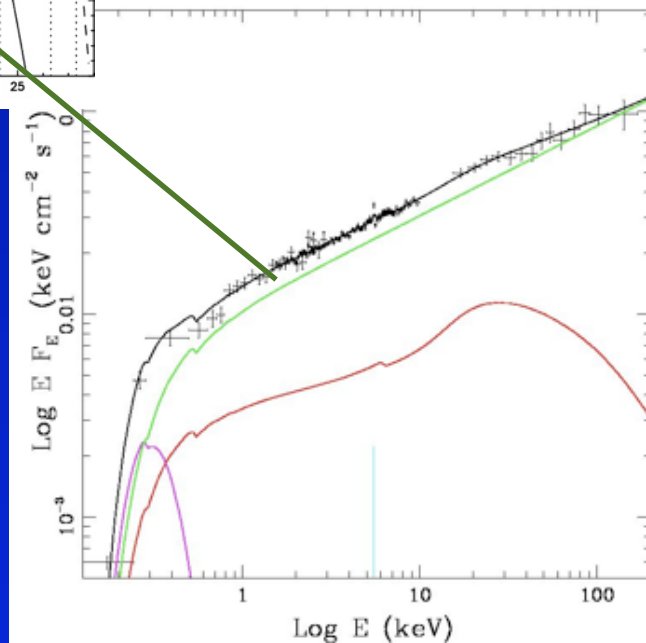
The X-ray dip is probably caused by the disappearance of a section of the inner accretion disk as it falls past the event horizon, while the remainder of the disk section is ejected into the jet, creating the appearance of a superluminal bright spot

In RL AGNs the accretion can be efficient. 3C273



Jet
simple power law
in the X-ray band

Seyfert-like features



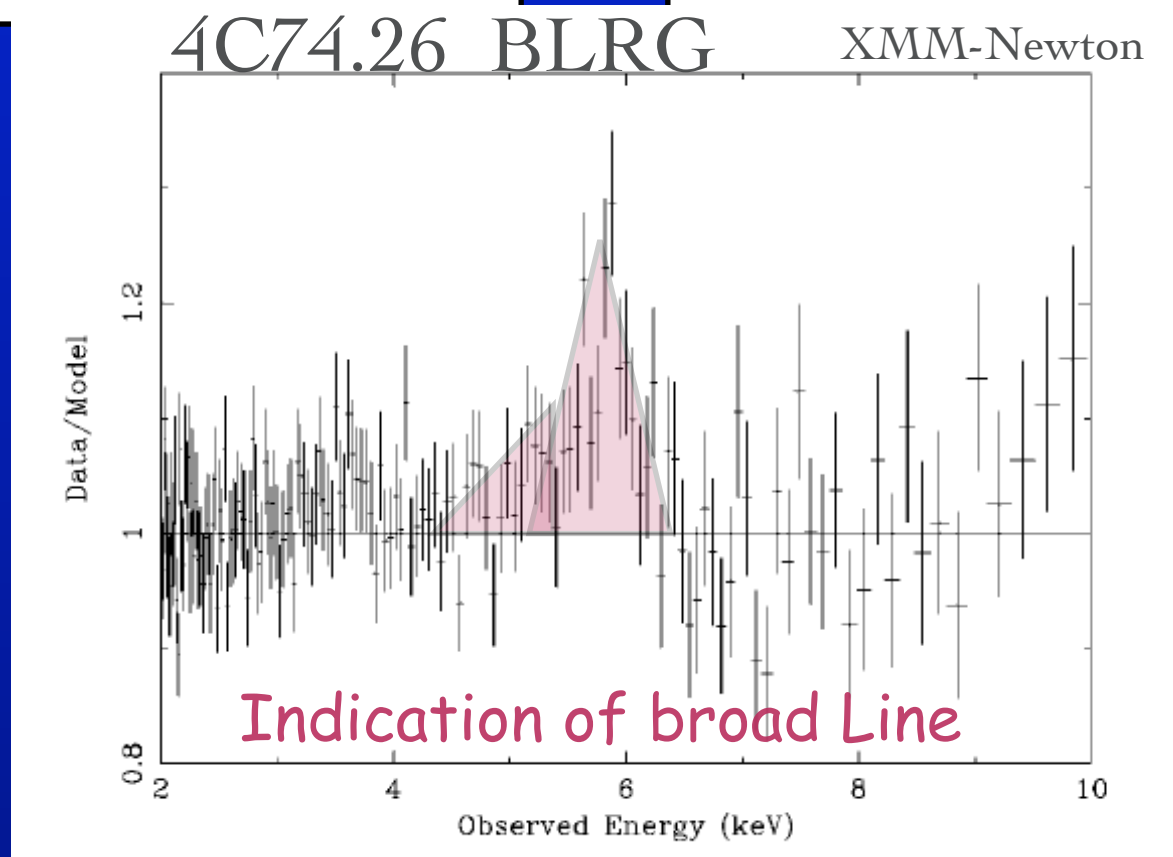
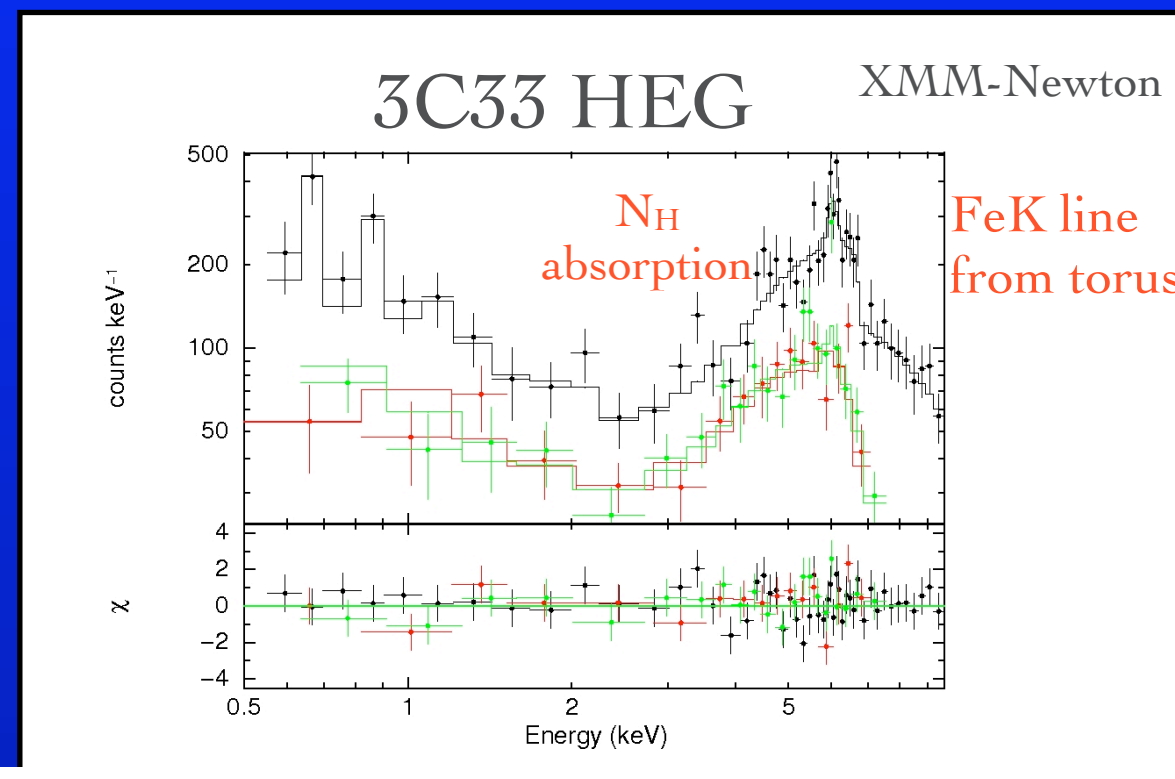
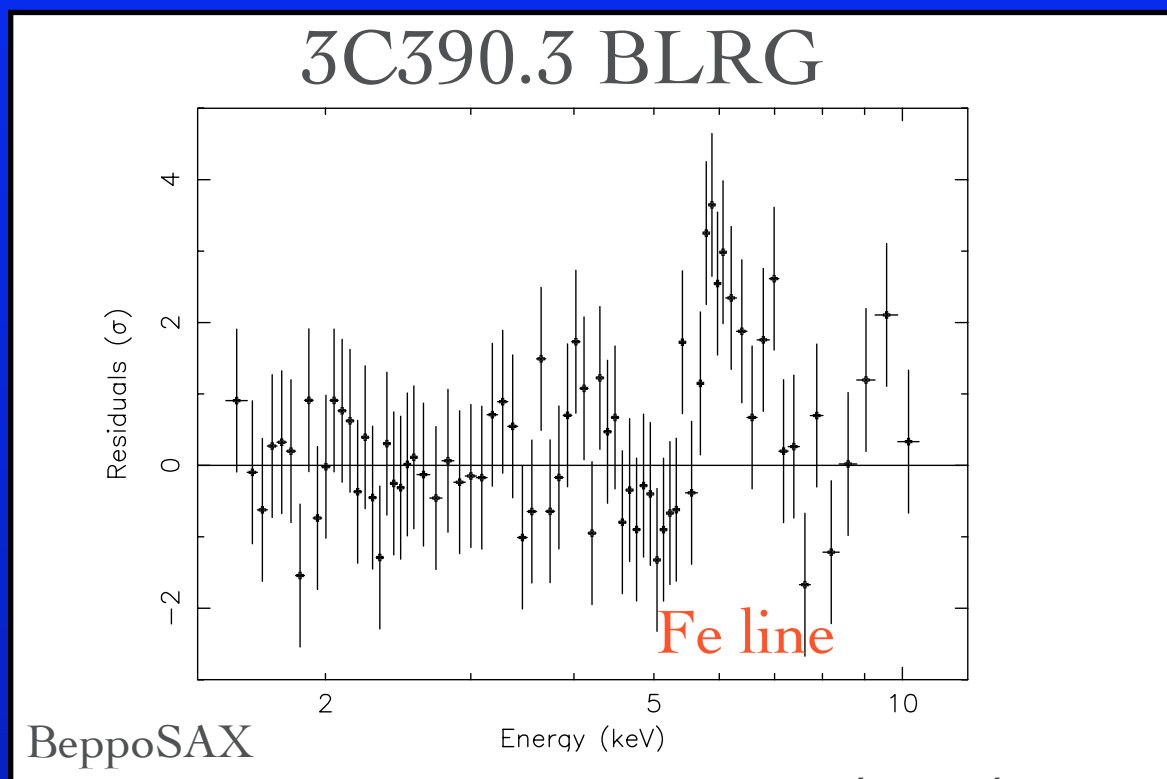
SS accretion disk
seen in Seyfert

The X-ray spectrum is the sum of two components:

- 1) an efficient accretion flow
- 2) a jet

The spectrum is usually dominated by a non-thermal power law (jet).
Sometime the jet fades and the accretion disk emerges

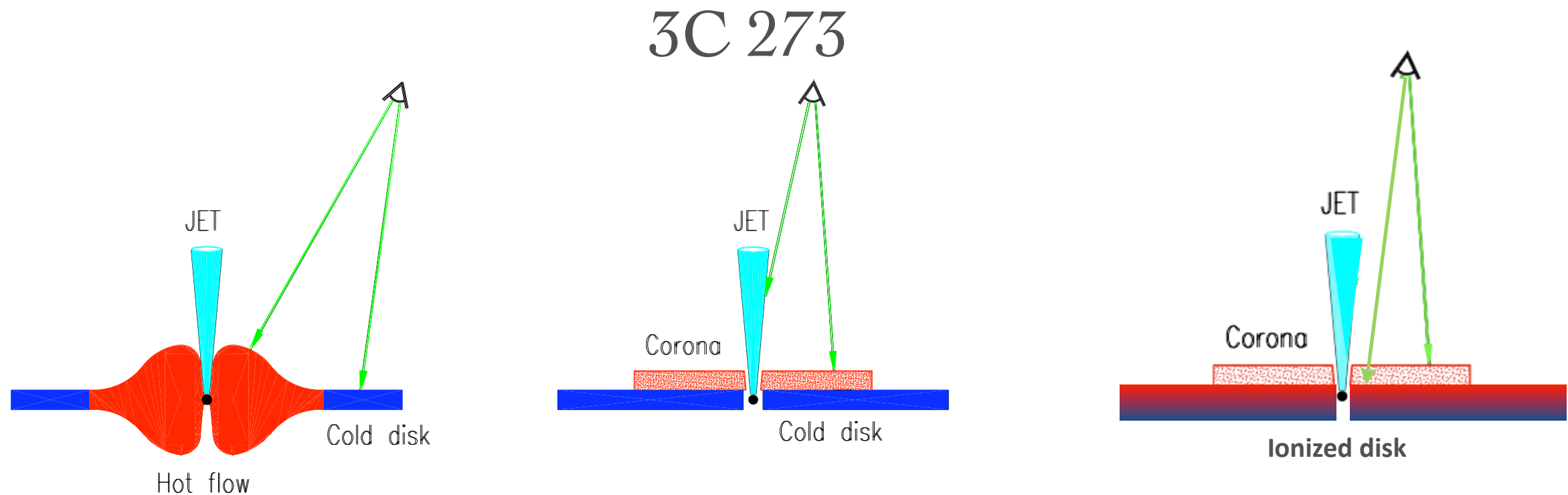
In **FRII** BLRGs and NLRG/HEGs, X-ray spectra show reprocessing features typical of cold matter surrounding an efficient accretion disk



Is the disk thin and optically thick (SS) in FRII RL AGN?

Still open question

In BLRGs the Fe line is usually weak and narrow.
The Compton reflection weak or absent



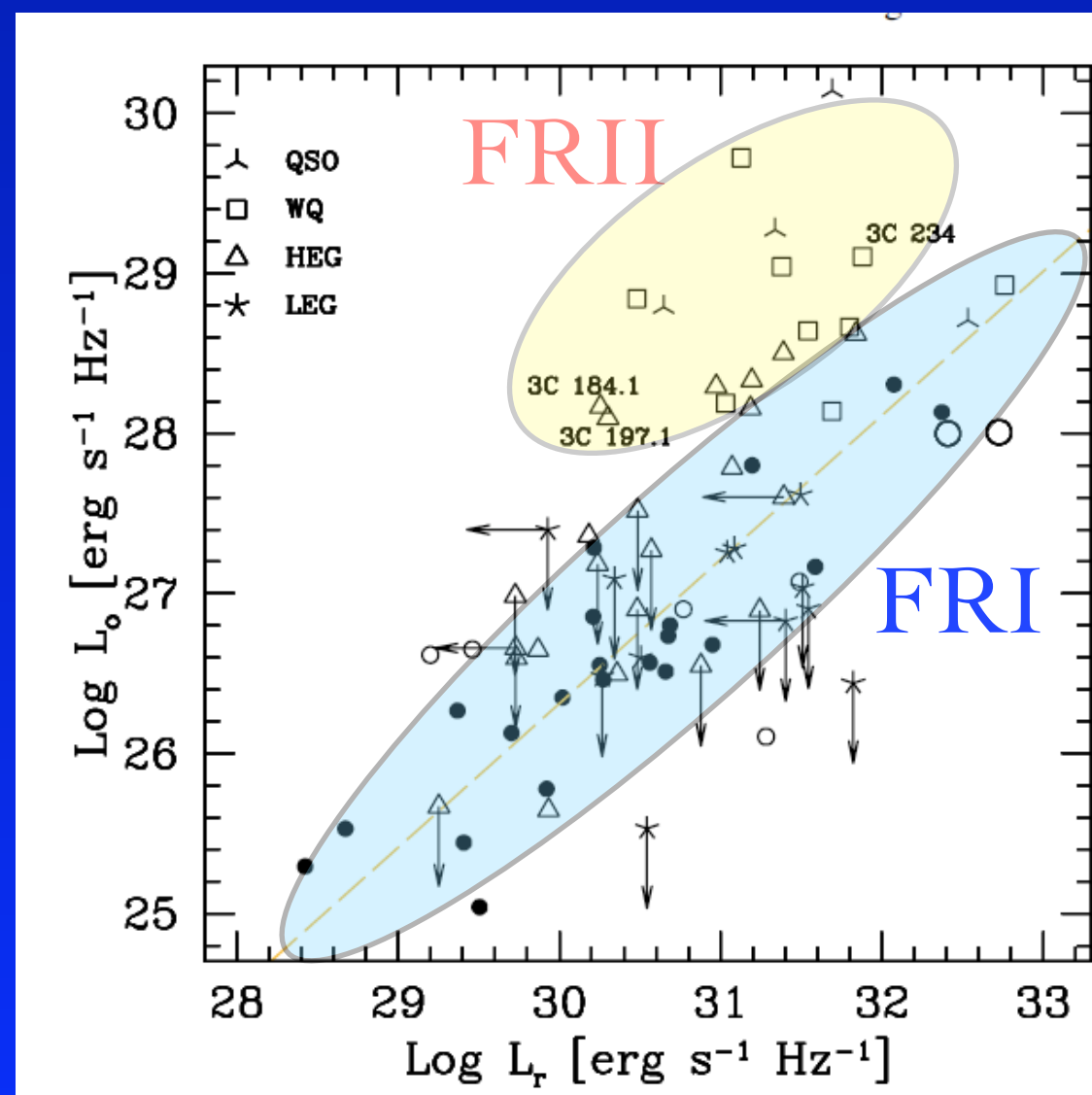
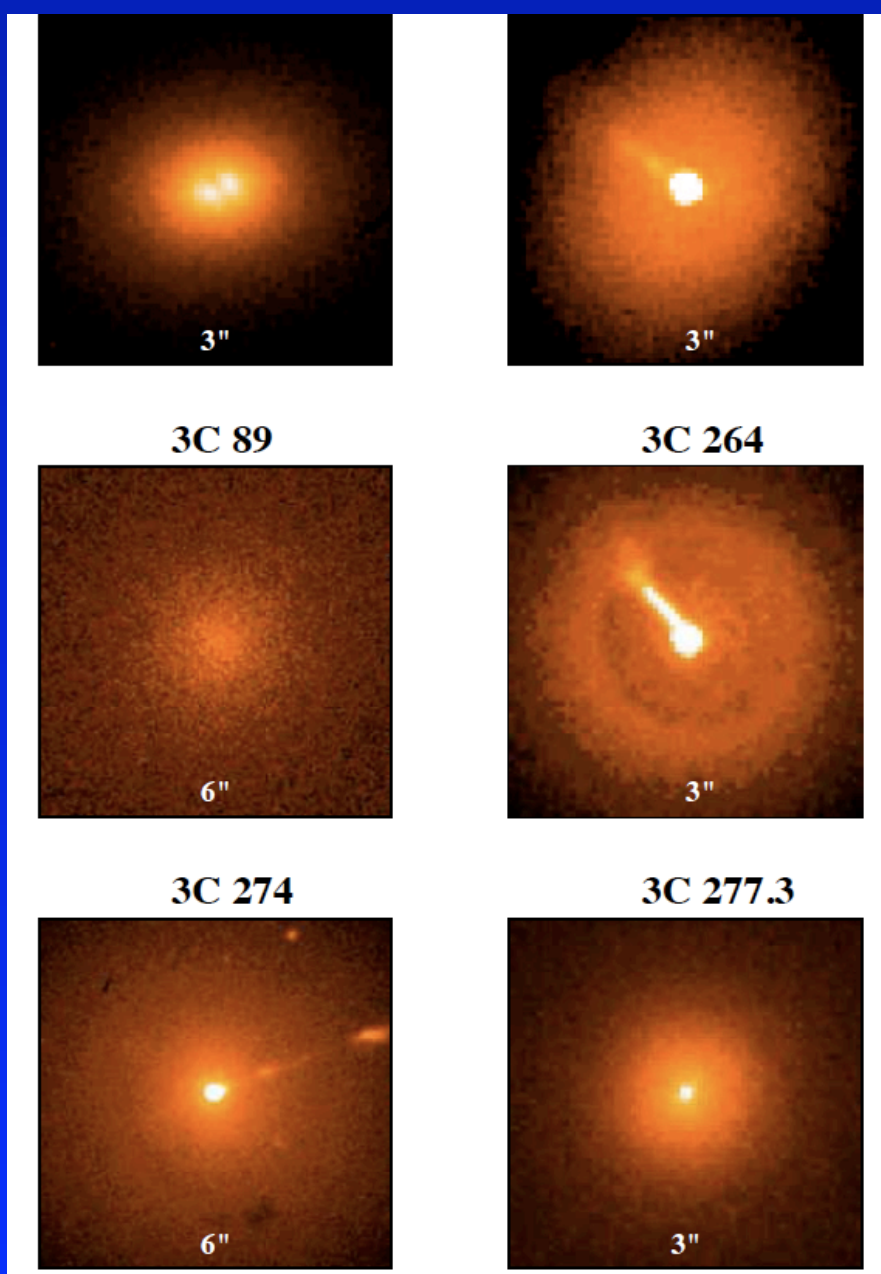
If an ADAF is in the inner region or the disk is strongly ionized the
line production is inhibited.

Then the reprocessed features could be produced in a torus or in
the Broad Line Region

In FRIs the accretion is not efficient

There is no nuclear absorption in HST images: the weakness of the optical lines is not due to obscuration

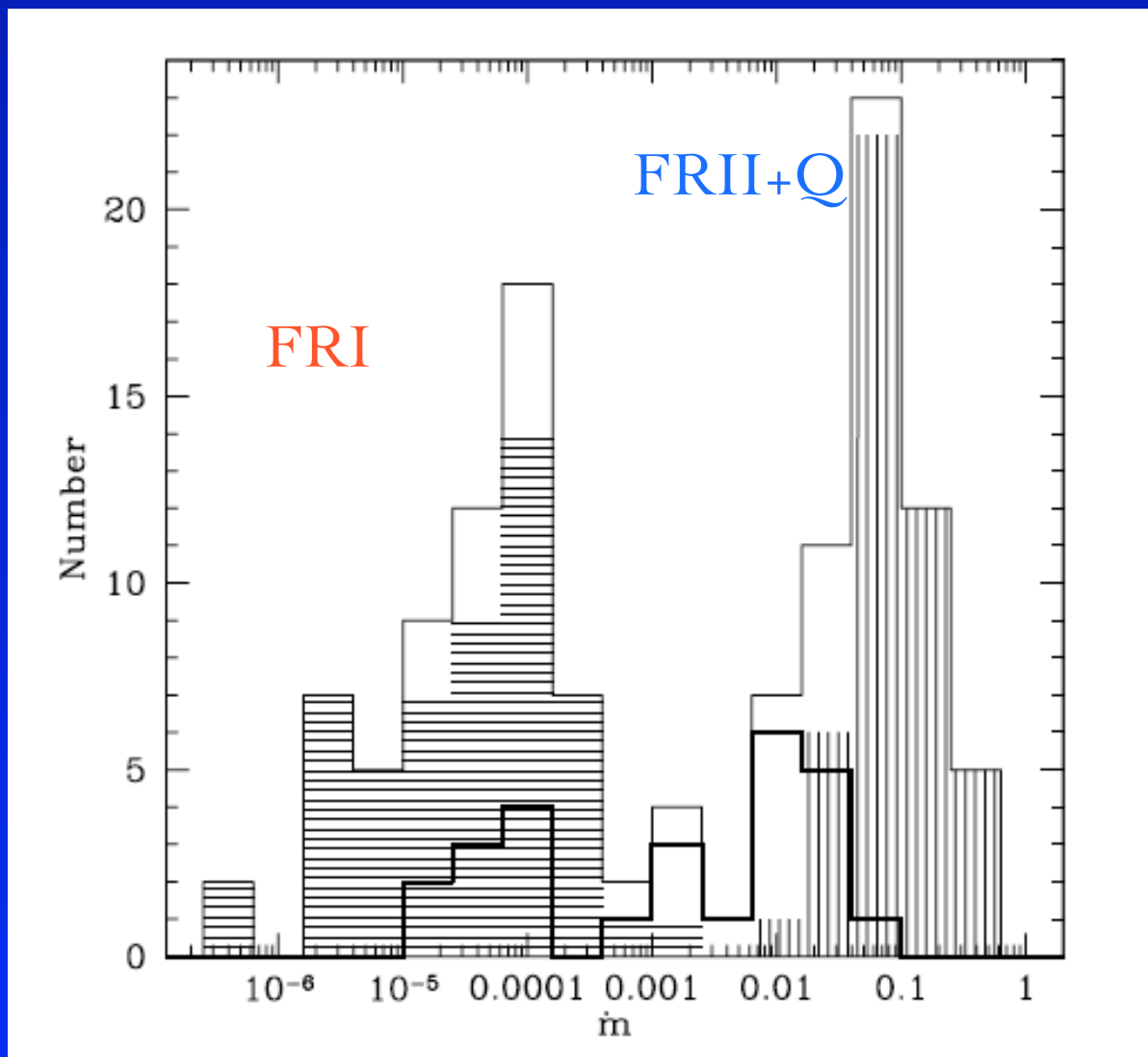
The optical flux of FRI shows a striking linear correlation with the radio core one over four decades, arguing for a non-thermal synchrotron origin of the nuclear radiation



The accretion rate distribution is
bimodal:

Low accretion rates => FRI

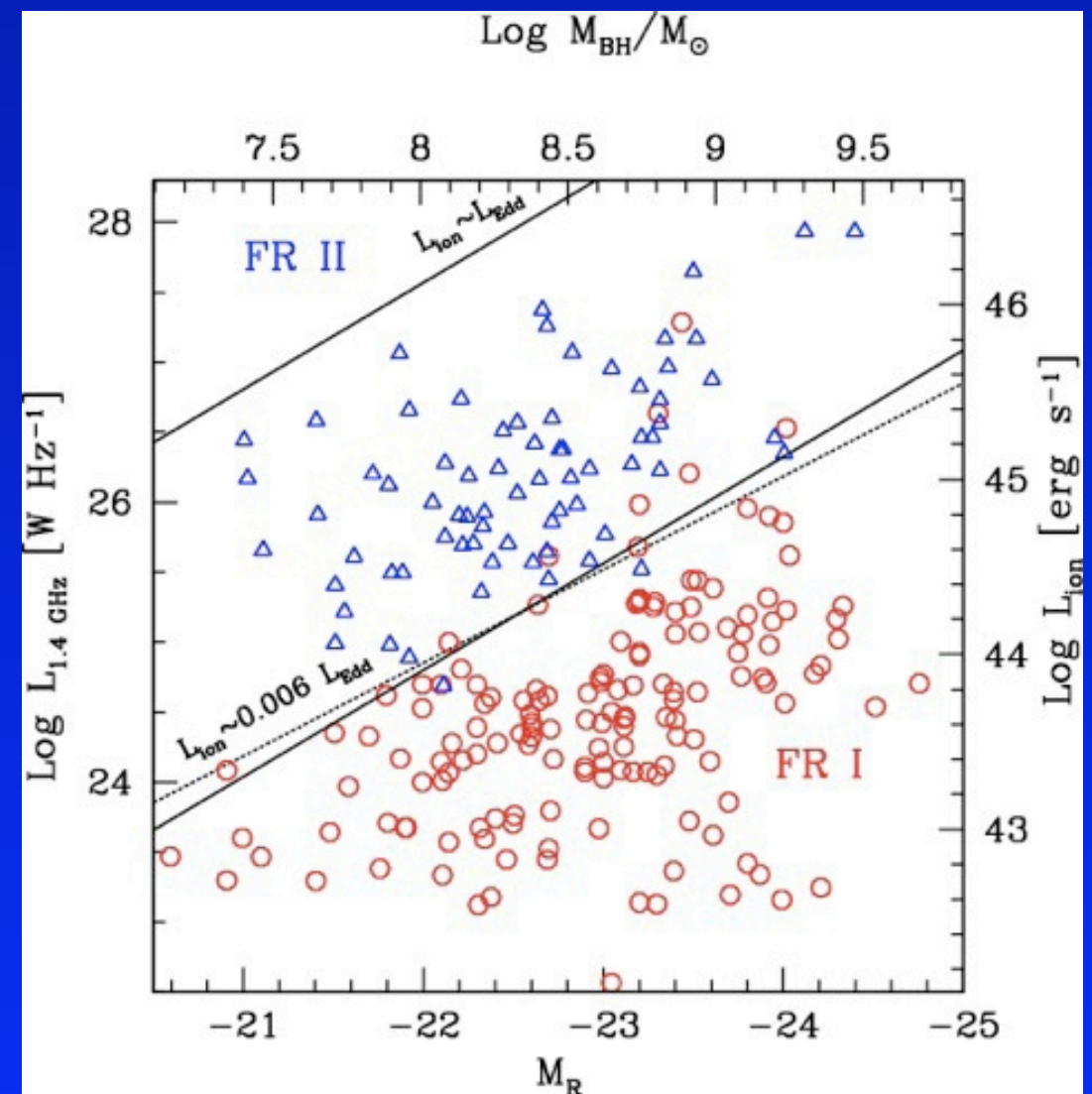
High accretion rate => FRII + Quasar (Q)



The division between FR I and FR II then turns
out to be a separation at constant $L_{\text{ion}}/M_{\text{BH}}$.

It is described by

$$L_{\text{ion}} \sim 6 \times 10^{-3} L_{\text{Edd}}$$

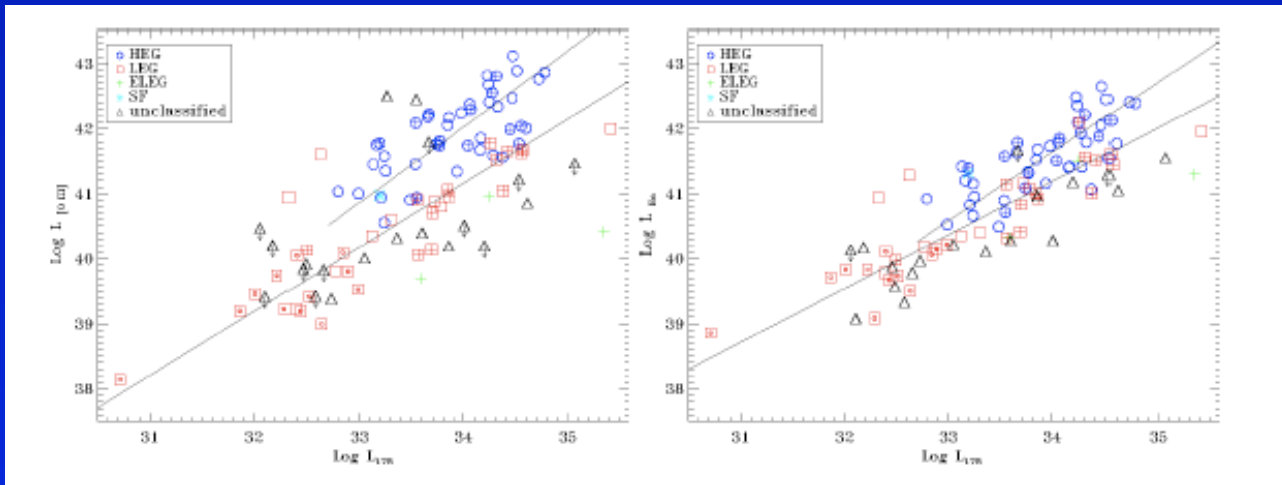


In summary:

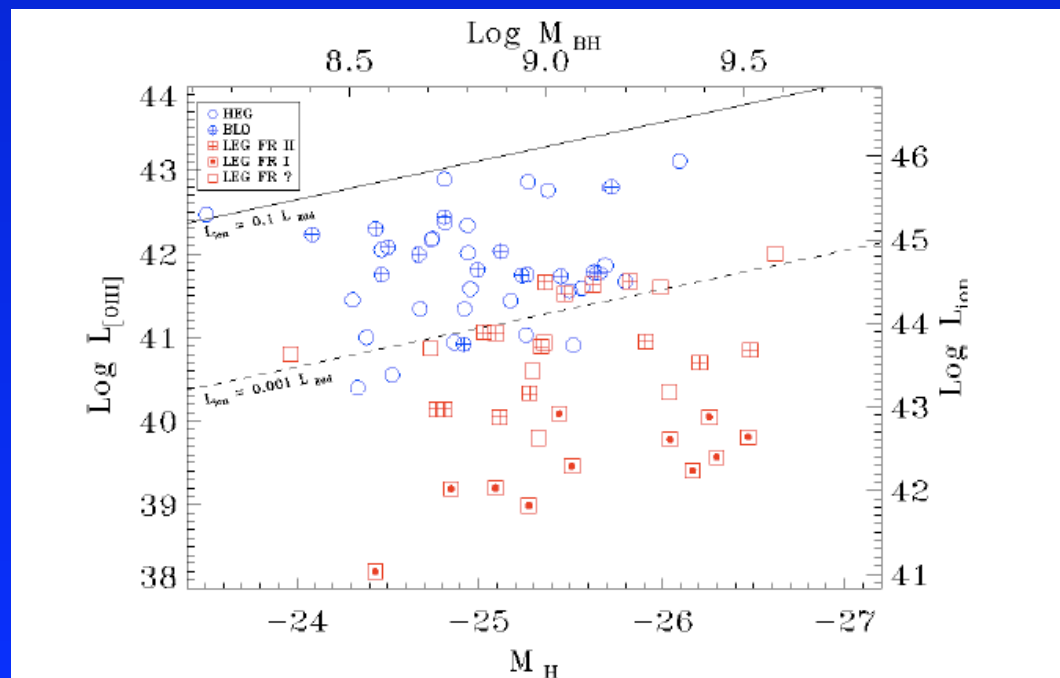
Powerful jets have efficient accretion disks (FR II)

Weak jets have inefficient accretion flows (FR I)

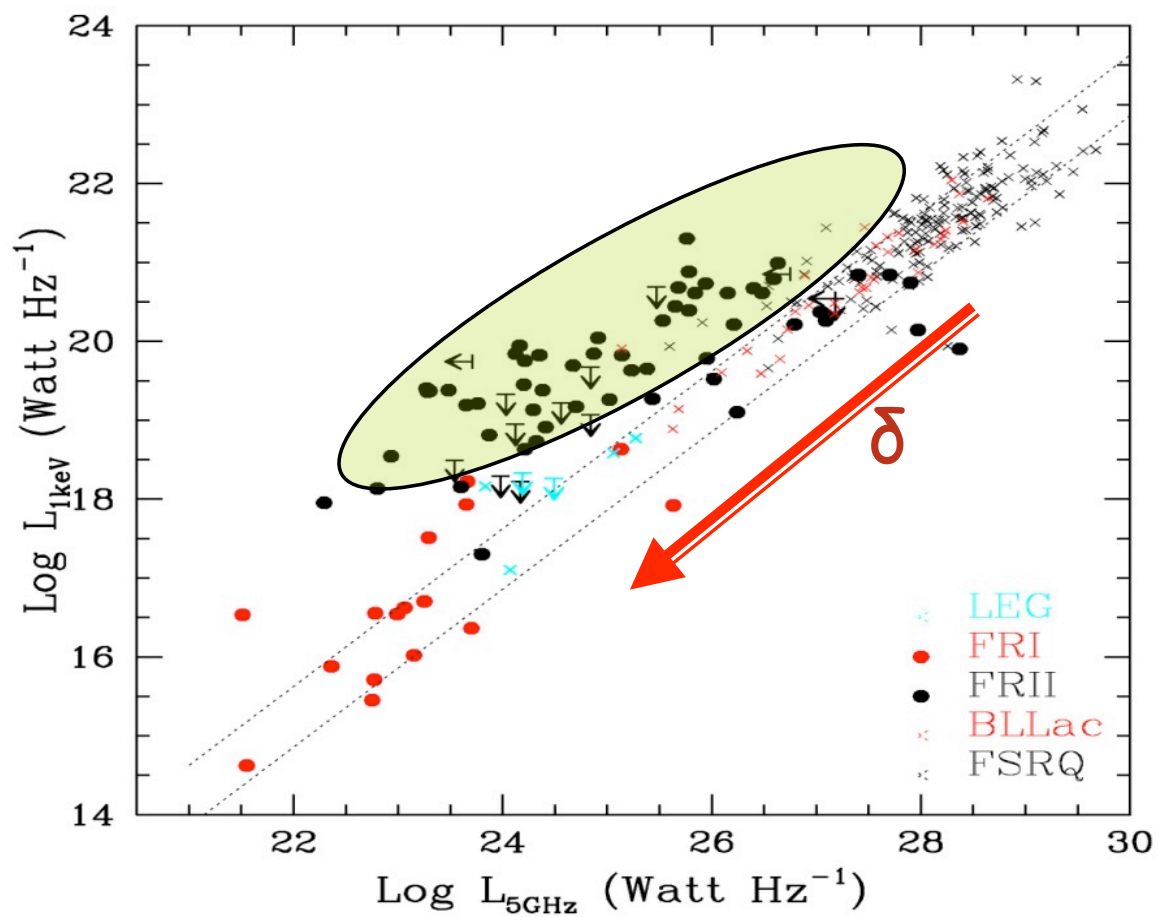
too simple.. HEG-LEG dichotomy



HEG are located in general at higher line luminosity with respect to LEG of similar radio luminosity.

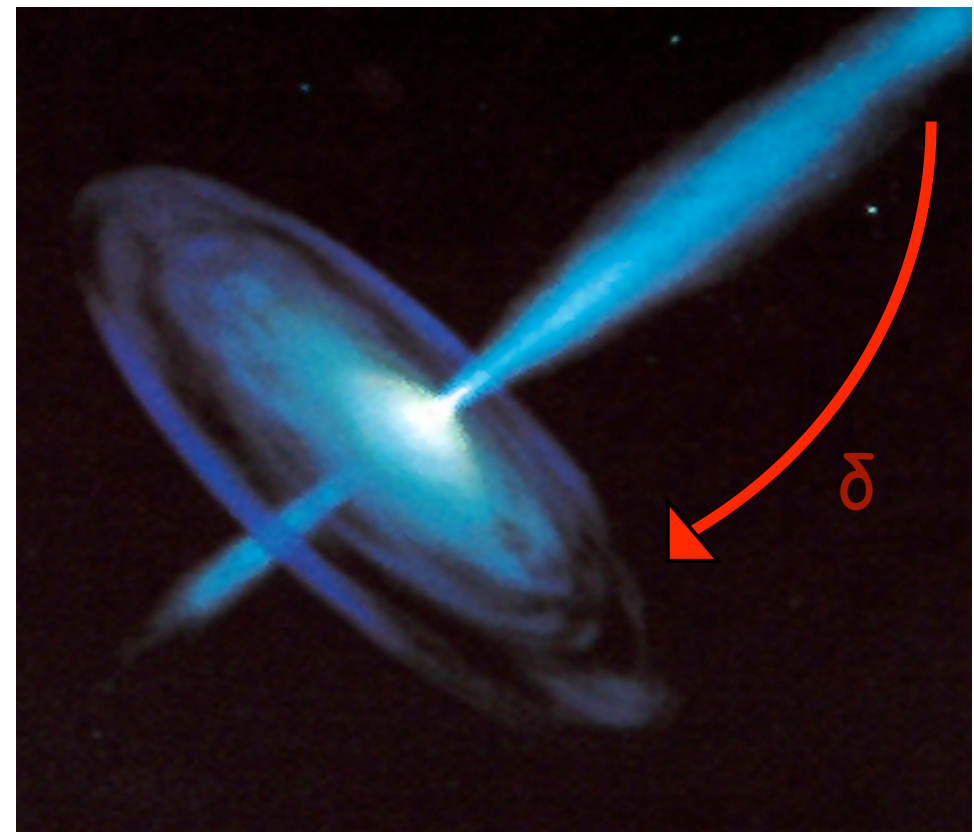


HEGs and LEGs occupy different region of the $L[\text{OIII}]-M_{\text{BH}}$ plane. Indication of a less efficient accretion flow in LEGs



In the green region

$L_{1keV} = L_{Ther} + L_{NTher}$, with $L_{Ther} \gg L_{NTher}$



LT = Lum Ther \Rightarrow Accretion

LNT = Lum Non-Ther \Rightarrow Jet

The dotted lines delimit a region where FSRQs and BL Lacs are expected to pass through when the angle of sight increases (i.e. when the beaming effects $\delta = [\gamma(1 - \beta \cos \theta)]^{-1}$ decreases).

LEGs probably host inefficient accretion flows but could also hide strongly obscured (powerful) disks. X-rays can definitely solve this still debated question.

5. MAGNs:

a different perspective on
relativistic jets

News from
Fermi!

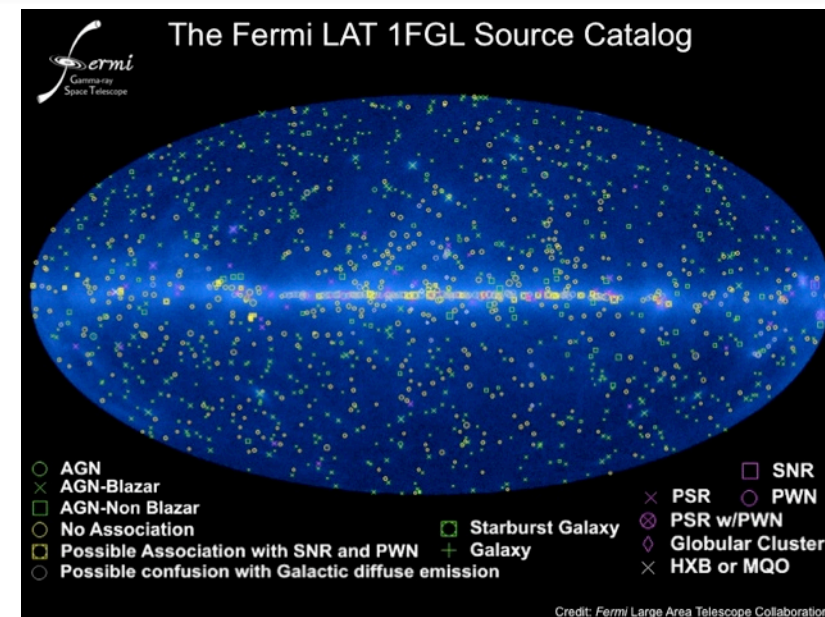
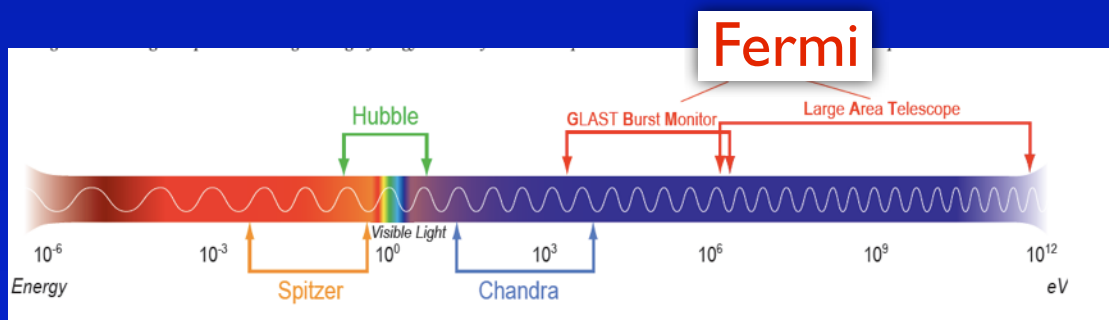


Within the AGN Unified Model, an increase of the angle of view implies a deamplification of the jet emission that can be quite severe at relatively small angles.

As a consequence large inclination Radio Sources should be lost by gamma-ray satellites if a pre, one zone homogeneous Synchrotron-Compton model is adopted.

The LAT-Fermi detection of new misaligned sources is opening a new field of research, that we can explore...

A sample of 11 MAGNs has been recently discovered by the Fermi satellite



The Fermi spacecraft orbits the earth in about 96 minutes. On alternate orbits Fermi rocks to the left and right, allowing the LAT to cover more of the sky.

With a field of view of 2.4 sr, the LAT see" 20% of the sky at any instant and will scan the entire sky (4π sr) once every two orbits, or three hours.

Quantity	LAT (Minimum Spec.)	EGRET
Energy Range	20 MeV - 300 GeV	20 MeV - 30 GeV
Peak Effective Area ¹	> 8000 cm ²	1500 cm ²
Field of View	> 2 sr	0.5 sr
Angular Resolution ²	< 3.5° (100 MeV) < 0.15° (>10 GeV)	5.8° (100 MeV)
Energy Resolution ³	< 10%	10%
Deadtime per Event	< 100 μs	100 ms
Source Location Determination ⁴	< 0.5'	15'
Point Source Sensitivity ⁵	< 6 x 10 ⁻⁹ cm ⁻² s ⁻¹	~ 10 ⁻⁷ cm ⁻² s ⁻¹

¹ After background rejection

² Single photon, 68% containment, on-axis

³ 1-σ, on-axis

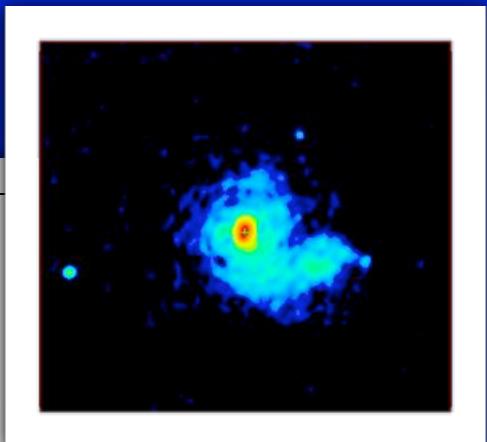
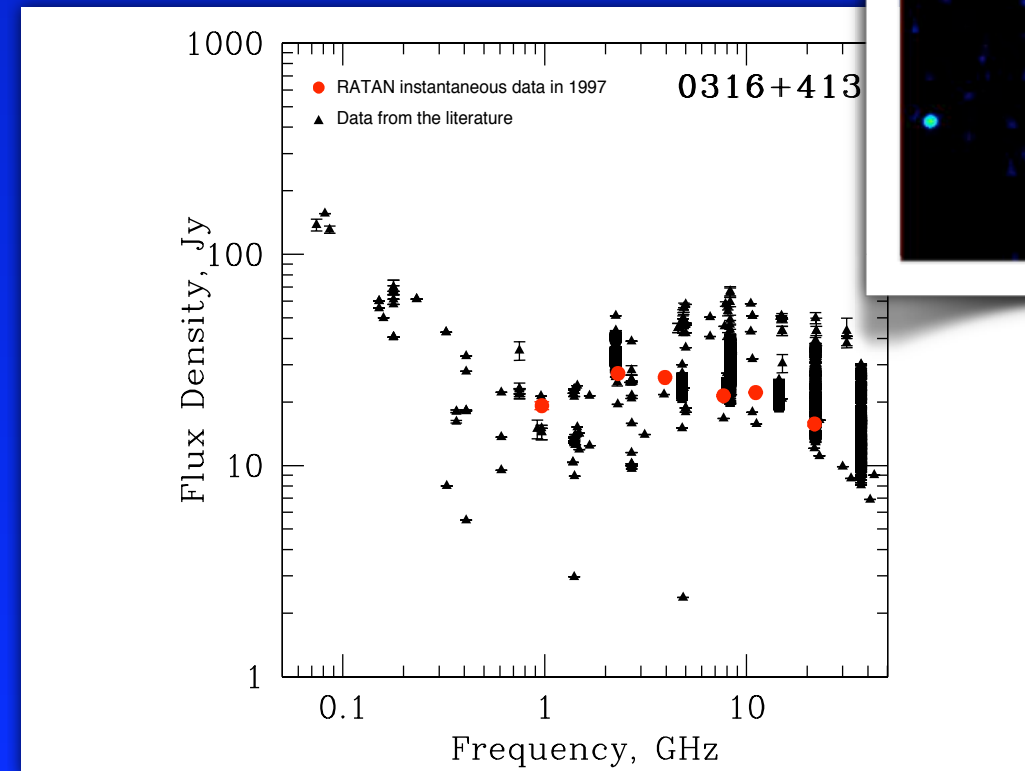
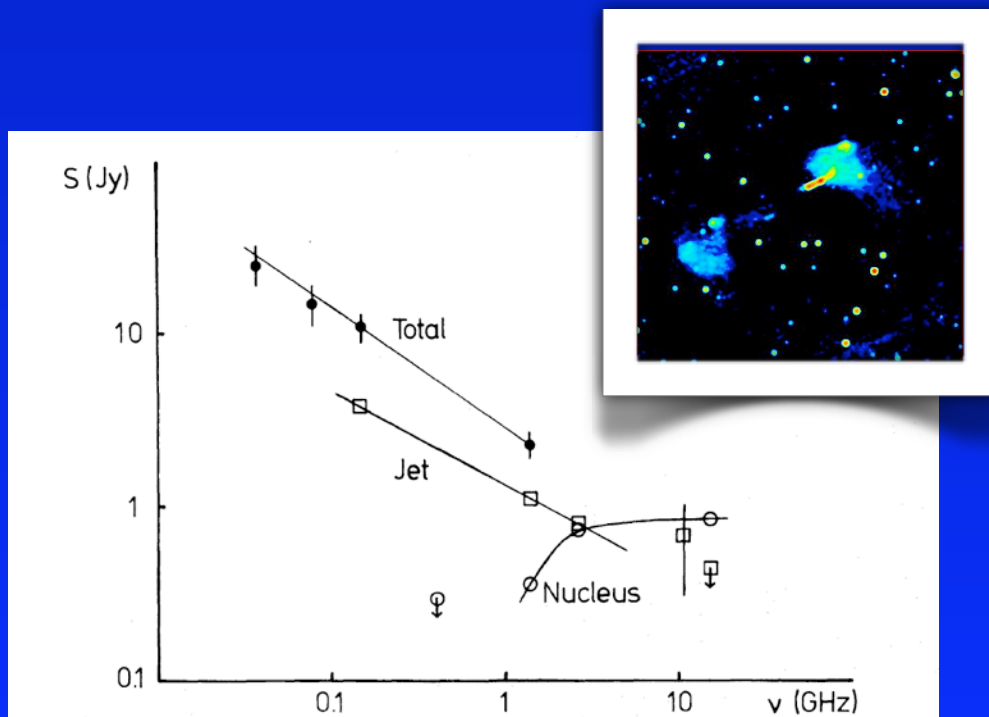
⁴ 1-σ radius, flux 10⁻⁷ cm⁻² s⁻¹ (>100 MeV), high |b|

⁵ > 100 MeV, at high |b|, for exposure of one-year all sky survey, photon spectral index -2

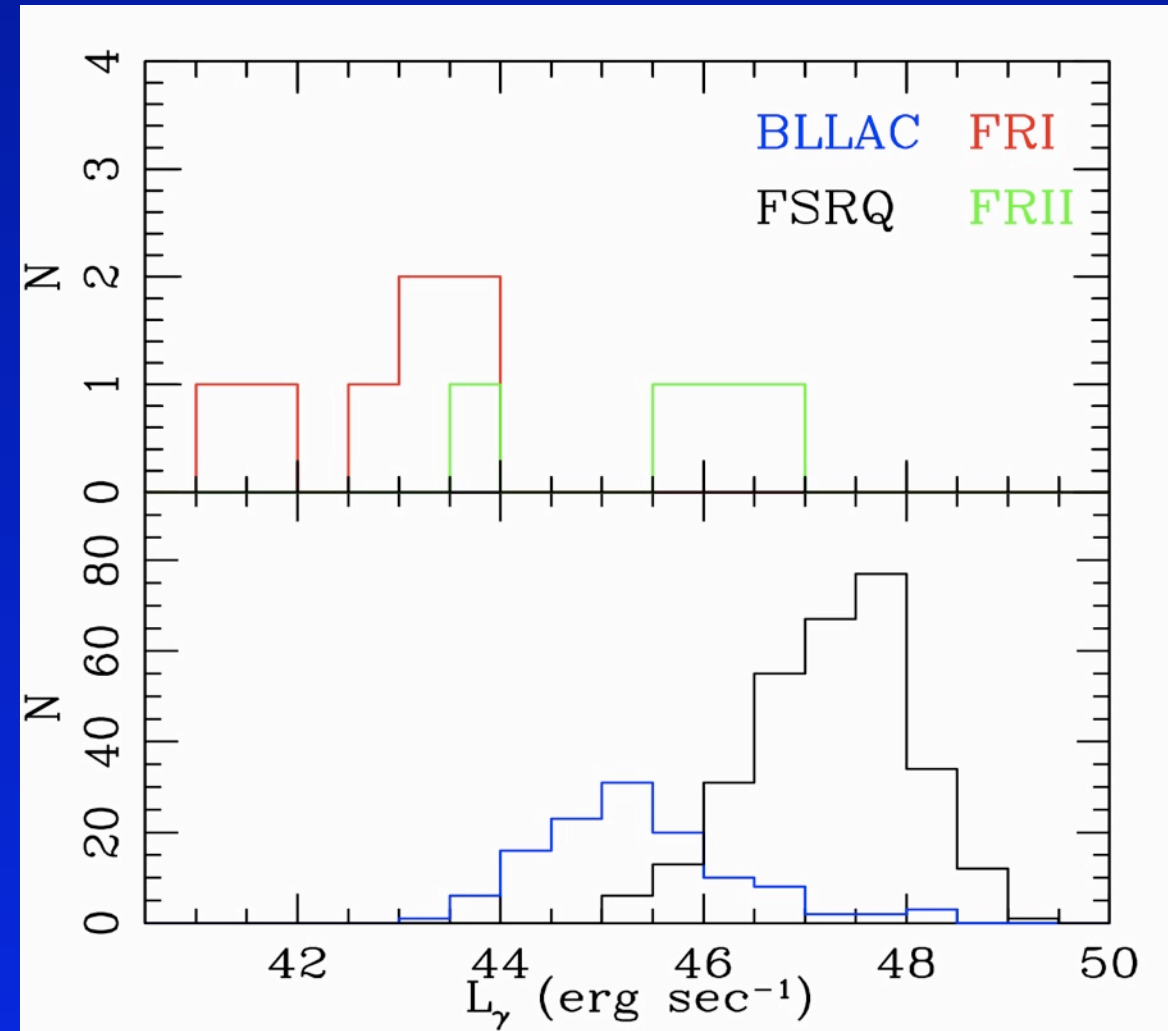
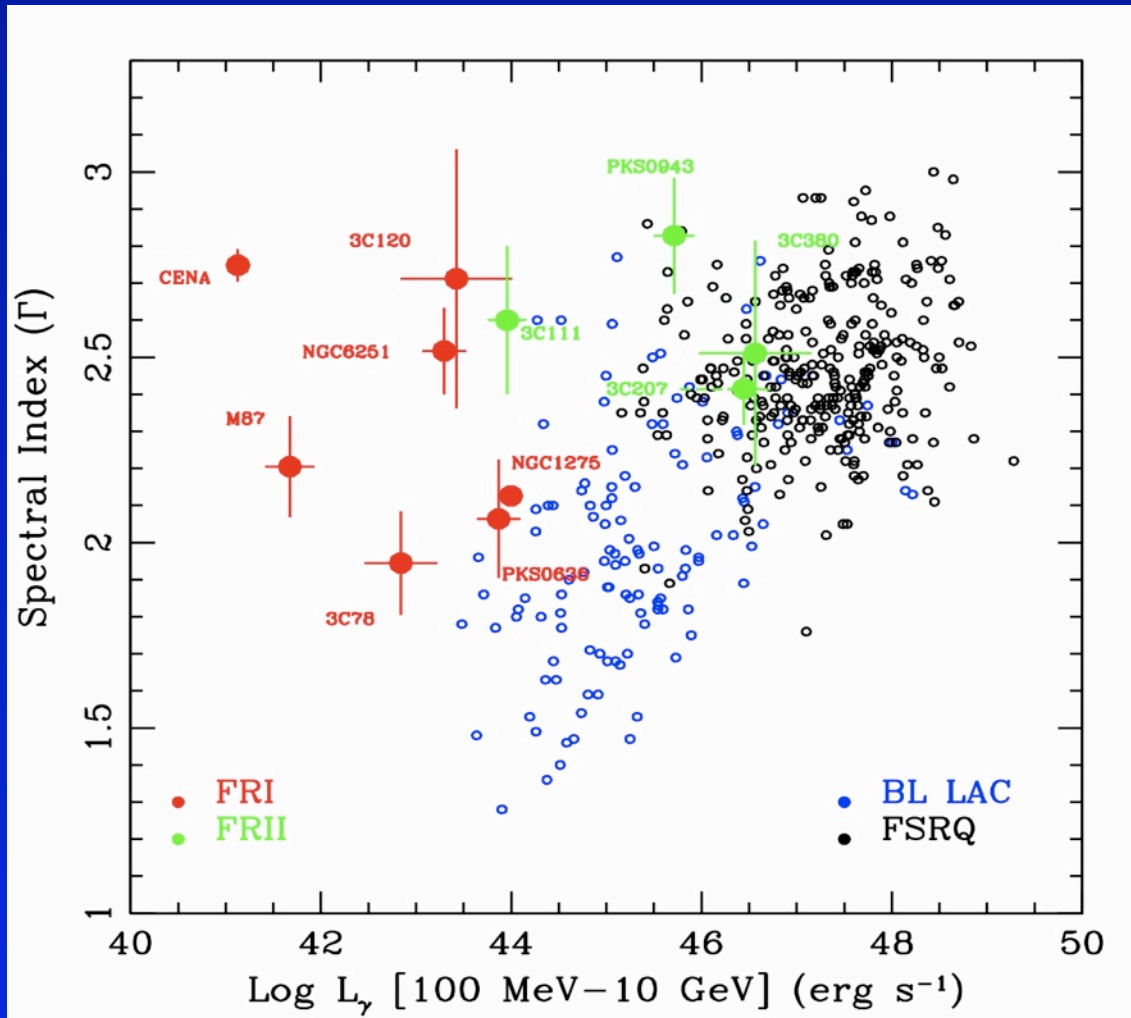
How can we find MAGNs at GeV energies?

The 3CR, 3CRR and MS4 samples are cross-correlated with the 11 month-LAT-list of AGN candidates

- ☀ The low-frequency selection criteria (178 and 408 MHz) select radio sources primarily on the relatively steep spectrum synchrotron emission of their extended lobes
- ☀ Radio (FRI vs FRII) and optical (Radio Galaxy vs Quasar) classifications are available for the majority of the sources.
- ☀ These surveys cover most part of the northern and southern sky



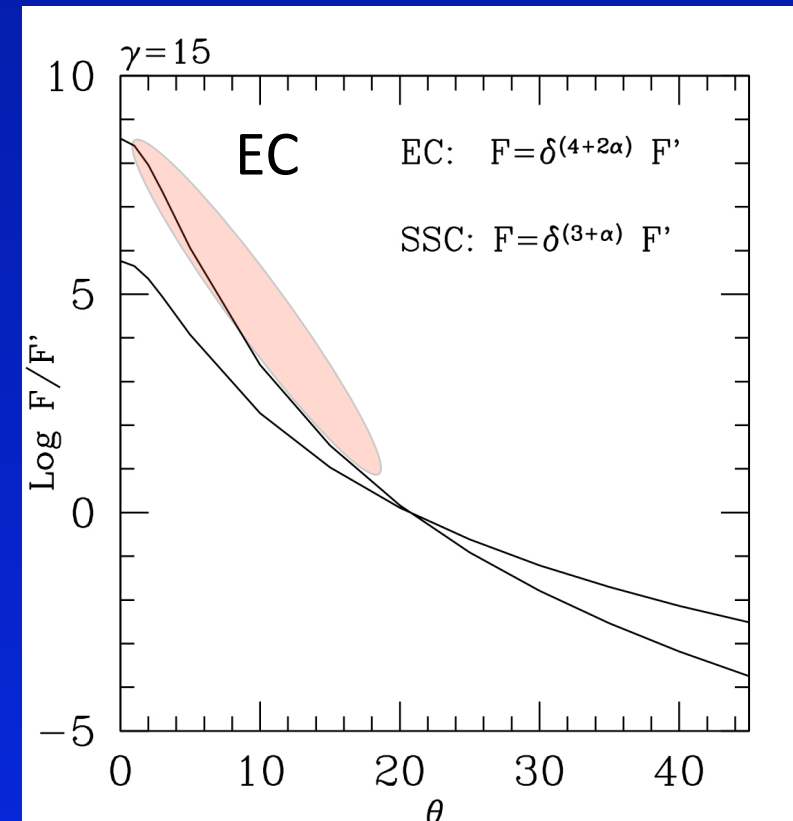
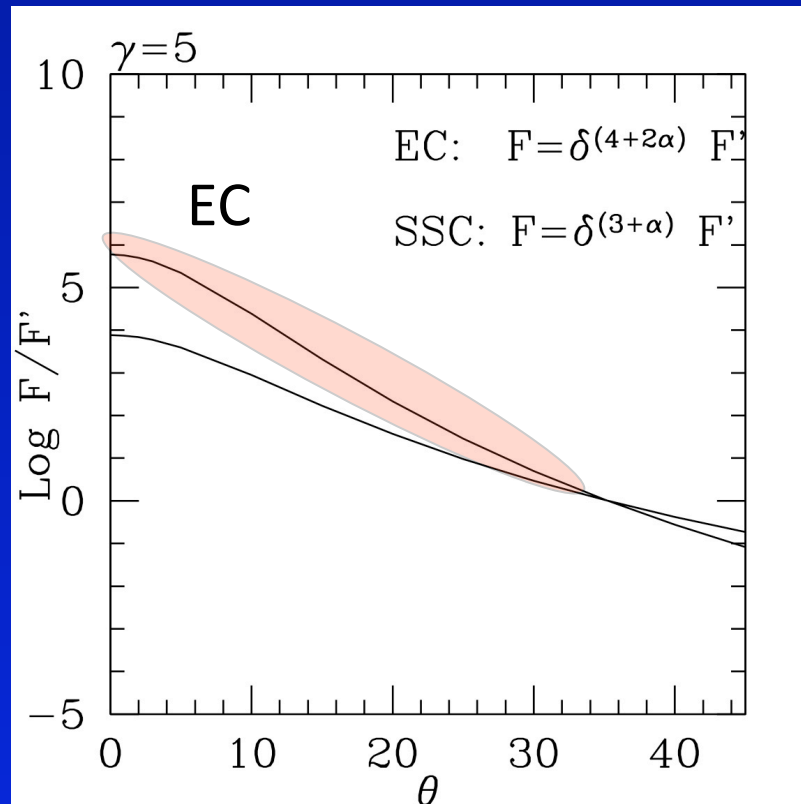
MAGNs versus Blazars



FRI > FRIIs

Misaligned AGNs generally occupy a separate region in the L_γ - Γ plane. In agreement with the idea that misaligned AGNs have smaller beaming factor $\delta = 1/\gamma(1-\beta \cos\theta)$ SSRQ (FRII) seem to lie at best in the outskirts of the FRSQ distribution.

Maybe SSRQs required a larger beaming that the other MAGNs

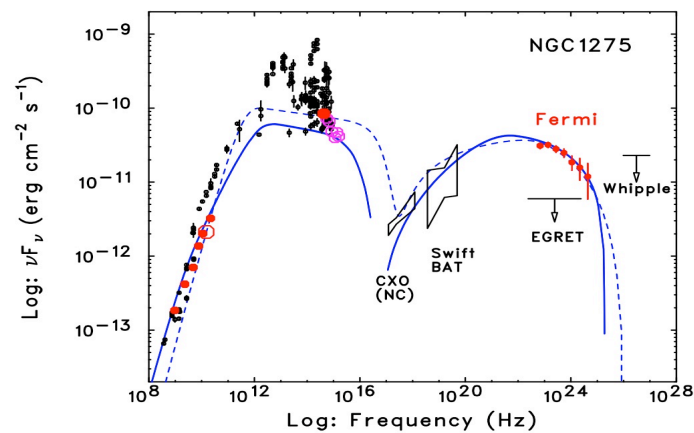


In FRII the jet propagates through a photon rich environment => EC dominant mechanism

EC emission is narrower in the beaming direction than the beaming pattern of SSC

What we are learning about the FRI jets

NGC1275



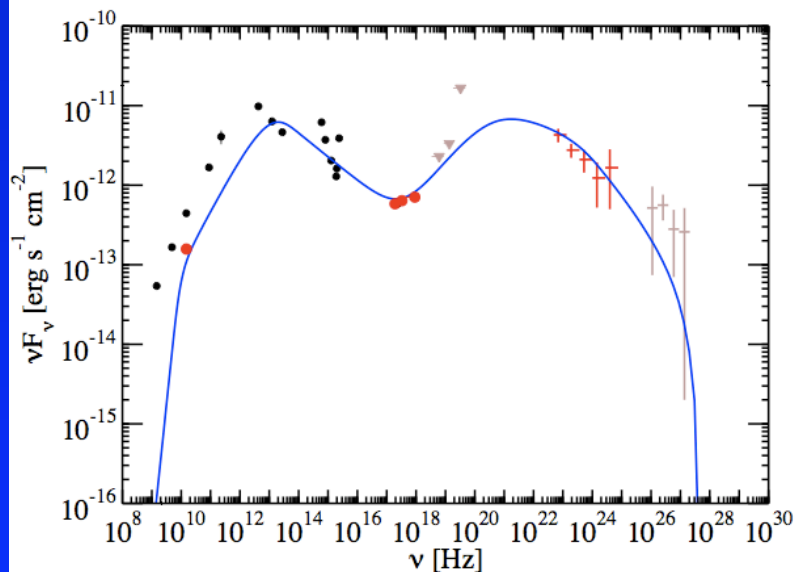
One simple zone SSC model

$$\gamma = 1.8 \quad \delta = 2.3 \quad \theta = 25^\circ \quad B = 0.05 \text{ G} \quad R = 2 \times 10^{18} \text{ cm}$$

$$n = \epsilon^{-p} \quad p = 2.1 \quad 800 \leq \epsilon \leq 960 \quad p = 3.1 \quad 960 < \epsilon \leq 4 \times 10^5$$

$$P_{\text{jet}} \sim 10^{44} \text{ erg sec}^{-1}$$

M87



SSC one zone model

Emission from sub-parsec scale jet (core) as suggested by 2008 VHE Chandra VLBA monitoring

$$\theta = 10^\circ, \gamma = 2.3, \delta = 3.9$$

$$n = k \epsilon^{-p} \quad p = 1.6 \quad [1, 4 \times 10^3] \quad p = 3.6 \quad [4 \times 10^3, 10^7]$$

$$R = 1.4 \times 10^{16} \text{ cm}$$

$$B = 55 \text{ mG}$$

Constraining the inclination angle

1. Superluminal motion

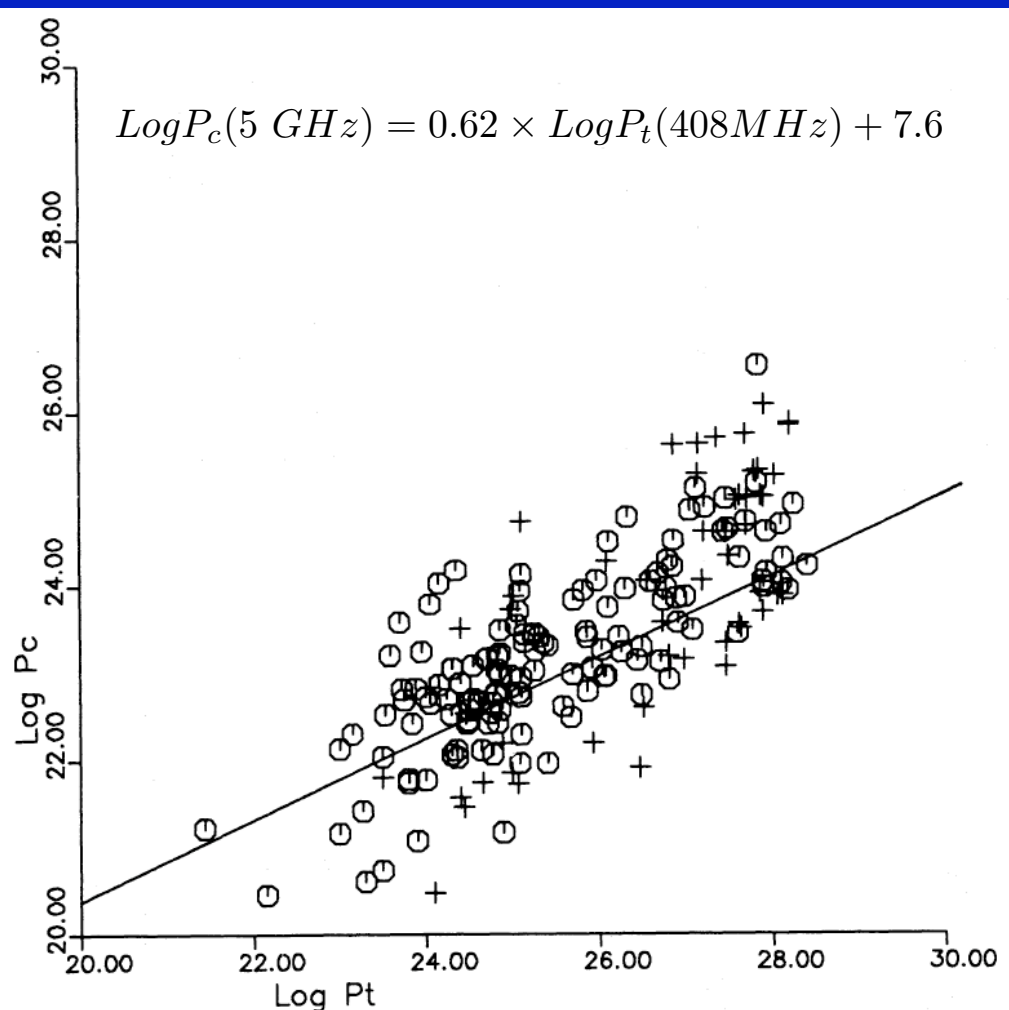
$$\beta_a = \frac{\beta \sin \theta}{1 - \beta \cos \theta}$$

2. Jet-Counterjet ratio

$$J = \left(\frac{1 + \beta \cos \theta}{1 - \beta \cos \theta} \right)^{2 + \alpha}$$

3. Core Radio Power

Assuming that sources are oriented at random angles, the best fit corresponds to the average orientation of 60°



$$P_c = P_i \delta^{2 + \alpha}$$

If $\alpha_{\text{core}} = 0$

from $P_t \Rightarrow P_c(60^\circ)$

$$P_c(\theta) = [\gamma (1 - \beta \cos \theta)]^{-2}$$

$$P_c(60^\circ) = [\gamma (1 - 0.5\beta)]^{-2}$$



$$\beta = (k - 1)(k \cos \theta - 0.5)^{-1} \text{ with}$$

$$k = [P_c(\theta) / P_c(60^\circ)]^{0.5}$$

NGC 6251

FRI Radio Galaxy $z=0.024$

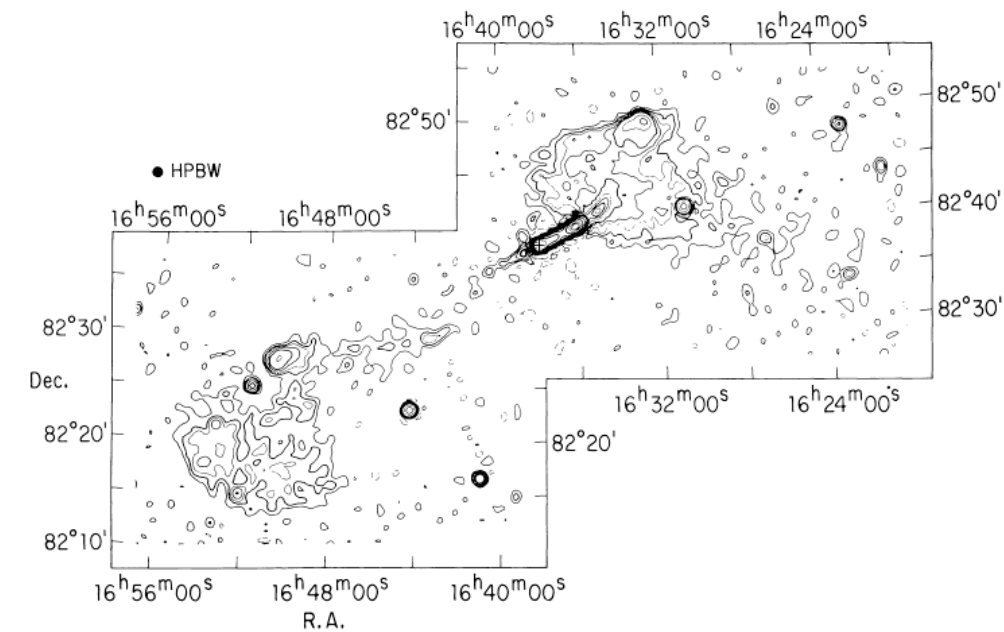
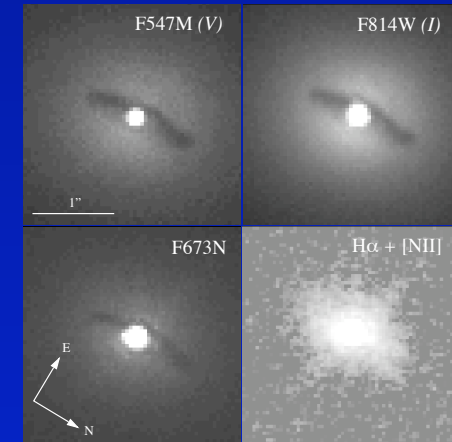
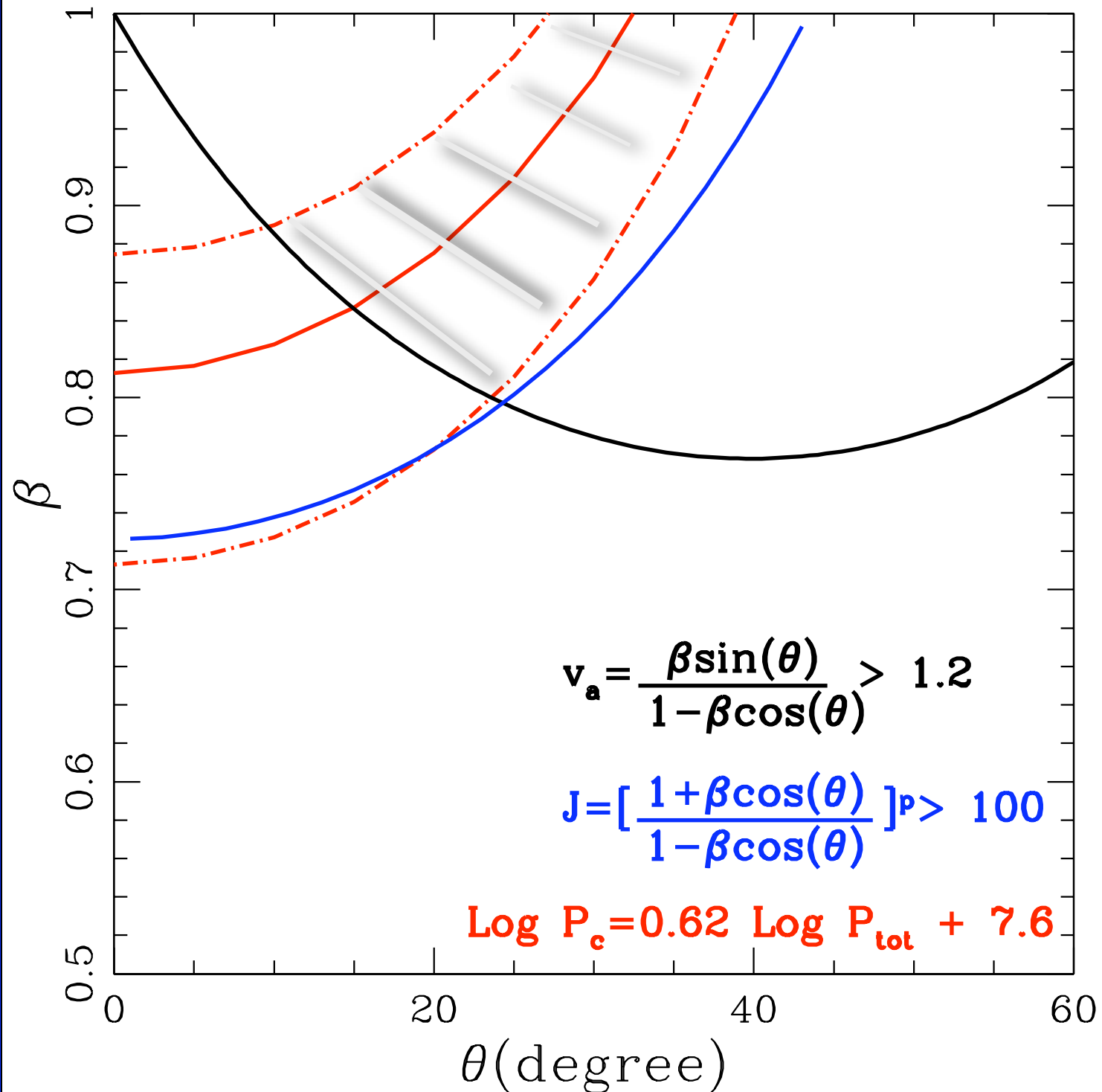
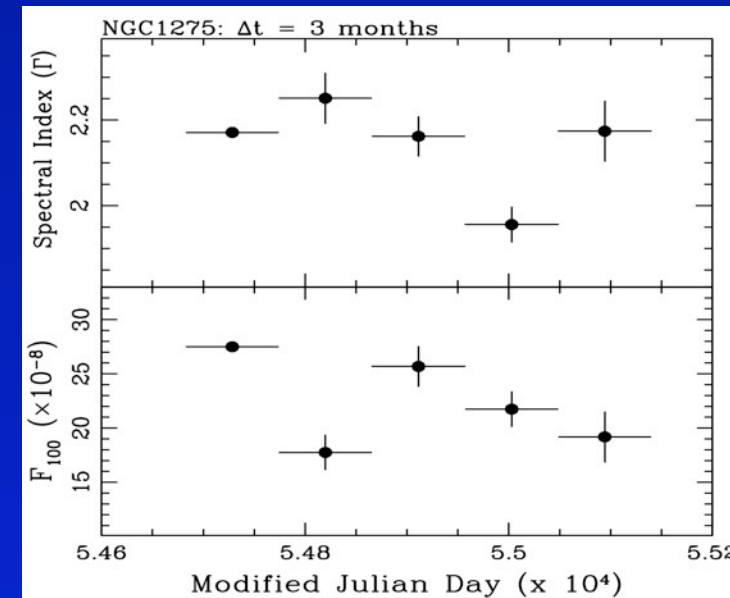


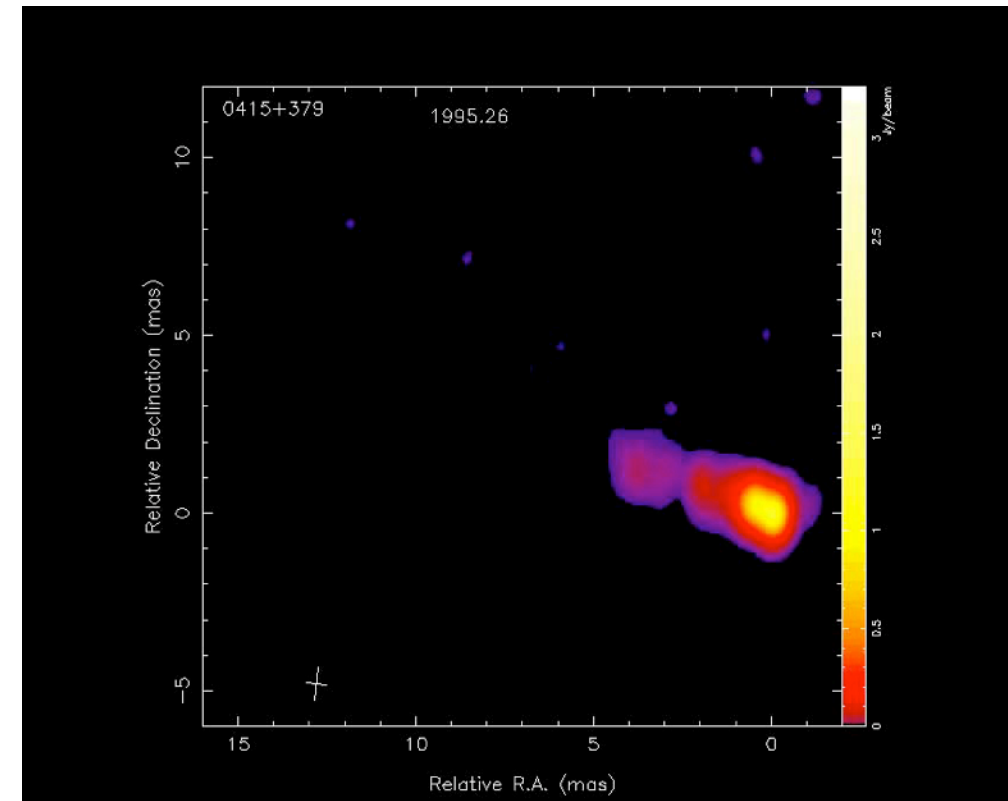
FIG. 1.—Map of the entire NGC 6251 source at 610 MHz with 50'' resolution (from Willis *et al.* 1982). The cross marks the position of the nucleus of NGC 6251.

Constraining the size of the γ -ray emitting region

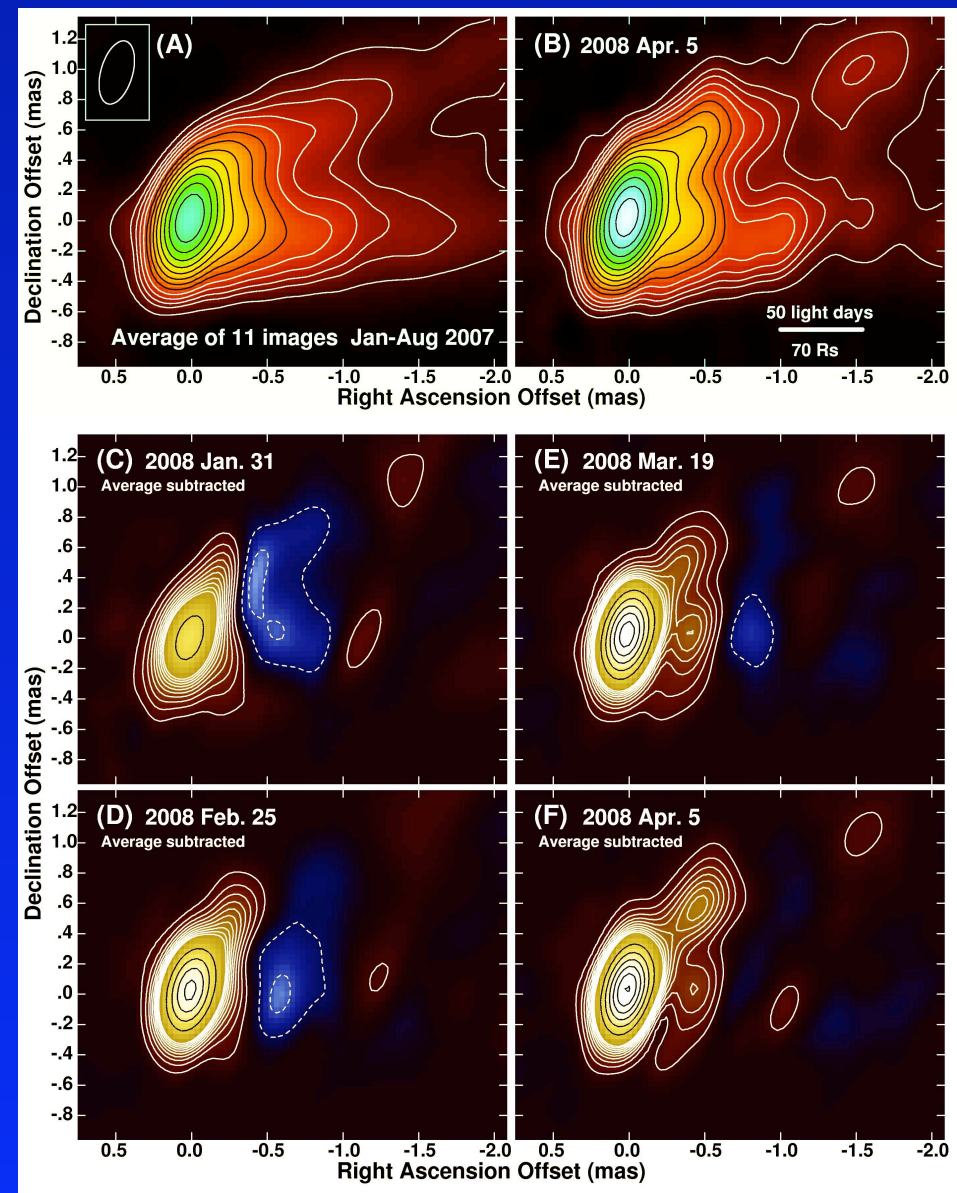
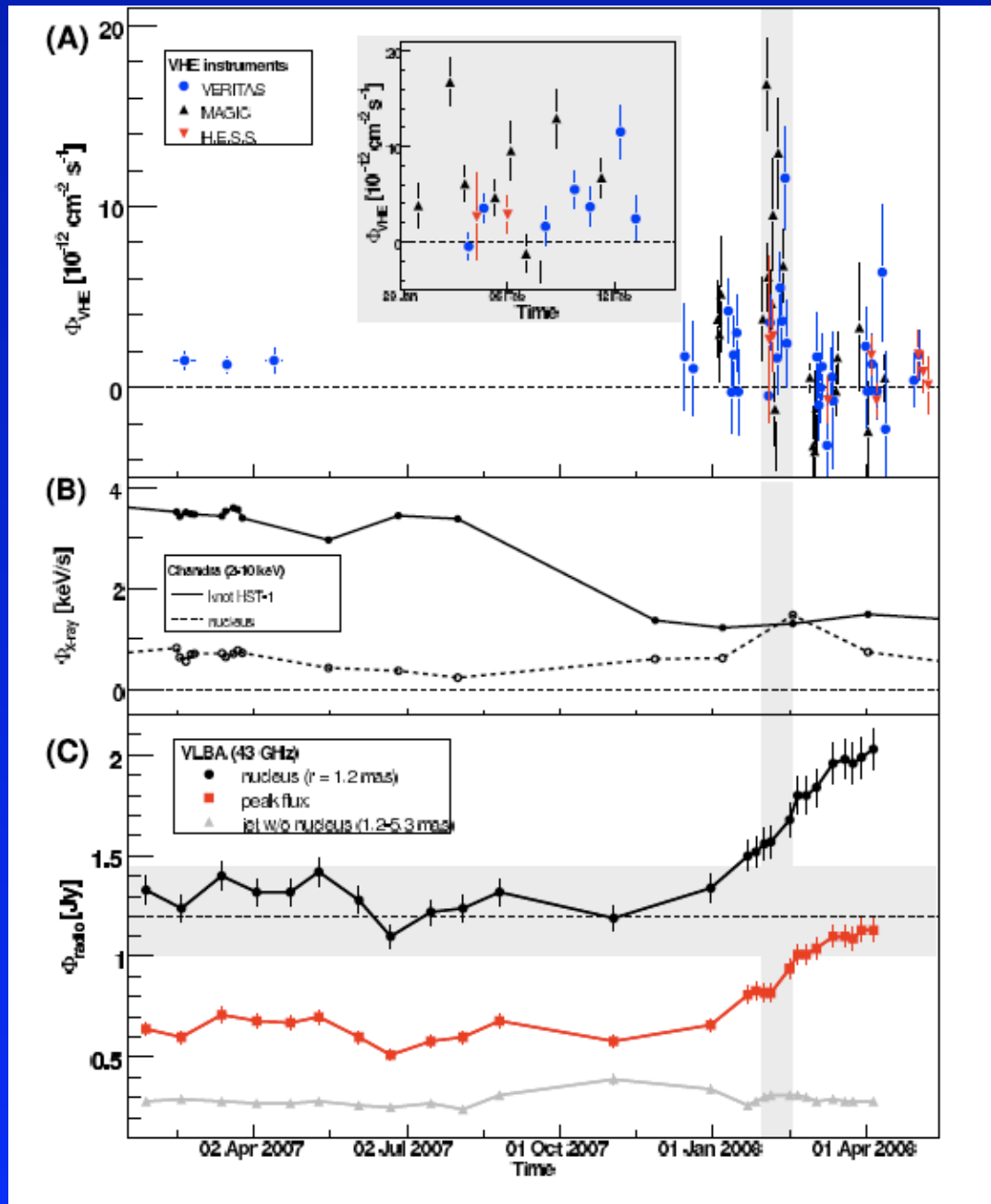
Flux Variability $R \lesssim c t_{var} \delta$



Radio core is assumed to be a possible source of gamma-ray photons (size \sim VLBI resolution : mas)

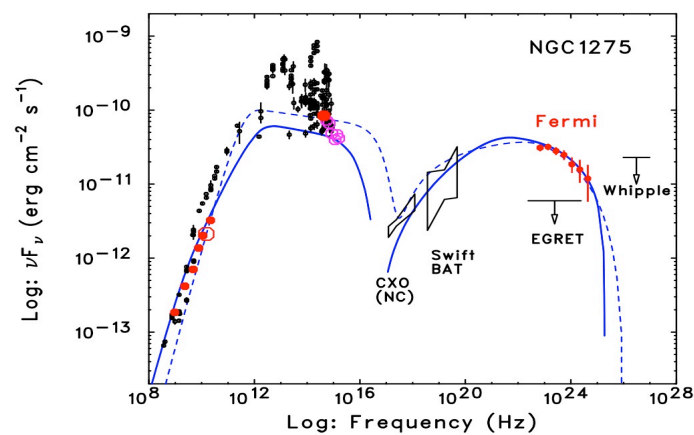


M87 suggests a core origin



What we are learning about the FRI jets

NGC1275



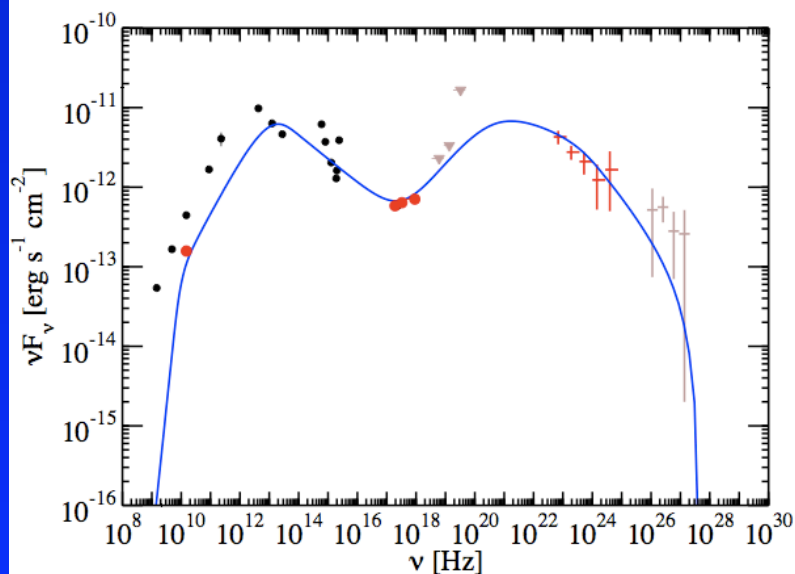
One simple zone SSC model

$$\gamma = 1.8 \quad \delta = 2.3 \quad \theta = 25^\circ \quad B = 0.05 \text{ G} \quad R = 2 \times 10^{18} \text{ cm}$$

$$n = \epsilon^{-p} \quad p = 2.1 \quad 800 \leq \epsilon \leq 960 \quad p = 3.1 \quad 960 < \epsilon \leq 4 \times 10^5$$

$$P_{\text{jet}} \sim 10^{44} \text{ erg sec}^{-1}$$

M87



SSC one zone model

Emission from sub-parsec scale jet (core) as suggested by 2008 VHE Chandra VLBA monitoring

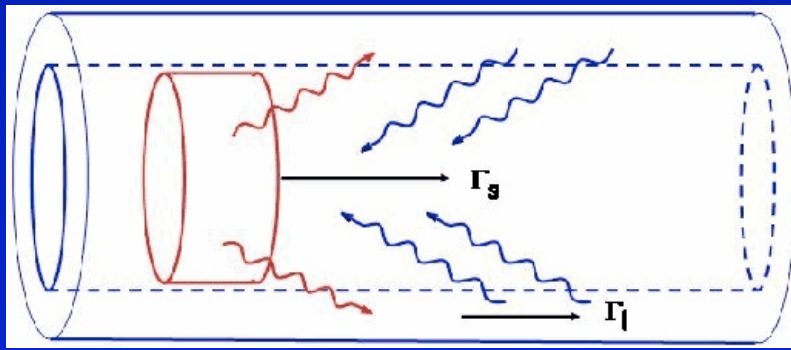
$$\theta = 10^\circ, \gamma = 2.3, \delta = 3.9$$

$$n = k \epsilon^{-p} \quad p = 1.6 \quad [1, 4 \times 10^3] \quad p = 3.6 \quad [4 \times 10^3, 10^7]$$

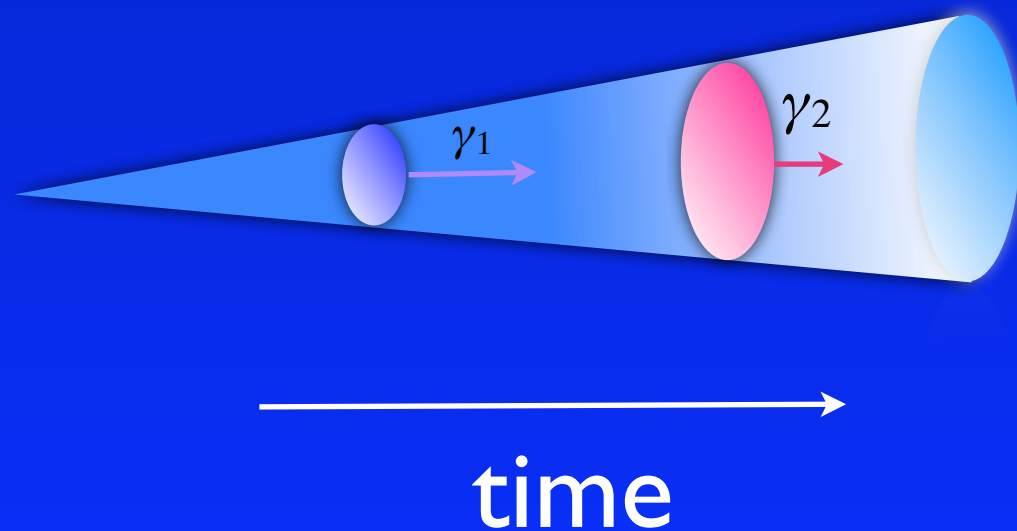
$$R = 1.4 \times 10^{16} \text{ cm}$$

$$B = 55 \text{ mG}$$

The bulk motion of the jet is too slow, when compared with that observed in Blazars.



The jet is structured



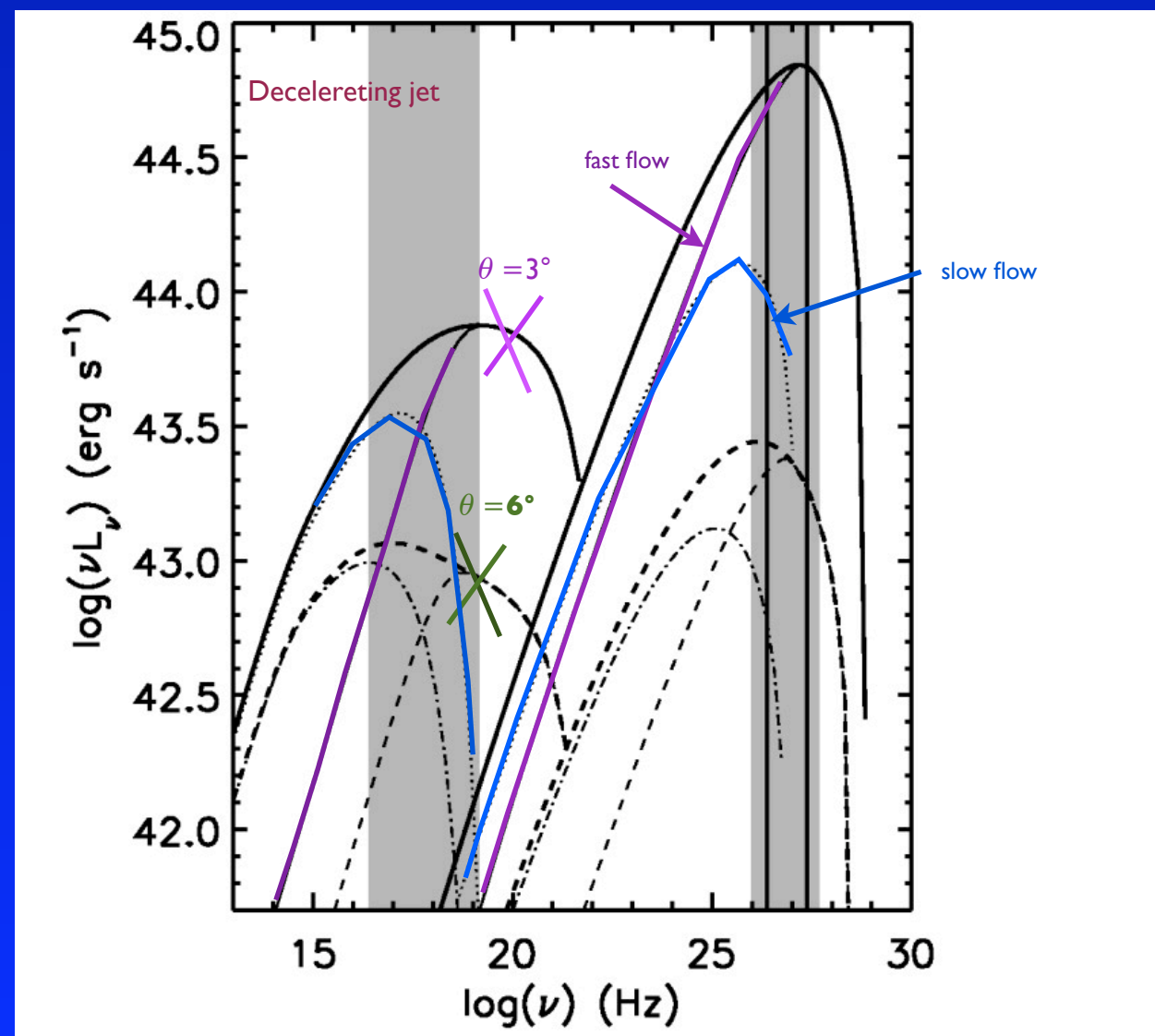
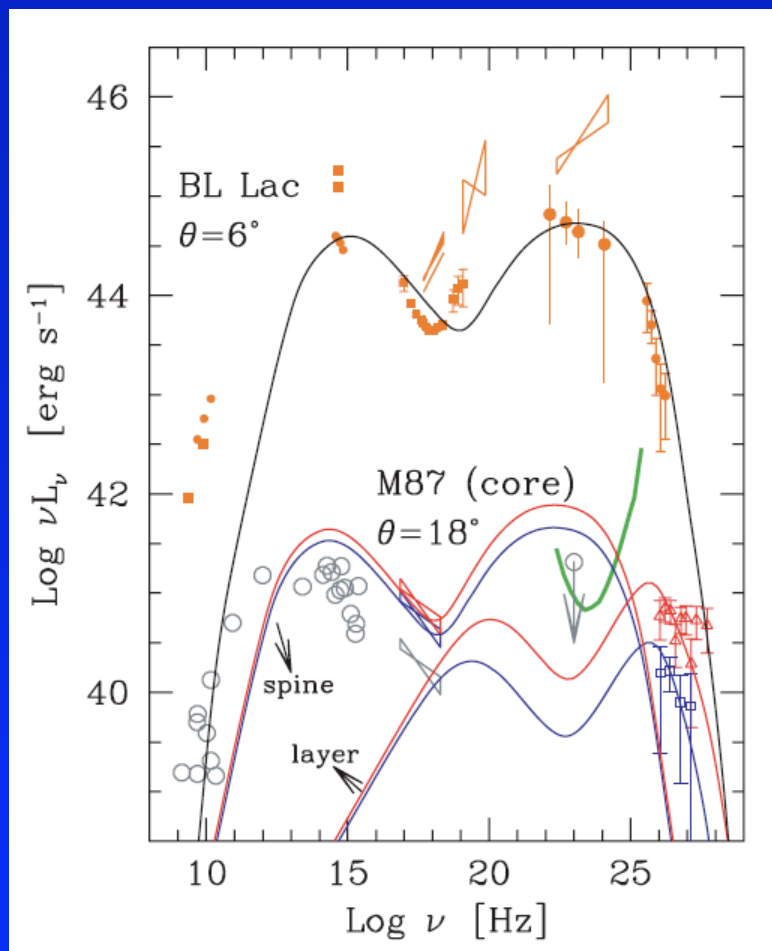
The jet is decelerated

The models in brief

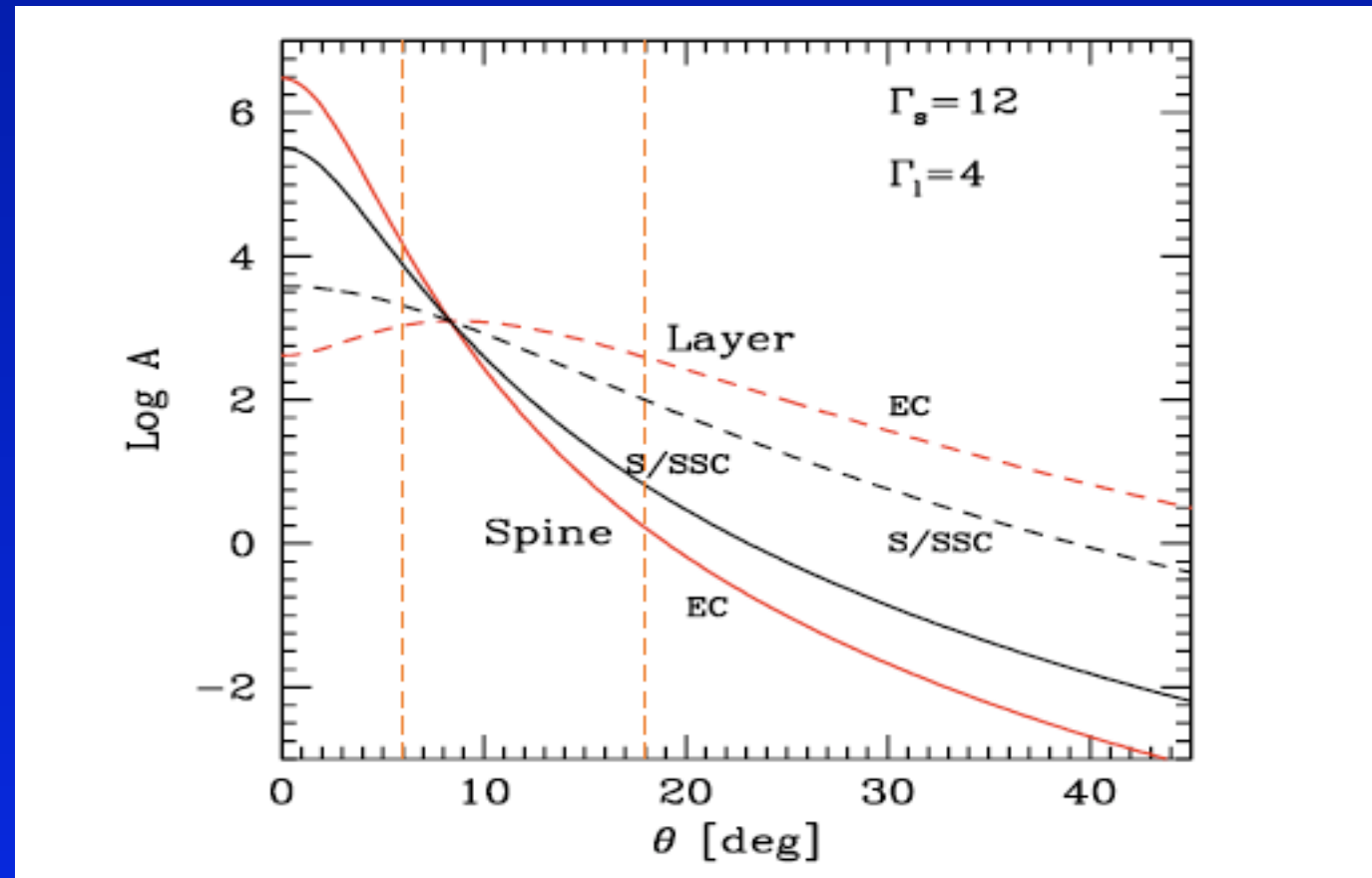
The seed photons relevant for the scattering processes are produced not only by the spine electrons but also by layer electrons.

The problem of missing photons is solved in the decelerating model assuming that the upstreaming energetic electrons from the fast base of the jet see the synchrotron photons produced in the slow part of the flow.

In both cases the effect is a strong feedback between the two components that increases the inverse Compton flux.



What about FRII sources?



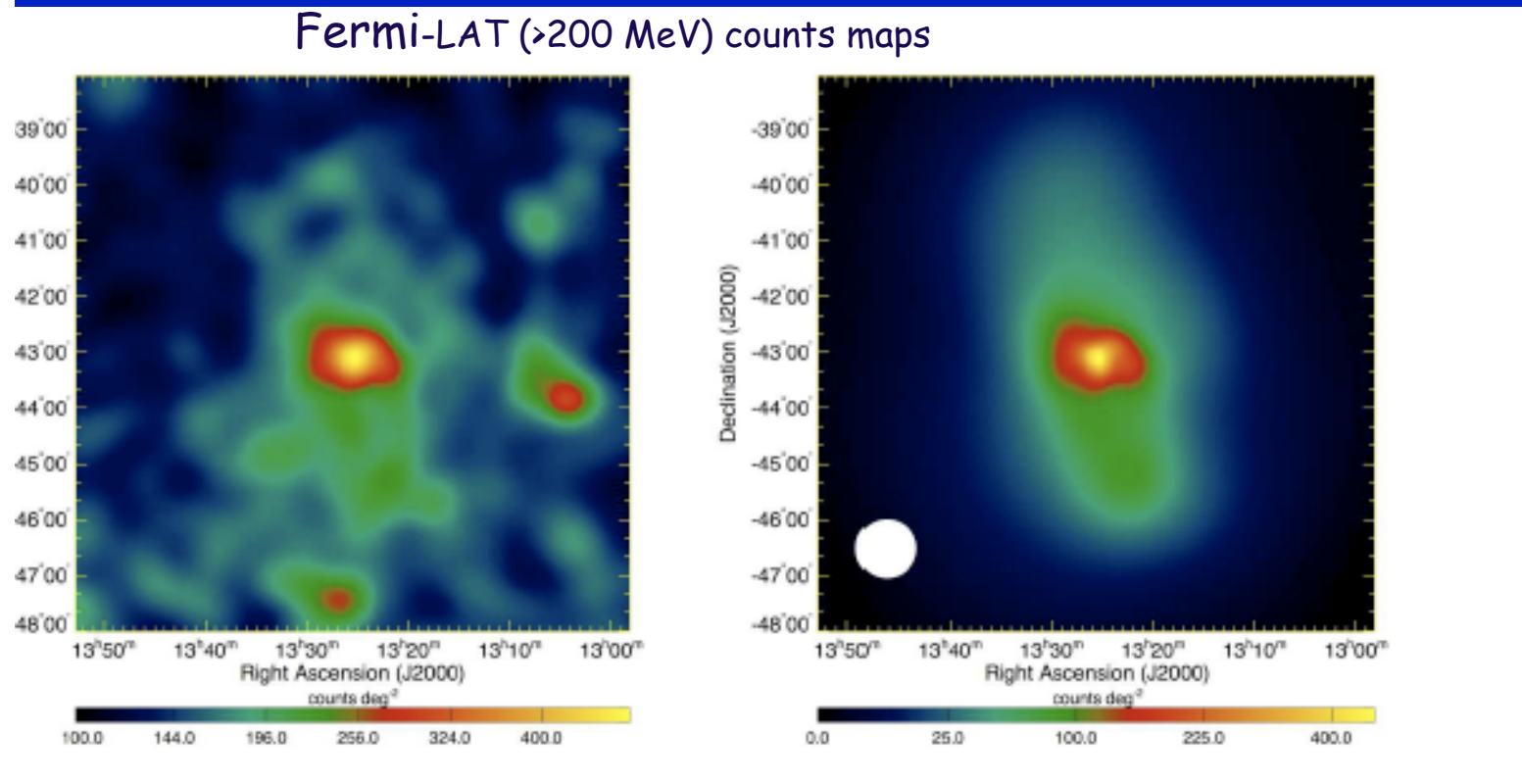
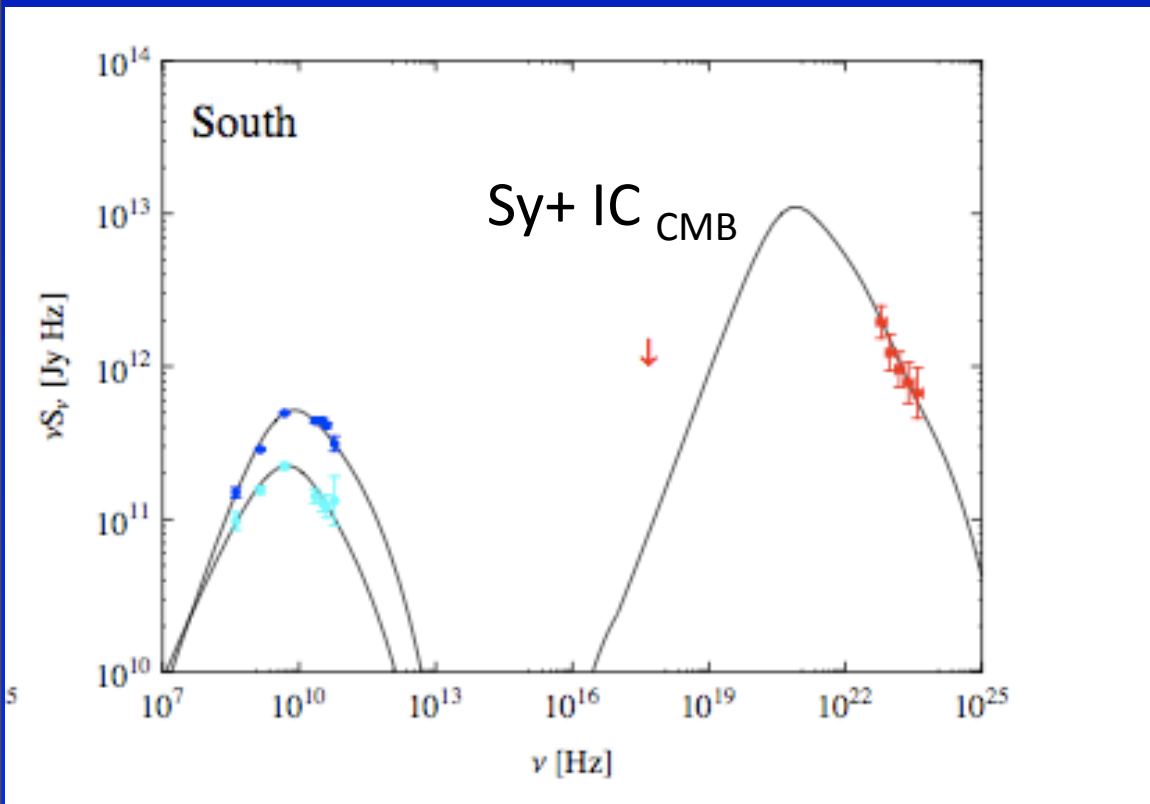
The small number of FRIIs with LAT associations could be simply related to their larger redshifts or indicate the presence of less structured jets (24 month analysis...)

Are we sure that the γ -ray are coming from the core ?

but we could also have a contribution
 → from large extended regions (kpc-scale structures)

CenA Lobes
 Abdo et al. 2010 Science

Inverse Compton of CMB
 by relativistic electrons

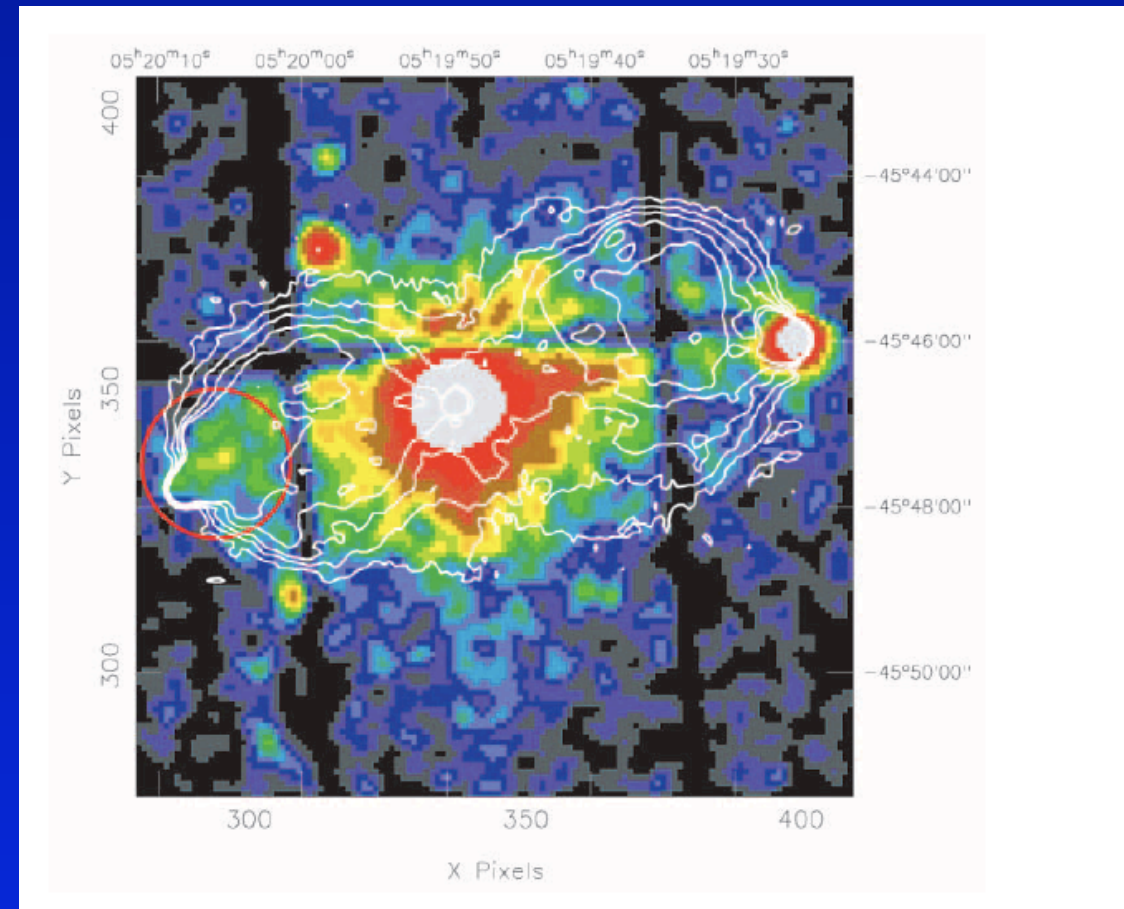
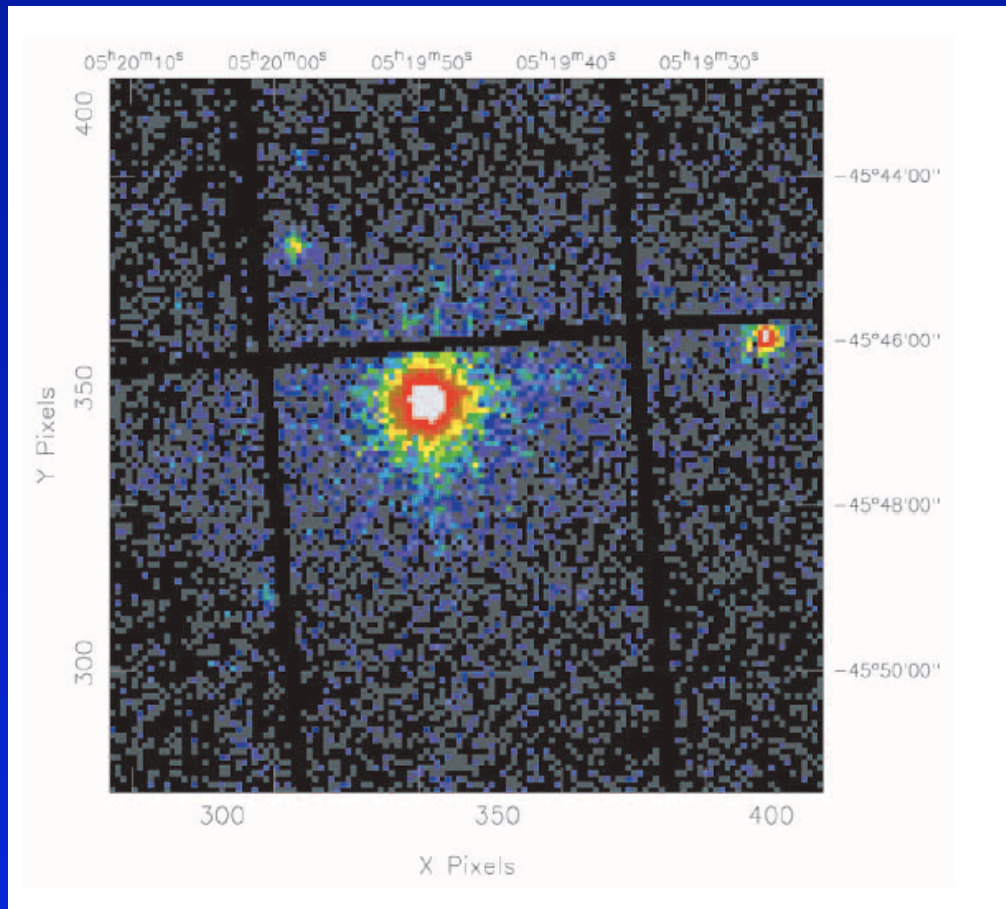


$n(\epsilon)$: broken pl + exp cutoff

$B \sim 0.9 \mu\text{G} \quad U_e/U_B \sim 2-4$

Detection significances: N Lobe 5σ - S Lobe 8σ

Note: Radio Lobes are sometime detected in X-rays



$$L_{syn} = C_{syn} k_e V B^{\alpha+1} \nu^{-\alpha} \quad L_{IC} = C_{IC} k_e V \nu^{-\alpha}$$

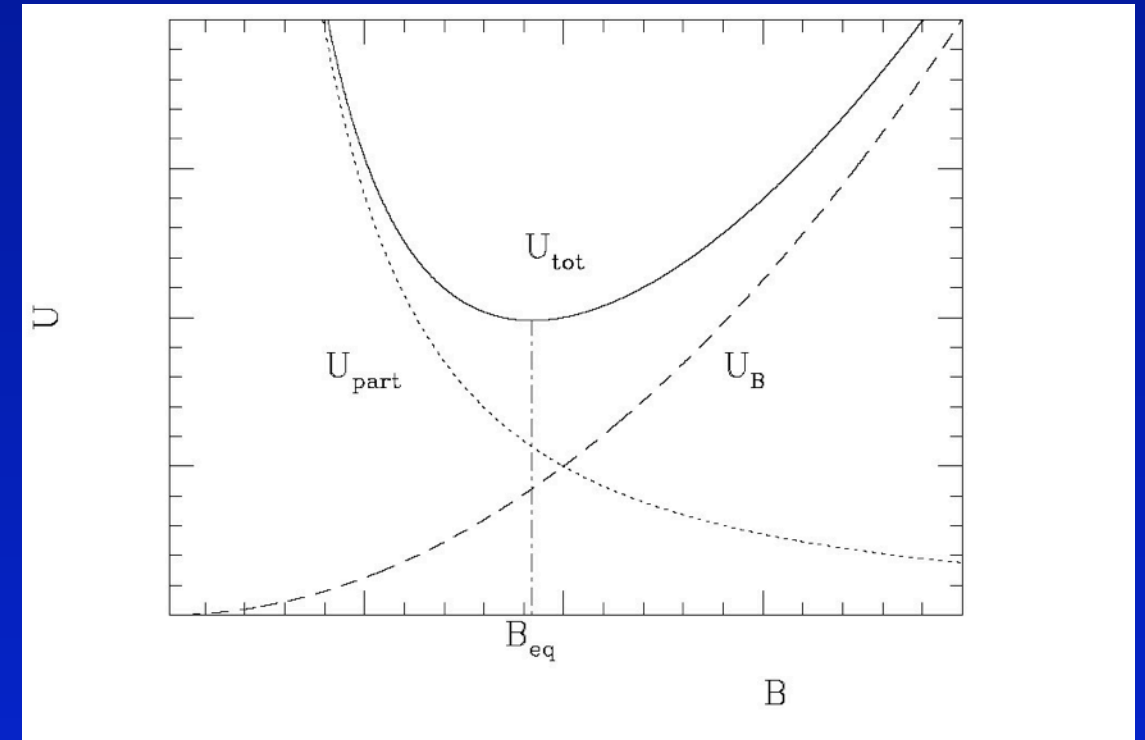
$$B_{IC} = \left[\frac{F_{1.4 \text{ GHz}} C_{IC}(\alpha) (1+z)^{\alpha+3}}{F_1 \text{ keV} C_{sin}(\alpha)} \right]^{\frac{1}{\alpha+1}} \left[\frac{\nu_{syn}}{\nu_{IC}} \right]^{\frac{\alpha}{\alpha+1}}$$

$$\alpha = \alpha_r = \alpha_x, V \text{ is the volume and } N(\gamma) = K e \gamma^{-(2\alpha+1)}$$

Condition of Equipartition

$$U_{\text{tot}} = U_B + U_e + U_p$$

$$U_p = kU_e, \quad U_B = B^2/8\pi$$



Powerful jets have efficient accretion disk, weak jets have inefficient accretion flow (FRI/FRII dichotomy)

The kinetic power of the jet, i.e., the energy flux of the relativistic flow through a section πR^2 of the jet, is given by $P_{\text{jet}} = \pi R^2 c \beta U \gamma^2$, where $U = U_B + U_e + U_p$ is the total energy density in the jet frame, caused by magnetic field, relativistic electrons, and, if present, protons ($L_{\text{jet}} = L_B + L_e + L_p = \eta P_{\text{jet}}$). η estimated by Laura is 1-10%.

There is a substantial equality of the jet and accretion power.

Powerful jets have efficient accretion disk, weak jets have inefficient accretion flow (FRI/FRII dichotomy)